PONTIFÍCIA UNIVERSIDADE CATÓLICA
DO RIO DE JANEIRO

Luisa Souza Neves Frade da Cruz

Shear Behavior of Concrete Beams Reinforced with Bamboo Culms

Dissertação de Mestrado

Dissertation presented to the Programa de Pós-Graduação em Engenharia Civil of PUC-Rio in partial fulfillment of the requirements for the degree of Mestre in Engenharia Civil.

Advisor: Daniel Carlos Taissum Cardoso

Co-Advisor: Flávio de Andrade Silva

Rio de Janeiro

September 2023

Pontifícia Universidade Católica
do Rio de Janeiro

Luisa Souza Neves Frade da Cruz

Shear Behavior of Concrete Beams Reinforced with Bamboo Culms

Dissertation presented to the Programa de Pós-Graduação em Engenharia Civil of PUC-Rio in partial fulfillment of the requirements for the degree of Mestre in Engenharia Civil. Approved by the Examination Committee.

Prof. Daniel Carlos Taissum Cardoso
Advisor
Departamento de Engenharia Civil – PUC-Rio

Prof. Flávio de Andrade Silva
Co-Advisor
Departamento de Engenharia Civil – PUC-Rio

Prof. Luisa Molari
UNIBO

Prof. Baolin Wan
Marquette University

Rio de Janeiro, September the 29th, 2023

Luisa Souza Neves Frade da Cruz

Graduated in Engenharia Civil from Universidade Federal de Juiz de Fora – UFJF in 2021.

Bibliographic data

Cruz, Luisa Souza Neves Frade da

Shear behavior of concrete beams reinforced with bamboo culms / Luisa Souza Neves Frade da Cruz ; advisor: Daniel Carlos Taissum Cardoso ; co-advisor: Flávio de Andrade Silva. – 2023.
111 f. : il. color. ; 30 cm

Dissertação (mestrado)–Pontifícia Universidade Católica do Rio de Janeiro, Departamento de Engenharia Civil e Ambiental, 2023.
Inclui bibliografia

1. Engenharia Civil e Ambiental - Teses. 2. Bambu. 3. Concreto. 4. Cisalhamento. 5. Sustentabilidade. 6. Cinemática da fissura. I. Cardoso, Daniel Carlos Taissum. II. Silva, Flávio de Andrade. III. Pontifícia Universidade Católica do Rio de Janeiro. Departamento de Engenharia Civil e Ambiental. IV. Título.

CDD: 624

Acknowledgements

To my advisor Daniel who supported me through all this journey, thanks for embracing my ideas and for being a great mentor and professor.

To Professor Flávio for always encouraging our ideas and sharing insightful advices.

To all my professors from PUC-Rio and UFJF for sharing their expertise and wisdom.

I would like to thank my committee members, Professor Luisa and Professor Baolin, for gently accepting the invitation.

My sincere thanks to all my family, friends, colleagues, and technicians from LEM-DEC who helped to create this work.

To my mother Cláudia,

To my father Inácio,

To my sister Helena, and to Lucas,

I deeply thank Paulo for accompanying me through this journey.

To Conselho Nacional de Desenvolvimento Científico e Tecnológico – CNPq for the financial support to the research.

This study was financed in part by the Coordenação de Aperfeiçoamento de Pessoal de Nível Superior - Brasil (CAPES) - Finance Code 001.

Abstract

da Cruz, Luisa Souza Neves Frade; Cardoso, Daniel Carlos Taissum; Silva, Flávio de Andrade. **Shear Behavior of Concrete Beams Reinforced with Bamboo Culms**. Rio de Janeiro, 2023. 111p. Dissertação de Mestrado – Departamento de Engenharia Civil e Ambiental, Pontifícia Universidade Católica do Rio de Janeiro.

As a renewable resource, highly available across the world, low-cost and eco-friendly material, bamboo has shown to be a promising alternative for achieving a more sustainable scenario in the construction industry. Therefore, this research aims to investigate the use of bamboo as reinforcement for concrete structures, focusing on the shear behavior of beams. Bamboo culms from the specie *Phyllostachys aurea* are used as longitudinal reinforcement while for shear reinforcement different techniques employing local materials are tested: discrete sisal fibers, bamboo stirrups, sisal yarn, and no shear reinforcement. The beams were subjected to three-point bending tests in order to analyze the shear behavior. Moreover, the Digital Image Correlation (DIC) technique was employed to acquire the crack kinematics and the contributions of shear mechanisms were estimated. The test results demonstrated improvements in the load-carrying capacity of the beams through the utilization of different materials. Bamboo stirrups increased the ultimate load by 15.85%, sisal yarn by 12.30%, and discrete sisal fibers by 1.32%, highlighting their positive impact on load-bearing capacity. This research underscores the possibility of replacing non-renewable carbon intensive materials such as steel with bamboo in low-rise buildings, particularly for social housing. Thereby it allows to promote sustainable and safe construction practices while empowering rural development and conserving global resources.

Keywords

Bamboo; Concrete; Shear; Sustainability; Crack kinematics.

Resumo

da Cruz, Luisa Souza Neves Frade; Cardoso, Daniel Carlos Taissum; Silva, Flávio de Andrade. **Comportamento ao Cisalhamento de Vigas de Concreto Armado com Colmos de Bambu**. Rio de Janeiro, 2023. 111p. Dissertação de Mestrado – Departamento de Engenharia Civil e Ambiental, Pontifícia Universidade Católica do Rio de Janeiro.

Enquanto fonte renovável, amplamente disponível no mundo, de baixo custo e ecologicamente amigável, o bambu tem se mostrado uma alternativa promissora para alcançar um cenário mais sustentável na indústria da construção. Assim, a presente pesquisa tem como objetivo investigar o uso do bambu como reforço para estruturas de concreto, com foco no comportamento ao cisalhamento de vigas. Foram usados colmos da espécie *Phyllostachys aurea* como armadura longitudinal e para reforço transversal diferentes técnicas empregando materiais naturais foram testadas: fibras de sisal discreta, estribo de bambu, cordão de sisal, além de vigas sem reforços. As vigas foram submetidas a ensaio de flexão em três pontos a fim de analisar o comportamento ao cisalhamento. Além disso, técnica de Correlação de Imagem Digital (CID) foi empregada para adquirir a cinemática das fissuras e estimar as contribuições dos mecanismos de cisalhamento. Os resultados dos ensaios apontam um aumento na capacidade de carga das vigas pelo uso de diferentes materiais. Estribos de bambu aumentaram a carga última em 15,85%, cordão de sisal em 12,30% e fibra discreta de sisal em 1,32%, destacando o impacto positivo desses artifícios na capacidade de carga. Esta pesquisa ressalta a possibilidade de substituir materiais não renováveis com alta pegada de carbono em construções de pequeno porte, especialmente em habitações populares. Isso permite promover práticas de construção sustentáveis e seguras, ao mesmo tempo em que fortalece o desenvolvimento rural e preserva recursos globais.

Palavras-chave

Bambu; Concreto; Cisalhamento; Sustentabilidade; Cinemática da fissura.

Figure List

List of Tables

SUMMARY

1. INTRODUCTION

1.1 Motivation

The construction industry is known for its high carbon footprint and energy consumption due mainly to the use of conventional materials and outdated techniques. According to Mehra *et al*. [1], steel production accounts for 32 MJ/kg of embodied energy and concrete around 1.9 MJ/kg, resulting in a large CO_2 emission. Other than the carbon dioxide released into the atmosphere by the production of the material itself, the whole manufacturing processing and transportation of these materials also generates a huge amount of CO_2, indicating the urgent need for the use of more eco-friendly materials and renewable resources. An *et al*. [2] state that the iron and steel industry is one of the main industrial emitters of CO_2, accounting for 7% of CO_2 emission of the total CO_2 production by human activity.

Taking into account the current scenario of the construction industry, bamboo emerges as a pertinent alternative to the use of steel in reinforced concrete structures. Bamboo is a widely spread, low-cost and lightweight material that presents a high ratio of strength by weight and a fast growth rate [3], [4], [5], [6], [7], [8]. Furthermore, bamboo is a very efficient carbon sink and thus it can play an important role in CO_2 absorption throughout its whole lifecycle. Other than reducing the environmental impacts of the AEC (Architecture, Engineering, and Construction) industry, bamboo can substitute unreinforced concrete structures used in regions where there is a deficiency in the production of steel for being expensive and not feasible, which can help to overcome housing problems [9], [10]. Nevertheless, some important material issues should be addressed in the replacement of steel with bamboo: brittle behavior, lower Young's modulus of bamboo, weakness of the nodes, and poor bonding performance [11], [12], [13]. Most of these concerns can be mitigated by adopting proper techniques.

Studies approaching the use of bamboo as flexural reinforcement for concrete elements have been reported by several authors [4], [10], [11], [13], [14], [15], [16], [17], [18]. Most of the researches [4], [15], [16], [17] focused on the flexural behavior of concrete beams reinforced with bamboo strips while fewer studies [13], [18], [19] investigated the use of bamboo culms. Also, the shear analysis of concrete structures reinforced with bamboo, as well as its application as transverse reinforcement, remains limited within the scope of existing literature [19], [17], [20], [21].

1.2 Objectives

From this perspective, the purpose of the present study is to examine the structural performance of concrete beams without steel reinforcement by primarily utilizing bamboo as a viable alternative. The main focus is on investigating the shear behavior of these beams and the shear strength mechanisms acting, specially, on slender beams. The research involves using bamboo culms as longitudinal reinforcement, since it presents lower technical requirements than splints do, and testing various types of shearing reinforcement. To analyze the shear mechanisms, three-point bending tests are performed on the beams with one span reinforced with steel stirrups and the other span reinforced with different techniques, which will be explained in subsequent sections.

1.3 Structure of the work

This work is divided in an initial part of literature review (Chapter 2) where topics regarding sustainability, bamboo contextualization, application of bamboo in concrete structures, and shear strength mechanisms overview are presented.

Chapter 3 describes the experimental program, presenting the process for preparing the materials, the assembling of the beams and the structural design as well.

Chapter 4 provides the results an analysis performed by DIC for the 3-point bending test. In section 4.2 the shear strength mechanisms are derived for specimens 02, 07, 08. Finally, Chapter 5 highlights the final remarks of this research and points out suggestions for further work.

2. LITERATURE REVIEW

2.1 Sustainability in the Construction Industry

The construction industry is characterized by a conservative *modus operandi,* that leads to substantial disposal of solid waste into the environment and the emission of hazardous gases into the atmosphere. Sandanayake [22] reports that the construction sector is accountable for approximately one-sixth of the world's freshwater consumption, one-fourth of wood extraction, and two-fifths of material processing. Statistics provided by the author underscore the construction industry's prominent role as one of the primary contributors to environmental emissions.

In this context, characterized by the urgent need to investigate alternatives to the materials conventionally adopted in the industry, bamboo stands out as a natural material of abundant availability in the national scenario. Owing to its capacity to capture CO_2 from the atmosphere, bamboo has the potential to mitigate the high ecological footprint inherent in the construction sector. According to Osorio *et al*. [23], when compared to tropical forests, bamboo is capable of releasing 35% more oxygen and sequestering four times more carbon dioxide per hectare per year. In addition to CO_2 capture, bamboo plays a fundamental role in reducing the energy demand of the production chain in the construction sector: compared to steel, bamboo has an approximately 60 times lower energy demand for production (MJ/kg) [24].

The replacement of steel, whether total or partial, through the incorporation of bamboo into traditional construction systems, can be regarded as an appealing alternative from an environmental perspective. Moreover, it is highly feasible concerning economic and social aspects, thus reaffirming the fundamental elements of the sustainability tripod. The utilization of bamboo enables the development of lightweight structures with renewable resource and low-cost material. However, when employing bamboo as a reinforcement for concrete, it is mandatory to implement specific procedures to enhance bamboo's durability and to improve the bond between bamboo reinforcement and concrete matrix. All of these methods must be carefully evaluated to preserve the ecological benefits of utilizing bamboo.

In the current research, a 'cradle-to-gate' Life Cycle Assessment (LCA) was conducted, comparing the ecological footprint of bamboo and steel. The cradle-to-gate LCA model evaluates a product's environmental impact, spanning from raw material extraction to its exit from the factory gate. The *SimaPro* software was utilized, employing the ReCiPe 2016 Midpoint (H) method. The analysis was conducted using an equal mass (in kg) of each material as input. Notably, the ReCiPe 2016 version features characterization factors suited for a global scale, unlike the ReCiPe 2008 version tailored for the European scale. The 'H' designation signifies the hierarchist perspective adopted, aligning with prevalent policy principles concerning time-frame and other considerations [25].

The ReCiPe 2016 methodology addresses 18 impact categories at the midpoint level and 3 categories at the endpoint level (human health, ecosystems, and resource scarcity). Given the research's environmental focus, 10 out of the 18 categories were selected for comparison. It is pertinent to acknowledge that the analysis encountered simplifications due to the inherent mass disparities between steel and bamboo, particularly considering structural applications where bamboo is notably lighter. However, even when evaluating the same material quantities, bamboo exhibited a reduced environmental impact across multiple categories, as depicted in Figure 1.

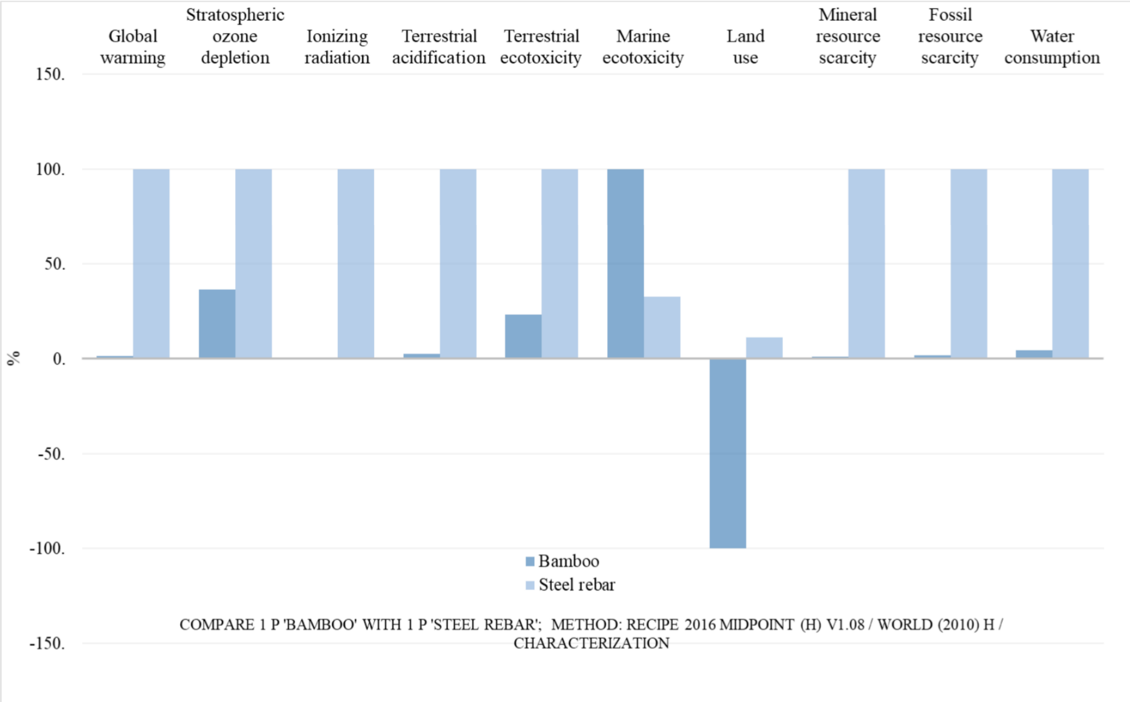

Figure 1 – Life Cycle Assesment (LCA) 'cradle-to-gate' comparing the impacts of bamboo versus steel according to results provided by SimaPro - ReCiPe 2016 Midpoint (H) method.

The cradle-to-gate LCA conducted corroborates the sustainable characteristics inherently associated with bamboo, as reported in the state of the art. Bamboo exhibits a significantly lower environmental impact, particularly in terms of global warming and resource consumption. Moreover, its capacity to recover degraded lands results in a negative footprint to land use. The observed marine ecotoxicity may be attributed to the use of artificial fertilizer considered by *SimaPro* for the bamboo production, a factor that could be addressed by substituting it with organic alternatives. Overall, the analysis underscores the ecological advantages of bamboo as a more environmentally friendly material choice when compared to steel.

In some research studies [12], [13], [26], counterarguments have been presented against using bamboo as reinforcement for concrete, citing concerns about high concrete volume and bamboo's inability to fully offset the concrete's impact. However, it is important to address the context where this technique is recommended. Besides being used for lightweight structures, bamboo can be utilized as a tool for empowering communities lacking access to conventional materials such as steel. The construction of full bamboo structures would require extensive training which may not be feasible in the present national scenario, whereas the use of bamboo culms in place of steel rebars would allow for the use of a pervasive technique, namely reinforced concrete, while it serves as a strategy to spread technical knowledge about the use of bamboo in EAC industry.

With the aim of minimizing the impact caused by the production of conventional concrete, strategies can be adopted to confer a more ecological character to the matrix. One possibility involves substituting the conventional coarse aggregate with recycled aggregate derived from construction and demolition waste (CDW). Mixtures using concrete with recycled aggregate reduce the environmental impact by approximately 70% compared to conventional concrete, considering that the by-products of the recycling process will not be discarded [27].

Furthermore, replacing traditional Portland cement with a low-clinker cement can be considered, as clinker is the primary responsible for CO_2 emissions in the atmosphere, accounting for about 6-7% of anthropogenic carbon dioxide emissions [28]. A promising material in this regard is geopolymers, which comprise a blend of aluminosilicates activated in an alkaline medium [29],[30],[31]. Compared to Portland cement, geopolymers can reduce CO_2 emissions by up to 0.73 ton CO_2/ton of cement, while also lowering the consumption of limestone and clay by the construction industry [32]. However, the materials required for producing geopolymers on a national scale are still challenging to commercialize. The complexity of obtaining the necessary resources hinders the widespread adoption of geopolymers as a replacement for conventional concrete with Portland cement, as well as complicates their use for large-scale research.

1.2
Bamboo

2.2.1
Basic characteristic of bamboo

According to López [6], bamboo is a woody plant belonging to the angiosperms, within the family Graminae (*Poaceae*) and subfamily *Bambusiudeae*. With approximately 121 genera and 1662 species, bamboo is distributed across both tropical and temperate regions, being naturally present on all continents except Europe [33]. Despite being commonly perceived as a tree, bamboo is, in reality, a giant arborescent grass, widely spread in warm and rainy areas such as the tropical and subtropical regions of Asia, Africa, and South America [4],[34].

This giant grass, with a millennial history of use, exhibits an accelerated growth rate of up to one meter per day. Bamboo is naturally found between latitudes 45°30' North and 47° South, distributed from sea level to high altitudes. For instance, in India, species of the genus *Arundinaria* can be found at altitudes of 3,000 meters [7]. According to Filgueiras and Gonçalves [35], Brazil presents the highest diversity of bamboo species among other Latin American countries, with around 230 species belonging to 34 genera.

Referred to as "green steel" in Eastern culture, bamboo is a plant that exhibits significant potential for engineering applications, making it suitable for structural purposes. The main species employed in the construction industry include *Guadua angustifolia*, *Dendrocalamus giganteus*, and *Phyllostachys pubescens*, with their natural distribution originating from South America and Asian countries such as Sri Lanka, Bangladesh, Nepal, Thailand, China, respectively [7]. The development of new techniques has allowed for a noticeable evolution in construction practices using bamboo, progressing from small dwellings to more complex structures, such as bridges, schools, and cathedrals (see Figures 2 and 3).

Figure 2 – Bridge constructed with bamboo Guadua in Colombia [36]

Figure 3 - Panyaden International School in Thailand [37]

Bamboo's abundant growth in tropical climate regions makes it a low-cost and highly efficient alternative for housing purposes in countries across Latin America, Africa, and Asia. Alongside its rapid growth, the plant offers considerably lower production costs (harvesting and treatment) compared to conventional materials. Some of the potential construction applications of bamboo include "*bioketro*" - a Brazilian term for using bamboo fibers in a cement matrix, GLB (glued laminated bamboo), which, in certain cases, can replace the use of wooden slats, or, as in the case of this study, bamboo culms or splints for reinforced concrete. In China, for instance, GLB is already employed on an industrial scale for products such as flooring, ceilings, paneling, furniture, laminates for flooring, among others [7]. To employ bamboo in engineering, standards for characterization, design and quality control have been developed, as outlined in Table 01.

Table 1 - Code and norms addressing the use of bamboo for structural applications and testing. Adapted from GATOÓ *et al.* [38]

Country	Code	Norm
Brazil		NBR16828-1 Bamboo Structures - Part 1: Design (12/2020) NBR16828-2 Bamboo Structures - Part 2: Determination of physical and mechanical properties of bamboo

China		JG/T 199: Testing method for physical and mechanical properties of bamboo used in building (PRC MoC, 2007)
Colombia	Reglamento Colombiano de Construcción Sismoresistente – capítulo G12 Estructuras de Guadua (Guadua structures) (ICONTEC, 2010)	NTC 5407: Uniones de Estructuras con Guadua angustifolia Kunth (Structural unions with Guadua angustifolia Kunth) (ICONTEC, 2006) NTC 5525: Métodos de Ensayo para Determinar las Propiedades Físicas y Mecánicas de la Guadua angustifolia Kunth (Methods and tests to determine the physical and mechanical properties of Guadua angustifolia Kunth) (ICONTEC, 2007)
Ecuador	Norma Ecuatoriana de la Construcción – capítulo 17 Utilización de la Guadua Angustifolia Kunth en la Construcción (Use of Guadua angustifolia Kunth in construction) (INEN, 2011)	INEN 42: Bamboo Caña Guadua (bamboo cane Guadua) (INEN, 1976)
India	National Building Code of India, section 3 Timber and bamboo: 3B (BIS, 2010)	IS 6874: Method of tests for round bamboos (BIS, 2008) IS 15912: Structural design using bamboo – code of practice (BIS, 2012)
Peru	Reglamento Nacional de Edificaciones, Section III. Code E100 – Diseño y Construcción con Bamboo (ICG 2012)	
USA		ASTM D5456: Standard specification for evaluation of structural composite lumber products (ASTM, 2013)
International		ISO 22156: Bamboo – structural design (ISO, 2004a) ISO 22157-1 Bamboo – determination of physical and mechanical properties – part 1: requirements (ISO, 2004b) ISO 22157-2: Bamboo – determination of physical and mechanical properties – part 2: laboratory manual (ISO, 2004c)

Considering its diverse range of applications, bamboo cultivation can significantly contribute to the microeconomy by fostering the growth of small and medium-sized producers and generating new employment opportunities. In countries across the African and Asian continents, such as South Africa and China, the cultivation and utilization of bamboo plays a significant role in supporting local communities [39]. In addition to the positive economic impacts, opting for bamboo as a construction material makes housing more accessible to low-income populations, especially when combined with support programs provided by the government.

2.2.2. Morfology and biologic characteristics of bamboo

As part of the "C4" group of plants, bamboo plays a significant role in sequestering CO_2 from the atmosphere, thereby contributing to the reduction of greenhouse gas emissions. According to Pinto *et al.* [40], bamboo species categorized as "C4" exhibit minimal CO_2 emissions during their respiration process due to a gas storage mechanism within the plant's fibers.

Bamboo is composed of two main parts: an aerial portion known as the culm and an underground part consisting of the rhizome and roots (see figure 4.a). The culms are approximately cylindrical, featuring hollow internodes with varying lengths along the longitudinal axis (see figure 4.b). Transverse separations called diaphragms provide greater rigidity and resistance against local wall buckling, granting bamboo the ability to withstand wind forces and its self-weight [7].

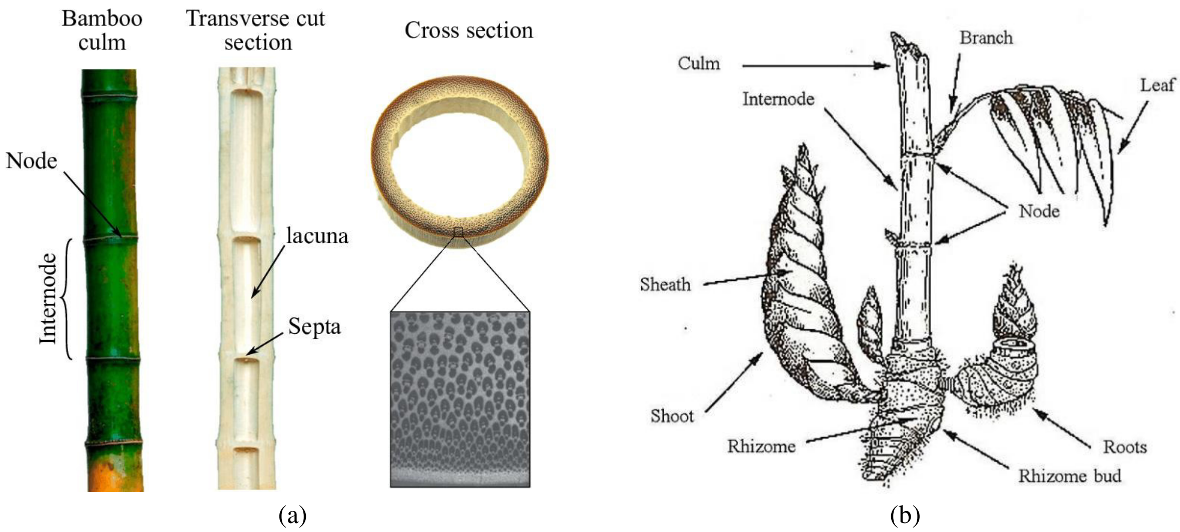

Figure 4 – Structure of bamboo: (a) Outer and inner morfology of aerial part of bamboo [41] (b) Morfology of bamboo, aerial and underground part [42]

The aerial part of bamboo can exhibit various characteristics, such as solid, hollow, or partially hollow culms, which can be erect, arched, supportive, or climbing. Culms may also vary in shape, ranging from cylindrical to grooved or slightly flattened. The coloration ranges from shades of green to reddish tones, transitioning through brown and yellow hues. As for the surface texture, it can be smooth, papillose, rough, or striated

[43]. Alongside the diversity in the plant's aesthetic patterns, there is also a significant variation concerning the number of nodes, the length of internodes, and the dimensions of the outer diameter and wall thickness of bamboo culms.

Regarding the underground part, known as the rhizome, it not only generates new culms and roots but also stores and transports nutrients from the aerial part. Additionally, the rhizome provides greater protection against wildfires. Almeida [44] highlights that bamboo was the first plant to grow after the nuclear attacks in Nagasaki and Hiroshima, thanks to its high resilience, mainly attributed to the rhizome.

2.2.3.
Anatomy and properties of bamboo

Despite considerable variation in the physical, anatomical, and mechanical characteristics among different bamboo species, the culm is generally composed of approximately 50% parenchyma cells, 40% fibers, and 10% conductive tissues [7][23][45]. Bamboo is a naturally composite, heterogeneous, and orthotropic material, meaning its properties vary along orthogonal axes [46]. According to Pereira and Beraldo [7], the primary factors influencing bamboo's mechanical properties include species, moisture content, edaphoclimatic conditions, age, and harvesting time.

Janssen [26] states that the most influential physical property affecting the mechanical performance of bamboo culms consists of its apparent density, which depends on the growth location, species, position within the culm, among other factors. Bamboo has apparent density values ranging from 500 kg/m³ to 900 kg/m³, depending on the species and type of rhizome. This property primarily varies with the culm's anatomical structure, such as the quantity and distribution of fiber bundles around the vessels, as well as fiber diameter and cell wall thickness [6].

Transversely to the culm, an increase in apparent density is observed from the inner to the outer wall. Longitudinally, the increase occurs from the base towards the top. A closely related aspect to apparent density is the moisture content of the material. For freshly cut culms, this content ranges from 40% to 150%, while for immature culms, the values are even higher than for mature culms. To improve the mechanical properties, it is crucial that bamboo undergoes a period of air drying for one to four months after harvesting, achieving a moisture content between 10% to 15% [7].

The influence of apparent density on bamboo's mechanical strength is also related to the presence of fibers constituting the sclerenchyma tissue. Analogous to the distribution described above, the fibers concentrate in the outer part of the culm wall, which has lower amounts of parenchyma tissue; and longitudinally, they concentrate towards the top, where small vascular bundles are also distributed [4], [46], [47], [48]. According to García [49], approximately 40-70% of the fibers are found in the outer part, while the remaining 15-30% are distributed in the interior. As depicted in Figure 5, the higher concentration of fibers in the outer portion of the culm walls enhances the rigidity of these layers, serving as a mechanism to withstand the wind forces that bamboo is often subjected to.

Figure 5 - Anatomy of bamboo and fiber distribution along its cross-section [50]

By analyzing the anatomical composition of bamboo culms, one can observe the presence of fiber bundles oriented along the longitudinal axis within the internodes and immersed in a lignin matrix [4], [51]. This fiber arrangement allows the plant to achieve a tensile strength of up to 370 MPa [14], [52]. According to Ghavami *et al*. [53], the superior tensile strength of bamboo, in comparison to other mechanical properties, is attributed to the parallel orientation of fibers along the culm axis, resulting in a tensile strength approximately 30% greater than the compression strength. However, at the nodes, there is a decrease in the amount of fibers compared to the internodes, and the diaphragms have even fewer fibers, leading to reduced properties such as tensile, compressive, and shear strength.

Furthermore, the modulus of elasticity parallel to the fibers varies based on the culm's position as well, and within the same species, the tensile modulus surpasses the compressive modulus. Concerning this property, values span across different species from 8 GPa to 25 GPa [53]. The concentration of stresses at the nodes and their low mechanical resistance is primarily due to the discontinuity of the section and the deviation of fiber bundles [7].

2.2.5. Durability and Treatments

Ensuring the sustainable use of bamboo in construction requires the adoption of precautionary measures and proper preservation procedures. To safeguard the material's properties, bamboo must undergo treatments to prevent insect and fungal attacks. The plant is susceptible to attacks by the insect *Dinoderus minutus*, popularly known as 'bamboo borer', which is drawn to the internal starch and leads to culm deterioration. The culms should be adequately dried, either through air drying or kiln drying, and stored appropriately. Also, as a biological material, bamboo requires protection through designs that shield it from weathering, such as constructing eaves and minimizing ground contact. By integrating suitable construction practices with proper treatment procedures, the lifespan of bamboo culms can be extended, making it a practical and environmentally-friendly choice for construction projects.

For most species, the top portion of the culm exhibits higher durability than the base and middle parts, which can be related to the increase in fiber content along the bamboo's height whereas the starch reduces. The soft internal walls are more susceptible to insect attack, especially in culms younger than one year. Additionally, when divided into strips, bamboo becomes more vulnerable to deterioration than when preserving its original geometry [6].

According to López [6], bamboo treatment methods can be classified as physical and chemical. The physical treatment, also known as curing, aims to remove or reduce the starch present in the culms, thereby minimizing the attack from *Dinoderus minutus* (bamboo borer). This low-cost method is traditionally used in rural areas and villages, particularly in Asian countries. However, it does not guarantee protection against termite and fungal attacks. Among the physical treatment methods, maturation or curing on-site, immersion curing, fire curing, and smoke curing can be employed.

On the other hand, chemical treatment can be categorized as temporary or long-lasting, and it includes methods using oil-based, oil-soluble, water-soluble, immersion in water-soluble salt solutions, or replacing sap with water-soluble salts [7]. Nevertheless, it is crucial to consider the pollution associated with certain chemical methods, as many of the substances used can be highly toxic. Such environmental damage contradicts the ecological nature of using bamboo. Therefore, treatment methods should be carefully considered as an integral part of the project planning.

2.3.
Bamboo-reinforced concrete

The investigation into bamboo's application in concrete structures began in the second decade of the 20th century, led by Chow [54], who conducted tests on bamboo-reinforced beams and columns during his thesis at the Massachusetts Institute of Technology. In addition to Chow [54], several authors [4], [14], [15], [55], [56], [57], [58], [59], [60] have studied the behavior of bamboo-reinforced concrete structures, exploring aspects such as material adhesion, reinforcement anchorage, and the performance of columns and beams, among others.

Although there are no national guidelines[1] for the design of concrete structures reinforced with bamboo, one observes the use of bamboo splints as components for structural elements in housing, particularly in the northeastern region of Brazil, known as "*bambucreto*". Its utilization is directly linked to the abundant availability and accessibility of this resource, which thrives in tropical and subtropical climates. However, these constructions are often built without proper engineering design, highlighting the need for discussions on standards capable of encompassing the analysis of structures that combine more traditional systems, like reinforced concrete, with unconventional materials like bamboo.

Bamboo can be employed in reinforcing concrete, as whole culms (with the tapered geometry) or as splints achieved through the longitudinal splitting of culms. As discussed further, bamboo can be used for elements such as beams, columns, or even as reinforcement in slabs. Another approach for reinforcing concrete structures using

---

[1] It is important to highlight the establishment of the Brazilian standard ABNT NBR16828 Bamboo Structures (Part 1: Design and Part 2: Determination of Bamboo's Physical and Mechanical Properties) in 2020, serving as a guideline for the utilization of bamboo as a construction material in structural applications.

bamboo involves creating bars by impregnating natural bamboo fibers into polymer resins, as depicted in Figure 6 (a, b). This is an interesting alternative, both economically and environmentally, compared to the use of inorganic synthetic fibers (such as glass or carbon), which tend to be more expensive and environmentally impactful.

Javadian *et al.* [61] developed bars composed of bamboo fibers immersed in a polymer matrix, intended for reinforcement in concrete structures, and conducted both physical and mechanical tests on *Dendrocalamus asper* bamboo (central and basal portions). Concrete beams reinforced with two and four bamboo bars were assessed in a four-point bending test. Additionally, a material characterization was conducted to determine the tensile strength, modulus of elasticity in tension, and flexural strength (Modulus of Rupture - MOR) of bamboo. The outcomes underscore the potential of this material as an alternative to steel bars or GFRP (Glass Fiber Reinforced Polymer) for concrete structures, in terms of mechanical capacity and technical feasibility.

(a) (b)

Figure 6 - Bars created with bamboo fiber impregnated into polymer resin for reinforced concrete structures [61]: (a) Bamboo longitudinal and transverse reinforcement for concrete structures (b) Bamboo tensile sample made with bamboo fiber impregnated into polymer.

2.3.1 Concrete-Bamboo Interaction

In the context of employing bamboo in construction, essential aspects to consider encompass the moisture content, age, species, and node distribution. When incorporated into a cementitious matrix, bamboo undergoes volumetric variations due to change in the moisture content and, to a lesser extent, temperature variations [4], [14]. This critical aspect demands careful examination in projects that involve the combination of bamboo and concrete, as bamboo's expansion due to water absorption during curing may lead to cracks in concrete, while its contraction after curing creates a zone of low adhesion.

Strategies can be employed within the realm of bamboo utilization in construction, including the application of waterproofing agents onto the bamboo, the use of concrete with a rich mixture (lower w/c ratio) and rapid setting to prevent cracks, and the selection of mature culms [7], [55].

Prior to the application of preservatives on the culms, it is essential for the bamboo to undergo a drying process to ensure its moisture content does not exceed a limit (approximately 15%) that may adversely affect its physical and mechanical properties [4]. It is worth highlighting that this concern is not exclusive to natural materials; a similar vulnerability is observed in conventional reinforced concrete structures with steel bars. In a comparative analysis of the preservation status of steel and bamboo bars used in concrete structures, Ghavami [4] presented documentation of a steel-reinforced column within the Rio de Janeiro subway system that exhibited significant deterioration after 10 years of service (figures 7.a, 7.b). In contrast, bamboo bars used in a concrete beam on the PUC-Rio campus and exposed to weathering showed satisfactory condition even after 15 years of life.

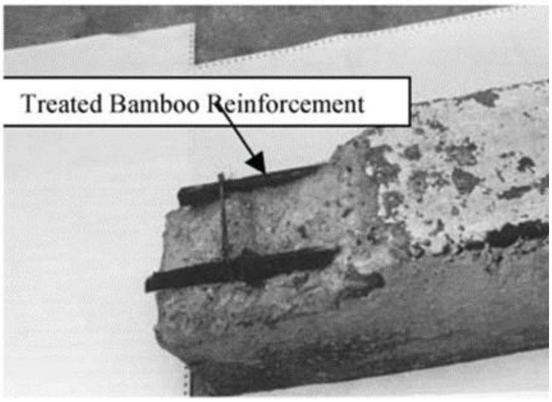

(a)

(b)

Figure 7 - Comparison between preservation condition of bamboo and steel rebars used for reinforced concrete structures.[4]: (a) Concrete beam reinforced with bamboo (b) Standard reinforced concrete column.

In terms of material adherence, owing to the smooth surface of bamboo, research studies [4], [7] suggest the sandblasting of bamboo culms or splints post-waterproofing to enhance surface roughness and thereby promote adhesion between bamboo and the matrix. The outer layer of bamboo is rich in cutin, a natural lubricant responsible for its smooth and shiny appearance, which causes greater slip within the concrete matrix. It is also recommended to utilize wires around the bamboo bars to modify the bamboo-concrete contact surface, thus enhancing the bond stress. Ghavami [4] conducted pull-out tests on bamboo segments with and without nodes, indicating that the bond strength of treated bamboo culms exhibited an average enhancement ranging from 50 to 90 percent over the untreated material for the Negrolin-sand and Negrolin-sand-wiring treatments, respectively. Notably, specimens with nodes showed over 50% higher bond strength compared to those without nodes. Azadeh and Kazemi [62] highlight significant benefits of corrugation in bamboo-concrete composites. Bamboo corrugation is proposed as a strategy to interlock bamboo and concrete, aiming to enhance cohesion, skin friction, and overall bond strength [62]. Corrugated bamboo strips also ensure an even distribution of load transfer, optimizing load-bearing capacity. According to the authors [62], these strips are practical for temporary structures, requiring no extra coatings or costs when integrated into mortar or concrete.

Furthermore, Al-Fasih *et al*. [63] correlated the structural performance of concrete beams reinforced with bamboo splints with the results from pull-out tests. As observed by the author, the responses to the three-point bending test were closely linked to the adhesive strength between concrete and bamboo determined through the pull-out test. The adhesive strength of Bambusa Vulgaris Vittata (BV) samples (0.667 MPa), which was nearly double that of Bambusa Heterostachya (BH) samples (0.345 MPa), led to a twofold increase in the load capacity of BV beams during bending compared to BH beams.

2.3.2. Concrete Structural Elements Reinforced with Bamboo

2.3.2.1 Beams

The utilization of bamboo bars in concrete structural elements is particularly enabled by bamboo's high ratio of tensile strength to specific weight. Bamboo exhibits satisfactory mechanical performance in constructions with low loadings and small spans (up to approximately 3.5 m); nonetheless, certain distinct characteristics of bamboo can influence its structural behavior. The presence of nodes in bamboo splints or culms leads to a reduction in the tensile modulus of elasticity and consequently creates regions prone to rupture without necessarily being areas of load concentration. In addition to potential rupture, nodes also contribute to the development of wide-opening cracks in beam cross-sections [11]. Muhtar [64] discusses the rupture in concrete beams reinforced with bamboo splints, attributing most crack patterns to bamboo slippage within the concrete matrix.

As previously mentioned, Al-Fasih *et al*. [63] conducted three-point bending tests on concrete beams (concrete compressive strength of 40 MPa) reinforced with bamboo splints, for different species: *Bambusa heterostachya* (BH), *Schizostachyum brachycladum* (SB), and *Bambusa vulgaris vittata* (BV). For the mechanical characterization, tensile tests were performed for bamboo samples according to ASTM D638, and also pull-out tests were carried out following ASTM C900 - ASTM Standard, 2013. For curved splints on one side, the authors achieved higher tensile strength results ranging from 100 MPa to 250 MPa. In the three-point bending tests, performed for concrete beams reinforced with *Bambusa vulgaris vittata* , specimens reached a load capacity of approximately 63% of that obtained for concrete beams reinforced with steel bars.

In a comparative study of bending behavior in concrete beams reinforced with bamboo (BB), steel (SB), and rattan (RB), Adewuyi *et al*. [65] conducted three-point bending tests on beams with the same reinforcement ratio and using steel stirrups. The strength of bamboo and rattan bars was found to be approximately 13% and 45% of that of steel, respectively, while tensile strength was 16% and 62% of steel's strength, respectively. The stiffness of bamboo and rattan-reinforced beams was 32% and 13.5% of that of steel-reinforced beams, with the flexural failure load being approximately 51% and 21% of SB. After the first crack, the authors recorded a residual flexural strength of 41% for BB and SB, and 25% for RB, with the first crack load being 55% for BB and 30% for RB compared to SB.

Adewuyi *et al*. [65] attribute the research findings not only to the inherent tensile strength of each material but also to the low adhesion at the concrete-bamboo and concrete-rattan interfaces. The authors observed that the failure mode for both SB and BB occurred due to shear, evidenced by diagonal cracks, while for RB, it was characterized by vertical cracks in flexure. Finally, it is emphasized that the use of bamboo bars to reinforce concrete beams should be reserved for lightweight structures with lower loads, necessitating treatments to enhance adhesion zones and consequently, load-bearing capacity.

Sutharsana [66] performed compression and tensile tests on bamboo sticks to characterize their mechanical properties, and then conducted bending tests on concrete beams reinforced with epoxy-coated bamboo splints. The results demonstrated a 77.7% increase in flexural strength of the bamboo-reinforced concrete compared to unreinforced concrete. Therefore, from the bending tests, it was concluded that the use of bamboo can enhance the load-carrying capacity of beams for the same dimensions. Nonetheless, the stress-strain graphs indicate that bamboo's modulus of elasticity is significantly lower than that of steel, emphasizing the need for prudent substitution.

It is noteworthy to compare these findings with the perspective put forth by Harries *et al.* [13] on the poor structural performance of bamboo-reinforced concrete elements in bending. The authors' key points are related to bamboo's lower modulus of elasticity and tensile strength compared to steel, along with its brittle behavior in tension, which renders it unsuitable as a direct replacement for traditional systems. They further highlight the need for treatments to enhance adhesion and structural element durability. According to Harries *et al.* [13], a concrete structure reinforced with bamboo must be designed to work without cracks, leading to a significant increase in element cross-section dimensions and a higher volume of concrete.

The arguments presented by Harries *et al.* [13] are supported in their research through experimental work comparing four types of beams in a three-point bending test: U beams (concrete only), S beams (concrete reinforced with steel bars and reinforcing ratio $\rho_g = 0.0047$), Bf beams (concrete reinforced with bamboo *Phyllostachys aurea*, equivalent strength, and reinforcing ratio $\rho_g = 0.0208$), and BE beams (concrete reinforced with bamboo *Phyllostachys aurea*, equivalent stiffness, and reinforcing ratio $\rho_g = 0.0543$). While the authors extend their arguments to both culms and splints, the tests were performed using only the culms as reinforcement in Bf and BE beams. The results indicated that bamboo-reinforced beams have higher structural capacity compared to unreinforced concrete beams. However, when compared to beams reinforced with steel bars, the performance, in terms of energy absorption, is about 8.17 times lower for Bf and 3.34 times lower for BE.

The failure modes of Bf and BE were characterized by brittle longitudinal splitting and loss of continuity of section, respectively [13]. This study underscores the need to explore methods to enhance the bonding between concrete and bamboo, as it directly influences the mechanical performance of structural elements. However, other factors, such as bamboo's lower modulus of elasticity compared to steel, do not invalidate its application in smaller-scale structures. Such applications contribute to advancing sustainable construction practices and enhancing concrete structural performance. Especially in areas lacking easy access to steel, this can be achieved by harnessing local resources such as bamboo.

In terms of studies addressing the shear strength of concrete beams reinforced with bamboo culms, the literature is limited, underscoring the significance of the current investigation. Silva [21] presents findings on the replacement of steel in concrete structures through the incorporation of bamboo stirrups. In addition to bamboo splints as longitudinal reinforcement, the author employed *Bambusa Vulgaris* for the development of stirrups in concrete beams. By cutting, selecting the outer layer, which contains a substantial amount of fibers, and bending the bamboo into a pre-defined geometric shape, pieces for bamboo stirrups were fabricated. While the analysis primarily centered on establishing a correlation between theoretical design and experimental results, the study did not explore the examination of crack kinematics.

Mark and Russel [20] conducted research on the utilization of various types of shear reinforcement, such as bamboo and cane stirrups, for concrete beams reinforced with bamboo in rural construction contexts. All the beams were subjected to four-point bend tests and were designed to fail in flexural tension while also resisting shear failure. However, during the study, failure mode due to flexural shear was observed in five out of the sixteen beams, including those reinforced with bamboo stirrups, cane stirrups, and steel stirrups. Moreover, occurrences of diagonal tension coupled with flexural shear, or diagonal tension along with shear bond, and also concrete crushing combined with flexural shear were noted. The authors concluded that shear capacity is heightened by an increased amount of tension reinforcement and the incorporation of web reinforcement. The concrete's strength significantly impacts both shear capacity and the concrete's failure mode, as lower strength concrete tends to experience concrete crushing before reaching full shear capacity [20].

2.3.2.2 Columns

The mechanical performance of concrete columns reinforced with bamboo has been investigated by researchers including Ghavami [4], Agarwal *et al*. [15], Sutharsana [66], Salau *et al*. [67], Kaware *et al*. [68], Min Lei *et al*. [69], among others. These studies have demonstrated the potential of bamboo as a substitute for steel in affordable housing projects, particularly in regions where concrete is widely used but steel bars are less available. Table 2 below provides a summary of the results obtained by some of the aforementioned authors.

Table 2– Compression strength for concrete columns reinforced with bamboo splints and steel rebars

Author	Bamboo		Steel	
	Reinforcement Ratio	Compression Strength (kN)	Reinforcement Ratio	Compression Strength (kN)
Salau	1.42%	332	1.42%	428
Min Lei	2.56%	366.67	0.72%	493.33
Kaware	3%	366	1.6%	370
Agarwal	3%	315	0.89%	444

Experiments performed by Ghavami [4] present contrasting results for concrete columns with circular cross-sections reinforced with bamboo splints of the *Dendrocalamus giganteus* species and concrete samples reinforced with steel bars for equivalent rectangular sections. The tests were conducted in accordance with Brazilian standards and indicate that 3% of bamboo reinforcement treated with Sikadur 32-Gel would provide performance comparable to conventional steel reinforcement in concrete structures. However, it should be noted that the use of inputs such as the aforementioned resin adds to the cost of reinforcement fabrication, a factor that demands careful consideration.

Kaware *et al*. [68] conducted a comparative analysis in their study on concrete columns with square, rectangular, and circular sections reinforced with *Dendrocalamus strictus* bamboo splints and steel bars. The load-displacement and stress-strain curves of the bamboo-reinforced column exhibited a pattern similar to the columns reinforced with steel. However, to achieve satisfactory performance, the lateral dimensions of the bamboo-reinforced columns were increased compared to the steel-reinforced ones. Additionally, the author suggests a minimum width of 2 to 2.5 cm for the splints and alternate positioning of basal and distal ends to achieve uniform reinforcement distribution along the length of the structural element.

Salau *et al.* [67] investigated the load-carrying capacity, deflection, and failure modes of concrete columns reinforced with bamboo splints and steel bars through compression tests. The use of splints was found to enhance the load-carrying capacity of the columns compared to unreinforced concrete, along with improving post-cracking behavior. However, this enhancement is not as pronounced as observed with steel reinforcement. According to Salau *et al.* [67], the increase in the volumetric ratio of bamboo reinforcement for concrete sections does not necessarily correspond to an increase in strength; it primarily contributes to enhancing the ductility of the section. Additionally, across all the examined research, the failure mode of the columns was consistently documented as concrete rupture.

2.3.2.3
Slabs

An interesting approach to utilizing bamboo can be achieved through the idealization of structures that serve both as formwork and reinforcement for concrete slabs. Ghavami [4] investigated the use of bamboo for this purpose and observed the influence of the shear strength of the bamboo diaphragm on the ultimate load capacity of the slabs. Despite the diaphragms establishing a positive interaction between bamboo and concrete, their shear strength is not sufficient to prevent failure. Through experiments, it was observed that most slabs initially failed due to debonding and rupture of the diaphragm, followed by failure in the concrete compression zone. However, by using connectors, the author recorded a nearly 200% increase in shear strength, resulting in an enhanced load-carrying capacity.

Ismail *et al.* [70] studied the behavior of bamboo-reinforced concrete slabs by conducting four-point bending tests to establish the load-deflection relationship. The experimental work determined the failure mode, load-carrying capacity, and deflection in the structure. The failure load was 33.77 kN for 2% reinforcement and 40.96 kN for 3.2%, indicating an improvement in flexural response as the reinforcing ratio increased. In both slabs, it was observed that cracks initiated at a certain distance from the supports in the tensile zone, gradually enlarging until reaching the failure, at which point the cracks propagated into the compression zone.

Concrete panels reinforced with a novel type of bamboo bar (rectangular splints with semicircular grooves) were experimentally investigated by Mali and Datta [17], who reported a slight enhancement in the structural behavior of flexural slabs compared to the conventional model with carbon steel bars. Although there is literature discussing the deficient performance of bamboo reinforcements for flexural applications [12], [13], this technique can be regarded as an advantageous solution in terms of both economic and environmental aspects for low-cost constructions involving elements with low load demand, such as roofing panels.

2.3.3 Structural Design

Despite the existence of standards for the design of bamboo structures at both national and international levels, there is still a lack of direct guidance for calculating concrete structures reinforced with bamboo. Given this gap in the literature, the use of ACI CODE-440.11-22 - *Building Code Requirements for Structural Concrete Reinforced with Glass Fiber-Reinforced Polymer (GFRP) Bars* [71] - is herein suggested as a reference for designing concrete elements reinforced with bamboo. The assumptions presented in *ACI 440.11-22* [71] align with the expected characteristics and behavior of a concrete structure reinforced with bamboo.

Regarding the assumptions made in flexural design, it is assumed that the sections remain plane (Euler-Bernoulli Theory), the maximum strain in concrete is 0.003, the tensile strength of concrete is neglected, the behavior of reinforcement is linear elastic until failure, and there is a perfect bond between concrete and the bar. For shear, it is assumed that the transverse reinforcement has a low modulus of elasticity, low shear strength, high tensile strength, and no yield point. Furthermore, the tensile strength in the bent portions of the transverse reinforcement is considered significantly lower than in the straight portions of the bars, and for calculation purposes, it is assumed to be 45% of the latter.

Some studies employ the guidelines NBR6118 (Design of Concrete Structures - Procedure) and ACI 318 (Building Code Requirements for Structural Concrete) for designing concrete structures reinforced with bamboo, as both use the Euler-Bernoulli theory for flexure [8], [21], [72]. Based on NBR6118, Tokuda [8] adapted a calculation method for designing concrete structures with bamboo reinforcement and rectangular sections subject to four-point bending. The author developed spreadsheets to obtain the equivalent bamboo area for a given steel reinforcing ratio. Silva [21] proposed a design approach for concrete beams reinforced with bamboo, focusing on allowable deflection. This recommendation stemmed from the concern that designing solely based on allowable load could result in excessive deformations due to bamboo's comparatively low Young's Modulus.

The reinforcing ratios used for concrete beams with bamboo vary between 1.25% and 8.33%, with the ideal percentage being approximately 3% for longitudinal bamboo reinforcement [3], [4], [10], [21], [72]. Janssen [26] indicates that, beyond 4%, the reinforcement percentage starts to pose practical difficulties due to the need for wider cross-sectional dimensions. As a solution, inverted T-sections can be used, yet this alternative highlights the practical challenges associated with utilizing bamboo as reinforcement in concrete [26]. Silva [21] attributes a significant portion of the design problems to the existence of various unknown variables, most of which are related to stress distribution in the material. This leads to the use of an allowable stress lower than the necessary stress to induce material failure [21].

Overall, a wide use of concrete guidelines (NBR6118, ACI 318-14) has been observed in the design of concrete reinforced with bamboo [8], [21], [72], [73]. Furthermore, a hybrid methodology, proposed by Geymayer and Cox [14], suggests designing beams neglecting bamboo reinforcement, treating the structural elements as plain concrete without any form of reinforcement. In this case, the maximum tensile strength of concrete corresponding to $8\sqrt{f'_c}$ (psi) is assumed. This approach also proposes using a 3-4% rate of splints as reinforcement to ensure a safety factor of 2 to 2.5. According to the authors, the calculation of ultimate stress should be adapted to failure occurring due to detachment between bamboo and concrete, rather than yielding of the reinforcement.

Several studies identified within the literature review suggest the use of ACI 440.1R-15 / ACI CODE-440.11-22 as a calculation method for concrete structures reinforced with bamboo [61], [74], [75]. Due to the structural similarities between bamboo and FRP bars (both of which exhibit a brittle behavior), this particular standard will be adopted for beam design within the scope of this study. Drawing a correlation between GFRP and bamboo, Archila *et al.* [12] highlight that both materials share characteristics of anisotropy, brittle behavior, and low shear strength. Since ACI CODE-440.11-22 does not allow the use of GFRP bars to contribute to compression strength, the same should be taken into account for utilizing bamboo. Additionally, in practical terms, during concrete casting, these materials tend to float, making the use of ties advisable to keep the bars in place.

2.4. Shear in Reinforced Concrete Structures

The lack of proper redistribution of internal forces during shear failure and its brittle nature highlight the importance of accurate design with respect to this mode of rupture for the safety of reinforced concrete structures. The approach used in design codes for reinforced concrete members subjected to shear forces is traditionally based on the analogy to the truss model developed by Ritter [76] and Morsch [77]. This theory associates the behavior of a diagonally cracked simply supported beam (stage II) with that of a truss with parallel and statically determinate chords, where both the reinforcement and concrete work together to resist shear forces [78]. The concrete in the upper part of the beam assumes the role of the compressed chord, the longitudinal steel reinforcement corresponds to the tension chord, the inclined struts are formed by the concrete compressed between the cracks (compressed diagonals), and the stirrups, with an inclination that can vary from 45° to 90°, function as tie (upright or tension diagonals).

Discussions persist regarding the various models for shear design of reinforced concrete structures, as addressed in Section 2.3.3. For renowned models such as Morsch truss, ongoing debates exist regarding the assumptions adopted, such as the inclination of the struts for truss modeling, given that tests demonstrate a different strut inclination from the traditional 45°. Additionally, conditions assumed, such as parallel flanges and an statically determinate truss, are simplifications since there is an arching effect in the upper concrete flange and the truss is statically indeterminate (with a connection in the compression struts).

Despite providing satisfactory results for Ultimate Limit State design, the Morsch truss analogy has limitations for more sophisticated analyses [79]. Researchers have explored a range of factors influencing shear strength of structural elements, leading to the development of models tailored for beams subjected to simple bending, flexural-compression, and flexural-tension [80]. In the case of flexural-tension, the commonly used truss model becomes inadequate, as it does not directly account for the interaction between various shear resistance mechanisms. Hirata [80] further highlights the size effect, where larger-size elements (e.g. hydroelectric plants, viaducts, etc.) exhibit a significant reduction in the shear strength stress. However, since the experiments conducted in the present study involve a three-point bending problem without axial load application, theories predicting shear strength for beams in simple bending will be discussed.

Podgorniak-Stanik [81] assessed the influence of concrete strength, distribution of longitudinal reinforcement, number of stirrups, and structural element size on the shear capacity of reinforced concrete. The author developed the Beta Method through an adaptation of the Modified Compression Field Theory (MCFT) for estimating shear strength in reinforced concrete elements. Other researchers have also explored MCFT, using it as a basis to develop simplifying theories, as presented by Bentz *et al.* [82]. Villela [79] applied MCFT to reinforced and prestressed concrete sections, computing the contribution of concrete to tensile strength and the effect of the biaxial stress field acting on concrete struts.

For concrete beams reinforced with material with stiffness lower than that of steel, as seen with bamboo reinforcement, a reduced depth of the neutral axis is observed after cracking. As emphasized by ACI CODE-440.11-22, the cracks are wider, and the compressed region in the cross-section is smaller, resulting in lower contributions from aggregate interlocking and compressed concrete compared to conventionally steel-reinforced beams. The following section addresses the main mechanisms contributing to shear strength in reinforced concrete beams.

2.4.1 Shear Strength Mechanisms

As will be further explained in section 5.1, different resistance mechanisms are developed in concrete structures subjected to shear stress. The main contributors for the shear resistance are: dowel effect, aggregate interlock, residual tensile strength of concrete, inclined compression chord or arch action, and for beams with shear reinforcement there is also a contribution from the stirrups. Several authors studied the shear behavior of slender beams developing methods of calculus to predict the mechanism acting in reinforced concrete elements. Cavagnis [83] approached the shear resistance mechanisms for reinforced concrete members without transverse reinforcement. Resende [84] investigated the shear mechanism for beams with and without steel fibers. Gomes [85] conducted the analysis for reinforced beams with FRP stirrups and basalt fibers.

Table 3 illustrates the primary studies and models used as a basis to calculate each strength mechanism.

Table 3– Reference adopted for each shear strength mechanism.

Mechanism	References
Aggregate Interlock	**Empirical Models**: Walraven and Reinahrdt [86]
	Micro-mechanics: Walraven [87]; Ulaga [88]; Guidotti [89]
	Semi-empirichal: Li and Maekawa [90]; Resende *et al.* [91]
Residual Strength	**Mechanical Model**: Hillerborg et al. [92]
Dowel Effect	**Empirical Models**: Vintzeleou and Tassios [93]; Fernández Ruiz *et al.* [94]
	Mechanical Models: Cavagnis *et al* [95]; Resende [84]; Vintzeleou and Tassios [93]; López *et al.* [96]
Compression chord / Arch action	**Mechanical Models**: Kani [97]; López *et al.* [96]; Cavagnis *et al.* [98]; Cavagnis [83]
Stirrup	**Mechanical Models:** Huber *et al.* [99] ; Campana *et al.* [100]; López *et al.* [96]

The shear transfer mechanism may be developed by beam or arch action. Some of the factors related to the prevailed mechanism consists in the shear span to effective depth ratio (a/d). For a ratio a/d < 2.5, the beam is designed as deep beam and the arch action becomes dominant. The arch action can be considered as a secondary physical phenomenon and it contributes to load transferring straight to the supports. For slender beams the ratio a/d is generally greater than 2.5 and the arching action can be disregarded. In such cases Shahnewaz [101] states that the shear deformation could be negligible while it must be taking into account for analysis and design of a deep beam. Moreover, Cavagnis [83] points out that, when the critical shear crack develops below the theoretical compression strut, the arching action starts governing.

Factors related to the flexural design and the capacity of shear transfer at the diagonal crack such as the neutral axis depth, the presence of a compression zone and the longitudinal tensile reinforcement ratio affects strongly the shear strength capacity of the structural element [84]. In beams where shear force is the primary cause of failure, the shear resistance mechanisms are directly integrated. For instance, lower longitudinal reinforcement ratio causes the cracks to exhibit greater depth and opening size, which reduces the strength by dowel effect and aggregate interlock as well [102].

A relevant aspect for the shear strength of bamboo-reinforced concrete beams is the bonding of the longitudinal reinforcement, which can cause the bars to slip along the matrix and prevent diagonal failure to happen. According to Kani [97], for poor bond, fewer cracks are generated and the crack spacing is larger. However, the poor bond was surprisingly associated to an increase in the diagonal load-carrying capacity. Another important issue for this research consists of the use of self-compacting concrete that causes the shear strength of the beam to be lower than for a similar beam with vibrated concrete due to the lower content and/or smaller maximum size of coarse aggregate that this type of concrete typically has [103].

By using digital image correlation (DIC), one may use the crack geometry and kinematics to elaborate mechanical models capable of describing and represent the shear-transfer mechanisms that acts on the structural element. The shear transfer mechanisms acting in a cantilever subjected to point load are illustrated in figure 8. V_{agg} corresponds to the aggregate interlock and it is developed by the contact in rough cracks, generating normal and tangential stresses which allows for the shear forces transferring. By integrating the stresses along the crack in the vertical direction one derives the shear force V_{agg}.

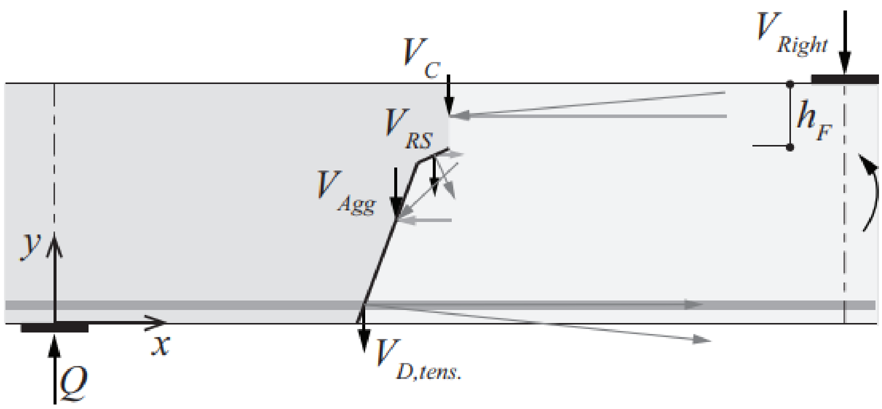

Figure 8 - Shear mechanisms acting in a concrete beam. [83]

The residual tensile strength of concrete, indicated by V_{RS}, is described by Cavagnis [83] as the capacity to transfer tensile stresses through the fracture process zone of the crack. The crack inclination creates a component in the vertical direction for the normal stresses which represent the V_{RS}. Hillerborg [92] informs that the crack is propagated as the stresses at the tip of the crack reaches the tensile strength, but when this occurs the stress does not fall to zero immediately; instead, it decreases as the crack width increases. Regarding the dowelling action (V_D), it is linked to the capacity of longitudinal reinforcement to transfer shear forces across the crack when the flexural reinforcement undergoes a transversal displacement. Dowel action is activated in cases when a critical crack intercepts the compression reinforcement as well ($V_{D,compr}$), but this contribution was not considered in the present work.

Finally, the inclined compression chord (V_C) corresponds to the capacity of shear transfer in the compression zone of the uncracked concrete above the tip of the critical crack. It is possible to calculate V_c from the shear transfer distribution along the cross-section. For instance, Morsch [77] considered the cross-section in stage II, the concrete with linear-elastic behavior and negligible tensile strength. From this assumption and given the shear stress with parabolic distribution above the neutral axis and with a constant distribution bellow the neutral axis, Morsch [77] derived V_C.

Cavagnis [83] obtained V_C from the vertical section between the tip of the crack and the extreme compression fiber of the concrete beam. Kani [97] described the mechanism of diagonal failure for reinforced concrete structures. According to the author, cracks start to develop well before reaching the allowable load and as the load is progressively increased, the cracks expand in both width and length, signaling a reduction in the area of the compressive zone. The concrete elements between two consecutive cracks can be considered as a short vertical cantilever anchored in the compression zone subjected to a horizontal force ΔT originated from bending (figure 9). This model is applicable for reinforced concrete beams with bond and the highest compressive strain is developed at the top fiber.

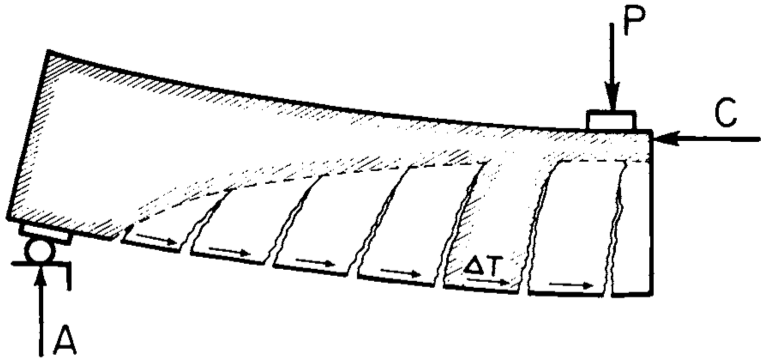

Figure 9 - Short vertical cantilever anchored in the compression zone. [97]

Furthermore, for cases where the beam is reinforced with stirrups, there is an additional shear strength mechanism. When the stirrup intersects the first and second crack branches, the tensile stresses is activated providing shear strength V_s [104]. Therefore, beams with sufficient amount of stirrups can bear further load even after the shear cracking, since the tensile stresses acting on the diagonal crack are redistributed to the shear reinforcement [99]. Two main factors can influence the stress developed in the shear reinforcement: the bond between the stirrup and the matrix, and the inclination of the diagonal crack. The angle of the crack indicates the number of stirrups crossing the crack; thus more stirrups are activated for smaller angles.

3. MATERIALS AND METHODS

3.1. Overview of experimental program and preliminary design

Three different techniques for the shear reinforcement were tested for the beams reinforced with untreated bamboo and then were compared to the performance of a beam with no shear reinforcement (beam 06) and a beam with steel stirrups (beam 05). The beam 02 was produced using discrete sisal fibers, beam 03 with bamboo stirrups (figure 2) and beam 04 with sisal yarn around the longitudinal reinforcement cage. As will be discussed in following sections, it was necessary to apply a coating in the bamboo for an effective beam action behavior. The treatment with castor oil and sand was applied for the beams with no shear reinforcement (beam 07) and with sisal yarn (beam 08). Also, a conventional beam with steel longitudinal and transverse reinforcement was casted (beam 01). Table 3 summarizes the experimental program, indicating the type of reinforcement and the respective name of the beam.

Table 3 - Types of studied beam with their respective longitudinal and shear reinforcement.

Beam	Longitudinal Reinforcement	Shear Reinforcement
01	Steel rebar	Steel stirrup
02	Uncoated bamboo	Discrete sisal fiber
03	Uncoated bamboo	Bamboo stirrup
04	Uncoated bamboo	Sisal yarn
05	Uncoated bamboo	Steel stirrup
06	Uncoated bamboo	No shear reinforcement
07	Coated bamboo (castor oil + sand)	No shear reinforcement
08	Coated bamboo (castor oil + sand)	Sisal yarn

As mentioned in Section 2.3.3, the design of the beams was performed with reference to ACI CODE-440.11-22 - *Building Code Requirements for Structural Concrete Reinforced with Glass Fiber-Reinforced Polymer (GFRP) Bars* [71]. The initial step involved calculating the flexural strength of the structure. With the flexural strength established, a rate of 70% of this value was adopted for shear strength, and the beams were designed to achieve this resistance. As recommended by Archila *et al*. [12], the spacing of the bamboo bars center-to-center should be at least three times the diameter of the culm to ensure proper concrete penetration between the voids. Hence, a minimum vertical spacing center-to-center of 4 cm was adopted.

The shear strength for beam 02 was estimated following the guidelines set by RILEM TC 162-TDF [105], using the experimental results obtained by Castoldi [106] as a basis. The shear strength is divided into the contribution portion from concrete (V_c) and the contribution from fibers (V_f), calculated using expressions 1 and 2, derived from RILEM TC 162-TDF. Furthermore, a comparison of the total shear strength was conducted by combining the previously computed V_c portion in accordance with ACI440 and the V_f component derived from RILEM.

$$V_f = 0.7k_f.k_1.\tau_f.b_w.d \tag{1}$$

$$V_c = [0.12k\left(100\rho_l f_{fck}\right)^{1/3} + 0.15\sigma_{cp}]b_w d \tag{2}$$

Where:

k_f = factor for taking into account the contribution of the flanges in a T-section; taken as 1 for rectangular sections

$k_1 = \frac{1600-d}{1000}$ (d in mm)

b_w = width of the web (mm)

$k = 1 + \sqrt{\frac{200}{d}}$ (d in mm)

$\rho_l = \frac{A_s}{b_w d} = 3.20$

$\sigma_{cp} = \frac{N_{Sd}}{A_c}$ (N/mm²), taken as 0 for reinforced concrete

$\tau_f = 0.18.f_{Rk,4}$, where $f_{Rk,4}$ is the nominal residual strength for Ultimate Limit State (ULS), considering CMOD = 3.5 mm, and it was obtained from Castoldi [106] - $f_{Rk,4}$ = 0.42 MPa.

The experimental load versus the expected load for beam 02 can be found in Table 4, and the calculation procedures are detailed in Appendix B.

Table 4 – Expected versus experimental load for beam 02.

BEAM 02			
$P_{expected}$ shear:		$P_{experimental}$	Failure Mode
ACI440.1R-15, RILEM TC 162-TDF	24.9	52.96	SHEAR
RILEM TC 162-TDF	59.6		

3.2. Material Characterization

3.2.1
Concrete

3.2.2.2
Concrete Ratio Mix

The preparation of the beams was carried out using self-compacting concrete to facilitate casting, especially given the reduced spacing between the bamboo stirrups and sisal yarn as well, which would make the use of a vibrator challenging. The concrete mix ratio is presented in Table 5 and was designed for a 28-day compressive strength of 30 MPa (f_{ck}). For each batch, a concrete volume corresponding to one beam and three cylinders for axial compression testing was calculated, accounting for a 10% material loss. The volume of each beam is 48.75 L, and each cylinder is 1.57 L, thus the mixture was prepared using a 400 L capacity concrete mixer. The cement used was CPIII RS, which has a higher slag content (70%) and is, therefore, more environmentally-friendly compared to other commercially available types of cement. The other components included crushed stone size 0, natural sand, reactive silica, and additives (superplasticizer and multifunctional). Superplasticizer ADVA 753 and multifunctional Miraset 818 were both provided by GCP Applied Technologies.

Table 5 - Concrete Mix

Material	1m³ of concrete
Cement	577
Silica	66.3
Sand	668
Aggregate	590
Water	300
Superplasticizer additive SP	2.47
Polyfunctional additive PL	2.47

3.2.2.3
Compressive Strength of Concrete

In order to obtain the strength of the concrete it was cast for each beam three cylinders, each one with 10 cm of diameter and 20 cm of height. After a 28-day curing process in the humid chamber, the cylinders were tested in the Controls machine (model MCC8) with a load capacity of 2000 kN, at a rate of 0.45 MPa/s. The axial compression tests resulted in strengths ranging from 29 MPa to 40 MPa, with a mean strength of 34.29 MPa. The results from the compression test are shown in Table 6.

Table 6 - Mechanical characterization of concrete in the compression test.

COMPRESSION STRENGTH (MPa)								
	BEAM 01	BEAM 02	BEAM 03	BEAM 04	BEAM 05	BEAM 06	BEAM 07	BEAM 08
CP1	-	27.3	34.6	31.9	33.0	30.9	39.4	39.9
CP2	-	30.5	34.09	34.1	37.06	37.2	32.1	37.9
CP3	-	29.5	34.4	33.03	35.8	28.6	40.9	37.2
MEAN		29.1	34.4	33.03	35.3	32.2	37.5	38.3

3.2.2 Bamboo

3.2.2.1
Physical characterization of bamboo

To utilize the entire culm as reinforcement for concrete beams, the bamboo species *Phyllostachys aurea* was carefully chosen due to its smaller diameter and high strength. Originating from China and primarily employed in the furniture industry, *Phyllostachys aurea* presents an interesting aspect regarding its workability when bending into splints which facilitates the stirrup creation process. The specie belongs to the monopodial bamboo group with creeping rhizomes that spread further in warm-temperate and well-watered regions. Its culms feature between 2 and 10 (12) meters in height and between 2 and 5 (7) centimeters in diameter [107]. The genera *Phyllostachys* shows a wide industrial application and high value-added production, standing out from bamboo panels for construction and house decoration to fiber extraction for paper-making, agrotechnical shoot production, among other uses [108].

In order to improve the material's durability, the batch of bamboo was prior to the purchase subjected to heat treatment in a chamber through direct flame. The physical properties of bamboo were determined according to the Brazilian guideline NBR16828 – Bamboo Structures - Part 2: Determination of physical and mechanical properties of bamboo [109], which was written in accordance with the international guideline ISO22157-1 Bamboo – determination of physical and mechanical properties – part 1: requirements (ISO, 2004b). The bamboo characterization was performed for the bottom, middle, and top parts of the culms, as recommended by the guideline. Six bamboo samples from the internode were selected for each region of the culm. Table 7 presents the values for moisture content and specific weight.

NBR16828-2 [109] establishes that the samples used for the moisture content tests must be prismatic 25 mm large and 25 mm long with a width equal to the culm. However, cylinder samples were adopted as suggested for the compression test. The height of the cylindrical specimen was determined according to the bamboo's diameters: for an outer diameter equal to or smaller than 20 mm, the height would be twice the outer diameter; for larger diameters, the height of the sample should match the outer diameter. To standardize the tests, a height-to-diameter ratio of 2:1 was adopted for all specimens.

The moisture content test concluded after reaching mass constancy, which occurred 72 hours after the initial measurements. A precision scale with an accuracy of 0.01 g and a hot air chamber maintained at a temperature of (103±2)°C were used. Measurements were taken at intervals greater than 2 hours, 24 hours after the test began. Mass constancy was determined when the difference between two successive measurements was equal to or less than 0.01 g.

According to NBR16828-2 [109], the specific weight can be determined by weighing (mass) and measuring the dimensions of the test specimen (volume). The standard allows for other methods to obtain volume, such as immersion of the specimen. Mass was determined using a scale with a precision of 0.01 g, and volume measurements were taken using a digital caliper with a precision of 0.01 mm. Due to the irregular geometry of the bamboo, three measurements were taken for the outer diameter and three for the inner diameter. The average of the diameters was then calculated, and with the height measurement, the volume of each sample was calculated.

Table 7 - Physical properties of bamboo.

PHYSICAL CHARACTERIZATION			
PROPERTY	BOTTOM	MIDDLE	TOP
Moisture content (%)	13.7	13.3	12.6
Specific weight (kg/m³)	823	850	913

As observed in Table 7, the moisture content values decrease for sections closer to the top part of the bamboo. This behavior can influence the material's mechanical characteristics, as a lower moisture content leads to a reduction in culm volume, thereby enhancing its mechanical properties. Several authors discuss the variation and influence of bamboo's moisture content, indicating that it is higher in the internode region and the inner part of the culms [5], [7]. Moreover, studies suggest that a moisture content range of 10 to 15% is ideal for bamboo's use in construction [110], [7]. Overall, from Table 7, an increase in the specific weight and a decrease in the moisture content can be observed along the height of the bamboo.

3.2.2.2 Mechanical characterization of bamboo

In order to evaluate the mechanical properties of the bamboo, the procedures to obtain the compression strength were adjusted based on NBR16828 [109]. As previously mentioned, the Brazilian code specifies the dimensions of the samples, hence it was adopted the ratio of 2:1 (height: diameter) for all the compression samples. The samples were instrumented with strain-gauges along the fiber direction (longitudinal to the culm). The maximum compressive stress supported by the bamboo samples was calculated using expression 1.1, where F_{max} is the maximum load supported by the sample and A is the cross-sectional area. Figure 10 (a, b, c) shows the result of the compression test.

$$\sigma_{max} = \frac{F_{max}}{A} \tag{1.1}$$

(a)

(b)

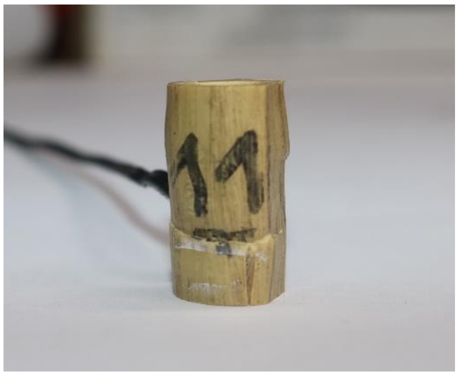

(c)

Figure 10 Compression samples from top, middle and bottom regions of the culm: (a) compression samples prior to been tested (b) compression sample instrumented with strain-gauge (c) compression sample after been tested.

The machine used to perform the compression test was EMiC Series 23 with a 30kN loading cell. NBR16828 [109] establishes the use of a device such as Teflon to even out the surface of the samples. The procedure to obtain the samples consisted in measuring and marking the required size followed by the application of tape onto the cut section to protect the bamboo fibers during the cutting step.

Additionally, a new technique was developed for testing the tensile strength, which involved using the entire culm of bamboo with its hollow and tapered geometry. To prevent premature failure in tension tests, a technique similar to the one used by Sabbir *et al*. [9] was employed. This involved spirally wringing the bamboo ends with galvanized iron to ensure a secure grip and prevent slippage. While Sabbir *et al*. [9] conducted the tests using splints, this research utilized the culm which is hollow, necessitating a strategy to avoid local failure at grips. To do so, the inner part of the bamboo was filled with

Sikadur. The procedures to prepare the samples for the tensile test can be seen in Figure 11.

(a)

(b)

Figure 11 - Sample preparation for tensile test.

The test was run in the MTS 311 machine at a displacement speed of 0.01mm/s, the tensile strength was obtained from the hydraulic actuator, and the sample strain and displacement were measured by the use of strain-gauges and displacement transducers (LVDT), respectively. Figure 12 shows the tensile test set-up and a typical failure mode for bamboo samples.

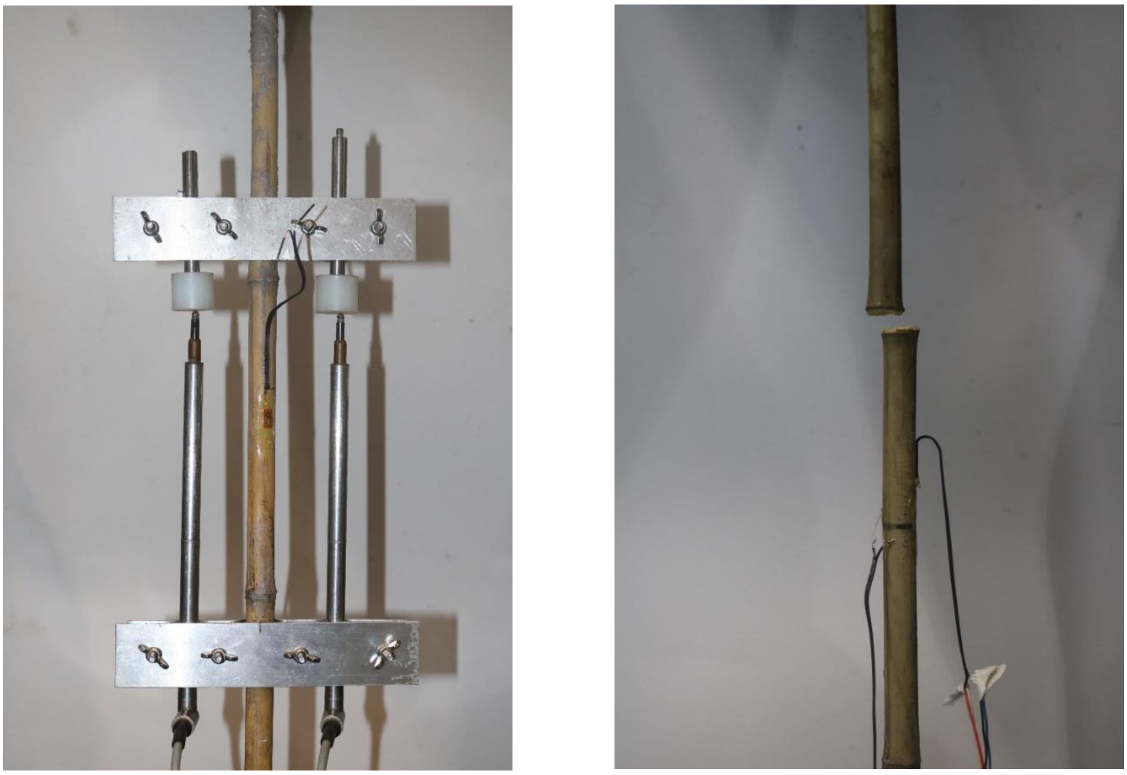

(a) (b)

Figure 12 - Tensile test set with displacement transducers: (a) Tensile test set-up. (b) Failure mode of the bamboo sample in the tensile test.

By using this technique only 3 out of 8 specimens worked out. Typical results were grip crush, node failure in the part reinforced with Sikadur, or node failure in the internode of the sample (Figure 13). Previously to defining the method, different procedures for the tensile testing of the bamboo samples were implemented, resulting in unsuccessful outcomes or unfeasible procedures. Some of the techniques experimented included the use of a steel pipe around the bamboo endings filled with Sikadur, for this case a sliding of the pipe over the course of the test was reported (Figure 14). Also, techniques using steel rebars inside bamboo endings filled with resin, and wrapped with fiberglass or sisal fibers were investigated.

(a) (b)

Figure 13 - Failure modes for the technique employed: (a) node failure (b) node failure in the grip part of the sample reinforced with Sikadur

(a) (b)

Figure 14 - Techniques tried for tensile test: (a) slippage of the pipe in the grip (b) steel pipe for protecting bamboo sample to be smashed by the grip of the machine.

As indicated by Table 8, for the mechanical properties, both the compression and the tensile strengths were higher for the middle part. For the tensile tests, the failure occurred as expected at the nodes of the bamboo, confirming the well-known weakness of this region. To ensure a safe design for the beams, the strength of the bamboo to be used must account for the nodes since the culm length used as reinforcement includes their presence. Overall, bamboo presents a Young's Modulus about 10 times smaller than steel, which is confirmed by the data obtained in the tensile tests ($E_{bamboo} \cong 10.05$ GPa). The following graphs (Figure 15 – a, b) show the curves stress (MPa) *versus* displacement (mm) for compression and tensile tests.

Table 8 - Mechanical properties of bamboo.

MECHANICAL CHARACTERIZATION			
PROPERTY	BOTTOM	MIDDLE	TOP
Tensile strength (MPa)	156.5	164.3	148.6
Compression strength (MPa)	73.2	66.4	69.9

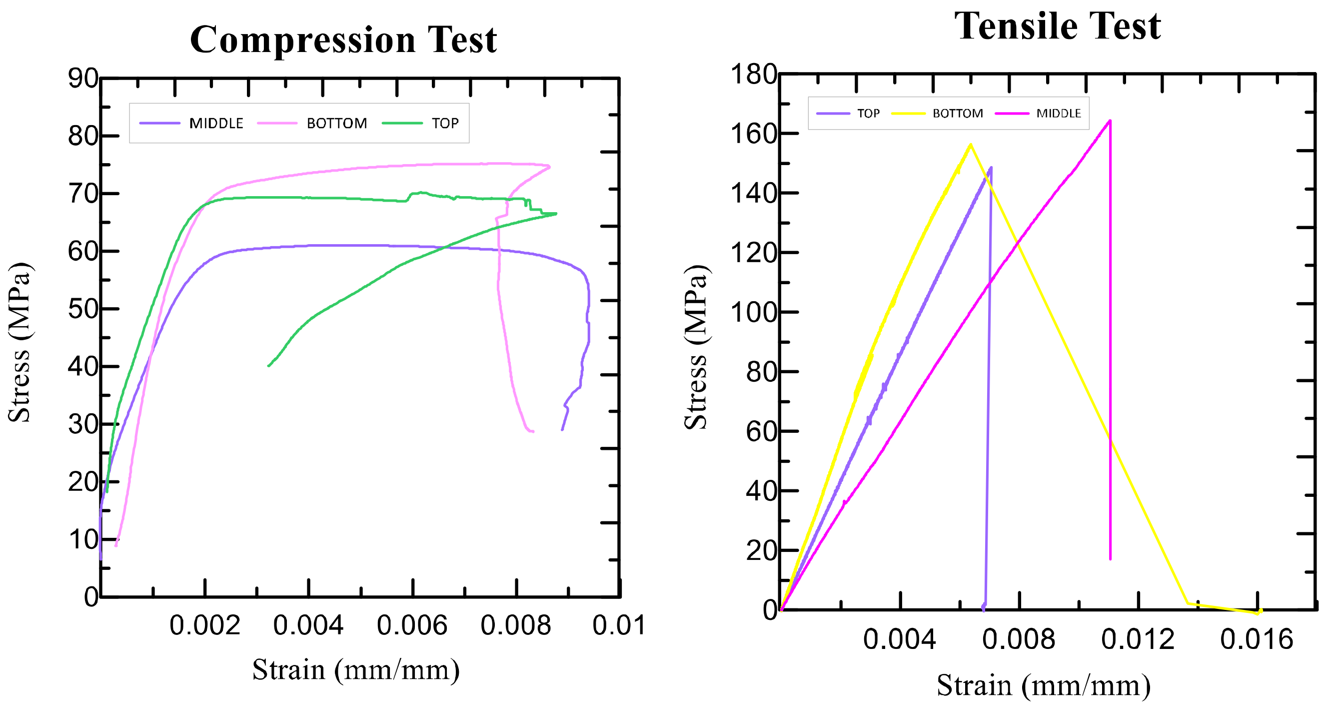

(a) (b)

Figure 15 - Graphs obtained from compression and tensile tests: (a) stress (MPa) versus strain (mm/m) graph for compression test (b) stress (MPa) versus strain (mm/mm) graph for tensile test.

3.2.3 Sisal

Sisal fibers incorporated into beam 02 were sourced from the municipality of Valente (Bahia), where they were gathered into bundles of long fibers. These fibers are derived from the leaves of the *Agave sisalana* plant through a mechanical process known as decortication [106]. As will be further explained, the fiber bundles underwent specific procedures to render them suitable for their intended application. The mechanical properties, as obtained from Castoldi [106], are presented in Table 9.

Table 9 - Physical and mechanical properties of sisal fiber. [106]

Physical and Mechanical Properties	**Sisal Fiber**
Diameter [mm]	0.19 ± 0.03
Linear density [g/m]	1.3 – 1.4
Tensile Strength [MPa]	383.88
Young's Modulus [GPa]	8.77

Sisal yarn was used as transverse reinforcement for beams 04 and 08. Additionally, the yarn was employed for tying the endings of bamboo stirrups, and for lashings connecting transverse reinforcement with longitudinal bars. For the sisal yarn, Santos and Cardoso [111] performed a physical and mechanical characterization of the material as shown in Table 10.

Table 10 - Physical and mechanical characterization of sisal yarn. [111]

Physical and Mechanical Properties	Sisal Yarn
Diameter [mm]	1.40 – 2.00
Linear density [g/m]	1.80 ±0.05
Tensile Strength [MPa]	112.8±9.2
Young's Modulus [GPa]	5.4±0.3

3.2.4
Castor Oil

Beams 07 and 08 were coated with castor oil that is sourced from an annual oilseed crop - *Ricinus communis* [112]. The material utilized is a plant-based polyurethane waterproof resin fabricated by the brand IMPERVEG, and it was used in proportions of 1 part component A to 2 parts of component B.

3.3 Material preparation

3.3.1
Bamboo Stirrups

Due to its natural and irregular nature, the development of bamboo stirrups often adheres to artisanal production standards, potentially posing challenges for large-scale manufacturing. Nevertheless, it is conceivable that methods could be enhanced to render their production more standardized and efficient. The procedures for the creation of the stirrups are explained below. Also, Figure 16 illustrates the bamboo stirrup and the assembly of beam 03. Thickness and width measurements for each stirrup are presented in Appendix A.1.


(a) (b)

Figure 16 – Longitudinal and shear reinforcement used for beam 03: (a) bamboo stirrup (b) assembly of longitudinal reinforcement with bamboo stirrups.

Some tools were developed at the Laboratory of Materials and Structure (LEM-DEC) of PUC-Rio for producing the stirrups. First, it was necessary to remove the bamboo diaphragms for then be able to cut the bamboo into strips. Figure 17 shows the device created to cut the bamboo strips. Also, in order to bend the strips, a wooden mold was fabricated with the stirrups' dimensions fixed by nails. The next step involved heating the bending parts of the stirrups to set the geometry and, lastly, the tips were tied together using sisal yarn. These steps are described as follows.

Figure 17 - Cutting tool developed for the production of bamboo stirrups.

1) Cutting of the culms with minimum length of 1m to account for losses during the process of cutting into strips.
2) Drilling of the culm's diaphragm.
3) Cutting of the strips using the tool shown in Figure 12.

4) Leveling the thickness into an approximate value of 1mm with the use of a thickness planer.
5) Production of molds in predefined measures to guide the bamboo stirrups' geometry.
6) Bending of the stirrups according to the molds.
7) Usage of hot air blower to fold the geometric shaping of the stirrups. The internal parts of the folded regions were heated to result in low loss of strength as the inner portion of the culm is richer in starch and the outer richer in fibers. This procedure prevented the fibers from being damaged by the hot air blower.
8) Removal of the stirrups from the molds, cutting of the ends and tying with sisal yarn.
9) Numbering the stirrups and measuring the width and thickness for calculating the respective mean area.

3.3.2 Sisal Fibers

A content of 6 kg/m³ of discrete sisal fiber was used for beam 02, as an alternative to the use of stirrup as for beam 03. Figure 18 illustrates the fibers before and after been prepared. To prepare the fibers, the following steps were adopted, as recommended by Castoldi [106]:

1) Weighting of the necessary fiber content considering 15% loss.
2) Immersion of the fibers in water, at a 70ºC temperature for a total of two hours.
3) Drying of the fibers at room temperature.
4) Fiber alignment with a comb.
5) Cutting the fibers to a length of approximately 5 cm using scissors.
6) Saturation of the fibers.

(a) (b)

Figure 18 - Preparation of sisal fibers for beam 02: (a) continuous sisal fiber before been subjected to the procedure to obtain the discrete fiber (b) sisal discrete fiber 50 mm long.

As observed for bamboo, the sisal fibers also present a hydrophilic behavior. This characteristic leads to high water consumption for the preparation of the concrete, resulting in workability issues. For this reason, the fibers were subjected to previous immersion in water for complete saturation before mixing with the rest of the concrete. The fiber content was adopted according to the results obtained by Castoldi [106], to assure residual stresses.

3.5
Assembly of the beams

Bamboo presents inherent characteristics of its nature that need to be taken into consideration when using it as reinforcement in concrete structures. One important aspect is the tapering of bamboo, resulting from the difference between the larger and smaller diameter at the ends of the culm. Therefore, when selecting bamboo to be used as reinforcement, one should seek the culms with greater linearity and cut the straighter sections. For each beam, reinforcements were utilized from both the top and the base portions of the bamboo. It is important that the top region is not disregarded, as it contains the highest concentration of fibers and, consequently, elevated mechanical properties.

Another relevant criterion in the selection and arrangement of culms as longitudinal reinforcement consists of the nodes distribution along the beam. As this region is weaker, it is crucial to avoid aligning nodes in the same cross-section to prevent chain failure of nodes and abrupt beam rupture. In addition to alternating the position of nodes, an alternation between the base and top of each culm was also adopted during the reinforcement positioning inside the formwork to achieve balance in the reinforcement area at each section along the beam's length.

For each beam, six culms were used as longitudinal reinforcement divided into two layers, resulting in an average reinforcement ratio ranging from 2.5% to 3%. Out of the six culms, five originated from the bottom of the bamboo, while one was sourced from the top. Additionally, two culms from the upper part of the bamboo were utilized for construction purposes. For each culm, the maximum and minimum measurements of both the inner and outer diameters were acquired across four distinct sections in order to derive the nominal area of bamboo reinforcement (Appendix A.2).

For the assembly of beams 02, 04, 06, 07, and 08, construction stirrups made from bamboo were employed. These stirrups were positioned at the beam's ends to maintain the geometric conformation of the longitudinal reinforcement (Figure 19). The components were crafted using the top portion of the bamboo selected due to its smaller diameters and high fiber content. Holes were drilled at the bamboo segments for the execution of the connections which were made with sisal yarn using the square lashing technique [113]. The stirrup was tied to the longitudinal reinforcement using sisal yarn as well.

(a) (b)

Figure 19 – Construction stirrup used for beams 02, 04, 06, 07, and 08: (a) bamboo construction stirrup (b) bamboo connection tied with sisal yarn.

For the beams produced with sisal yarn as shear reinforcement, the manufacturing process was simplified by just wrapping tightly the yarn around the culms after they were placed in the right position. The tips of the sisal yarn were tied in a knot at the bamboo endings. After the reinforcement assembly and material weighing, the concrete pouring process followed. The casting was carried out in layers, and compacted using a rubber hammer and a mechanical vibrator. Clamps were used at the edges of the formwork to ensure the correct width dimension of the beam as they were casted. As discussed in section 2.3.1, it is important for the bamboo to undergo treatment to enhance its adhesion to the matrix. To further investigate this matter, Masson [114] conducted four-point bending tests on beams and pull-out tests on concrete blocks using the following coating methods: (1) sikadur-32 with sand, (2) castor oil with sand, and (3) no coating. The concrete had the same mixture ratio as adopted in this research, and the bamboo used was of the *Phyllostachys aurea* species, from the same batch as the material used in the present work. Considering the results obtained from Masson [114] and prioritizing the development of an ecological and feasible structure, it was chosen to use uncoated bamboo.

3.5.1 Coated beams

For beams 07 and 08, a coating using castor oil and sand was applied to enhance the bond between the longitudinal reinforcement and the matrix. Initially, the outer surface of the bamboo was manually sanded to remove the waxy layer that lowers the adhesion of the coating. Special attention was taken to avoid the removal of the external fibers. After sanding the culms, the resin was applied with a brush, followed by manual sand spraying onto the culm's surface (Figure 20). As shown in Figure 20.b, the external lubricant layer was removed from the bamboo through sandpapering. This is evident from the contrast between the shiny outer surface on the right and the opaque surface on the left. Similar to the previous models, an alternation between the base and top of the culms was carried out as they were placed as longitudinal reinforcement.

(a)

(b) (c)

Figure 20 – Preparation of culms for use as longitudinal reinforcement: (a) Sanding the culm's surface to create a rough texture (b) Removal of the external lubricant layer by sandpapering it, evidenced by the contrast between a shiny outer surface on the right and an opaque surface on the left (c) Application of castor oil and sprinkled sand around the culm.

After the application of the coating, a reduction in the free horizontal spacing between the bamboo culms within the cross-section was observed, as the beam width, reinforcement cover, and number of layers remained unchanged. To ensure that the concrete penetrated the voids between the bamboo, a vibrating table was used, and the concrete pouring was done in layers, gradually adding concrete from the sides. Clamps were also used to maintain the beam's dimensions. Figures 21.a and 21.b represent the reinforcement with coated bamboo used for beams 07 and 08.

(a)

(b)

Figure 21 - Coated culms used as longitudinal reinforcement for beams: (a) 08 (b) 07

For the coated beams, the reinforcement was secured to the bottom of the formwork to prevent it from floating during the concrete pouring process and to maintain its original position. To achieve this, holes were drilled into the bottom of the formwork at three positions along the length of the reinforcement. Wire hooks were used to secure the reinforcements to the formwork. Figures 22.a and 22.b illustrate the process of fastening the stirrup to the formwork.

(a) (b)

Figure 22 – Fastening of the reinforcement to the bottom of the formwork: (a) shear reinforcement tied to the bottom of the formwork (b) formwork configuration to prevent bamboo from floating

3.6
Three-point bending test

The beams were set for a three-point bending test in a MTS machine with a 500 kN load capacity hydraulic actuator. The support plates were placed on rollers allowing for rotation and longitudinal displacements as well. The tests were conducted in displacement control at a rate of 1 mm/min. The shear span was analyzed through digital image correlation (DIC), and a displacement transducer (LVDT) was also used to measure the displacement at the load application section. The test started as the camera was synchronized with the actuator, and it was concluded when no significant increase in load-bearing capacity was registered. The results from DIC were used to investigate the crack kinematics and the shear mechanisms.

The length of the beam is 1300 mm with a cross-section of 150 mm width and 250 mm height. To ensure the beam exhibits slender behavior and to avoid the arch effect, the shear span was calculated to keep the ratio of a/d greater than or equal to 2.5; in which 'a' is the span between the load application section and the supports and 'd' is the effective depth of the beam [102]. This assumption resulted in a shear span of 500 mm. To force shear failure to occur on one side of the beam, the other span, which was 600 mm long, was reinforced with 6.3 mm diameter steel stirrups spaced 6 cm apart. A schematic representation of the beam and the test set-up can be seen in Figure 23.

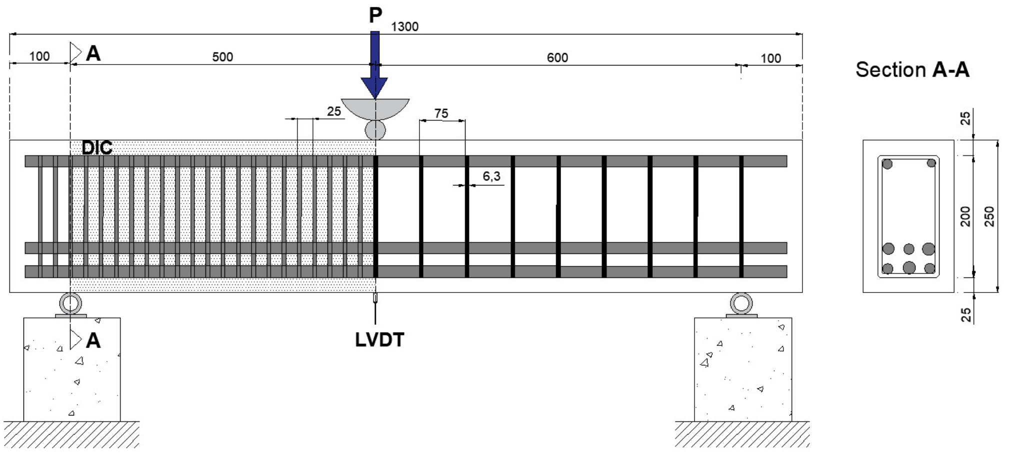

(a)

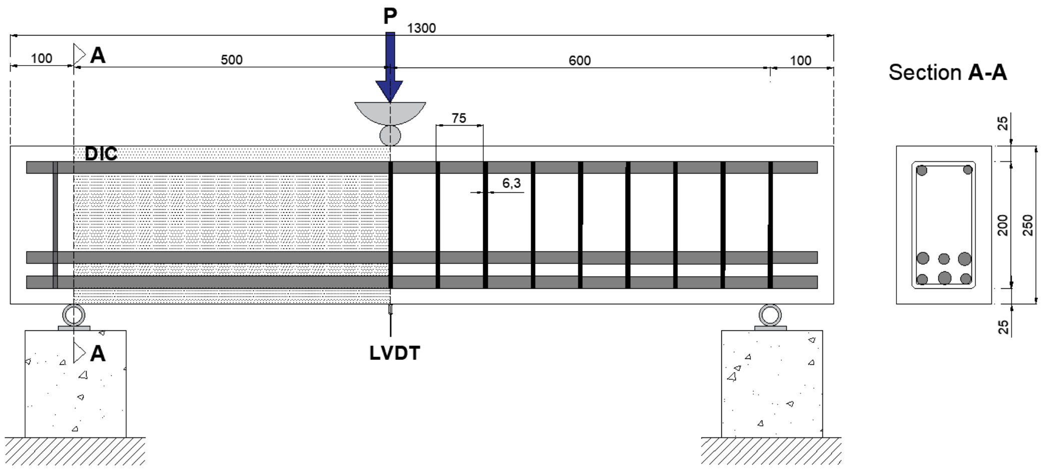

(b)

Figure 23 - Set-up for three-point bending test and cross-section of the beam (dimensions in mm): (a) beam reinforced with bamboo stirrup (b) general case.

3.6.1
Digital Image Correlation (DIC) instrumentation

The displacement and cracking data of the beams were obtained using digital image correlation (DIC). The specimens were prepared by first selecting the analysis span, applying a white painting, and then marking the investigation points using a roller. The criteria employed for determining the analysis point size were based on both the camera's resolution and the specific region of interest on the beam. The camera utilized had a resolution of 5 megapixels, and each analysis point needed to cover 4 to 6 pixels in the images. As a result, the analysis was conducted using a red roller with a point size of 1.27 mm, corresponding to an analysis span ranging from 39 cm to 103 cm. After preparing the beams, the camera was carefully positioned and calibrated to ensure proper brightness and image sharpness for subsequent data analysis. Vic-Snap software was utilized to capture images at 2-second intervals throughout the test duration.

4. RESULTS AND DISCUSSION

4.1
Failure Modes and Crack Pattern

After performing the three-point bending tests in the beams with untreated bamboo, it was observed that a dominant crack emerged vertically in the load application section characterizing a failure mode by bending, as can be seen in Figures 24c, 24d, 24e and 24f, respectively referring to beam reinforced with bamboo stirrups, sisal yarn, steel stirrup and unreinforced. For specimen 02 though it was noticed the appearance of a shear cracking. The vertical crack demonstrates the occurrence of the arch effect which can be caused, among other factors, by the lack of proper bonding between bamboo and concrete.

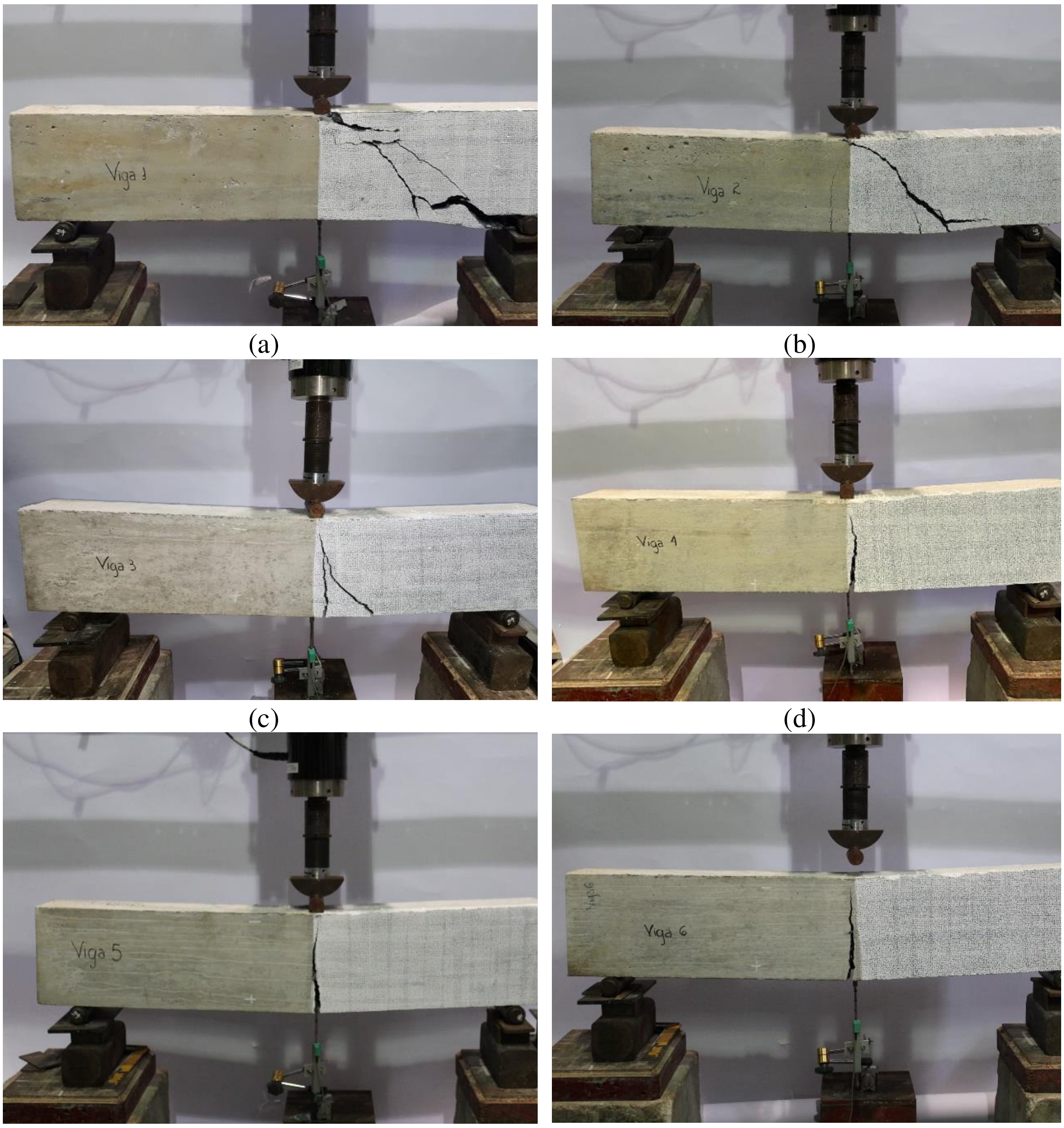

(a) (b) (c) (d) (e) (f)

Figure 24 - Failure modes for tested beams: (a) 01 (b) 02 (c) 03 (d) 04 (e) 05 (f) 06.

In order to obtain the shear failure of the beams, the culms were then treated with castor oil and sand to improve the bonding and allow for beam action to prevail. The treatment resulted in shear failure modes, thus confirming the importance of treating the bamboo to guarantee an efficient load distribution between the constituents. Figures 25a and 25b correspond, respectively, to beams reinforced with sisal yarn and without transverse reinforcement, both longitudinally reinforced with coated bamboo culms.

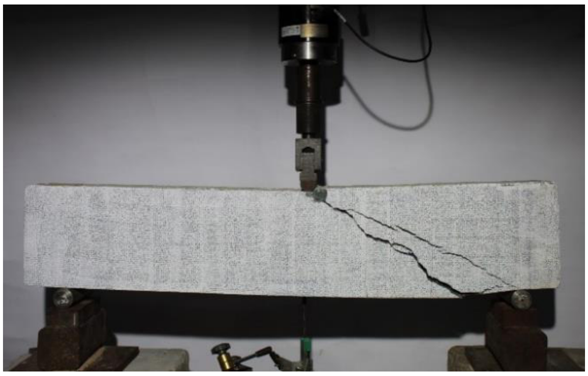

(a)

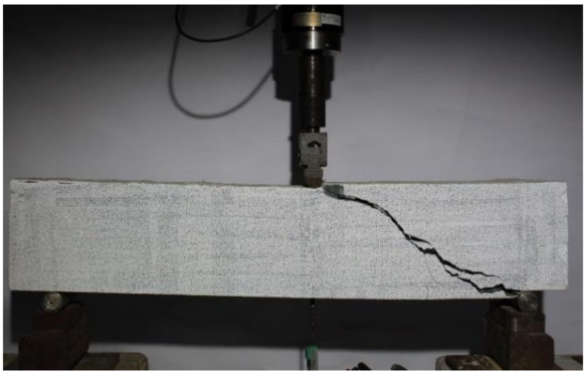

(b)

Figure 25 - Failure mode and crack pattern for beams 07 and 08.

The beam inspections conducted after testing provided a deeper understanding of the behavior of bamboo culms and other reinforcements employed. Figure 26 shows the result for specimen 03, indicating a node failure at the inclined cracking, along with the stirrup failure. This result is related to the stress concentration in the region of the nodes, known for its comparatively lower mechanical strength, which leads to failure in that particular area. Moreover, as previously mentioned, a displacement of the longitudinal reinforcement was observed for the beams 04, 05, and 06 causing a concrete cover greater than the value initially established (Figure 27). For beam 04, a horizontal displacement was also noticed.

(a) (b)

Figure 26 - Beam 03 after 3-point bending test: (a) nodes rupture (b) failure on bamboo stirrups.

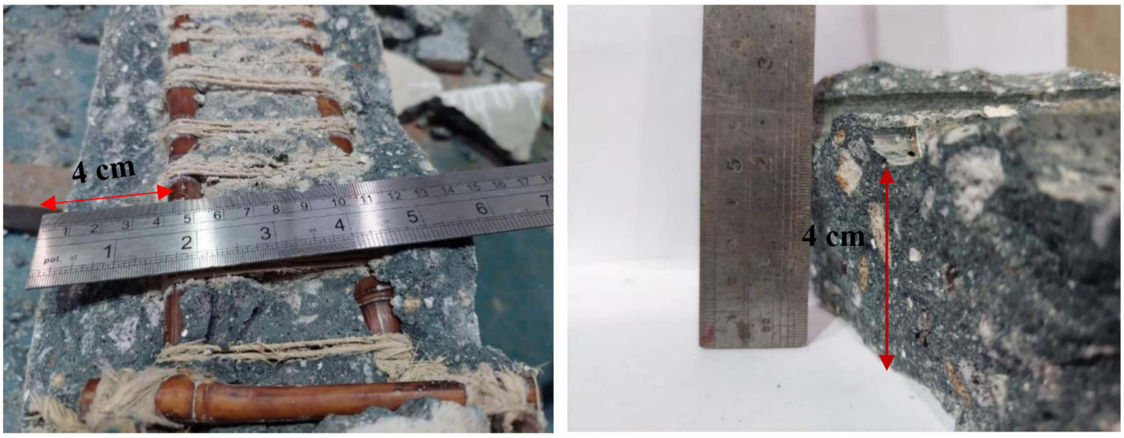

(a) (b)

Figure 27 – Horizontal and vertical displacement on specimens 04 and 06, respectively: (a) 04 (b) 06.

DIC instrumentation allowed to measure the crack opening values, as well as the cracking inclination (angle α) and the beams displacement. Moreover, other parameters were obtained for the shear mechanism calculation, such as the sliding between faces and the length of the critical shear crack. Figure 28 shows the use of DIC to measure the major principal strain acting on beams 03 and 07, corresponding to the testing time t=980s (V/V_{max} = 0.91, after beam failure) and t=800s (V/V_{max} = 0.74, after beam failure), respectively. For the specimen 07, one observes the development of several small crack opening in the vertical direction, obtained from DIC strain measurements.

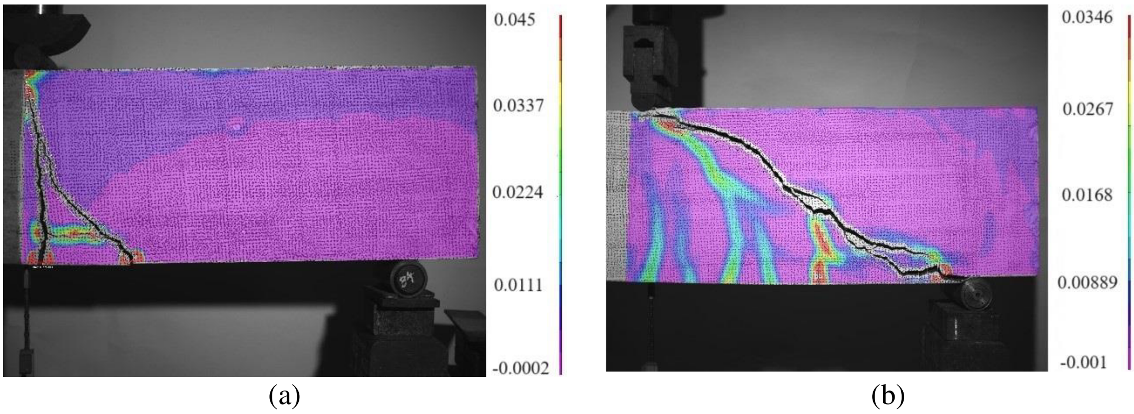

Figure 28 - Strain measurements e1 [Lagrange] using digital image correlation (DIC): (a) beam 03 - picture 490: V/Vmax = 0.91 (b) 07 - picture 400: V/Vmax = 0.91.

4.1 Load vs Displacement Curves

For untreated bamboo, the use of bamboo stirrups increased the load capacity of the beams by 15.85%, the sisal yarn by 12.30% and the discrete sisal fiber by 1.32%. The use of discrete fibers did not show an effective improvement in the load capacity, but allowed for a better crack control. For treated bamboo, the improvement in the load capacity for sisal yarn compared to the beam with no shear reinforcement was 17.90%. The load *versus* displacement curves for all the beams tested can be seen in Figure 29.a, while a comparison between the beams with sisal yarn reinforced with treated and untreated culms is shown in Figure 29.b.

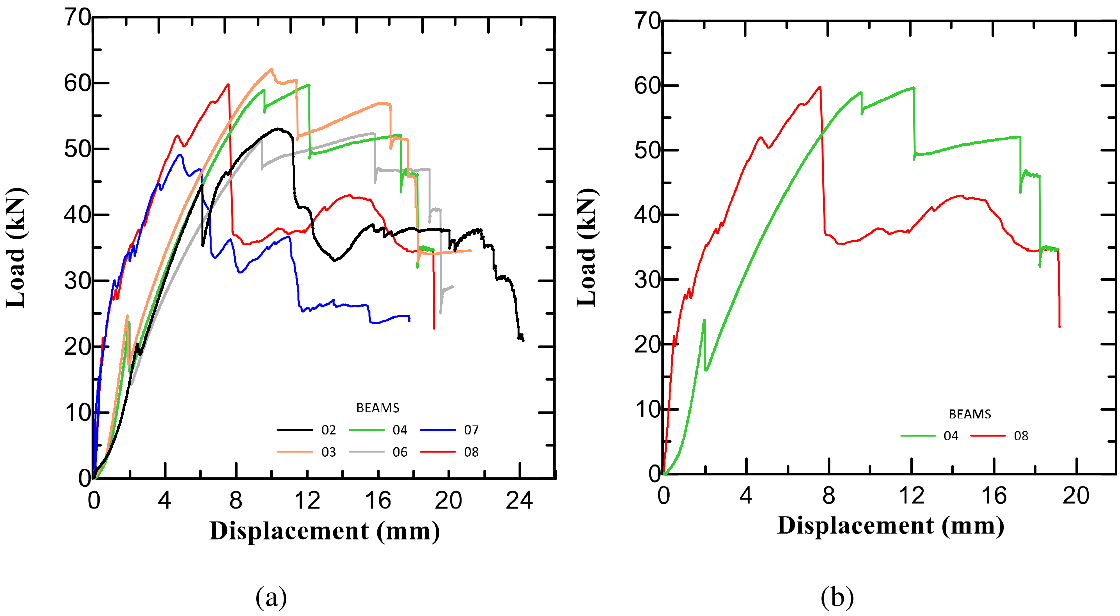

Figure 29 – Graphs of ‘Load’ versus ‘Displacement’ obtained from the three-point bending test: (a) graph Load vs Displacement for all the tested beams (b) graph Load vs Displacement comparing the effect of treatment (beams 04 and 08)

As evidenced by the aforementioned graphs, despite bamboo demonstrating a linear behavior under tension, the beams exhibit a pseudo-ductile behavior due to the gradual rupture of the nodes induced by incremental loading. Additionally, another factor potentially contributing to the peaks in the graphs is the slippage of longitudinal reinforcement, leading to a reduction in load, followed by stress redistribution, and ultimately an increase in load-bearing capacity. The drops in the curves are noticeable as the culms slip along the concrete matrix.

For the treated beams, it was observed that the maximum load occurred at smaller displacements compared to the untreated beams. As a hypothesis for this observation, the application of a castor oil coating was found to contribute to safeguarding the bamboo against water absorption and preserving its initial stiffness. This protective effect likely assists in maintaining the integrity of the fibers, whereas untreated culms may be subject to deterioration and possibly anatomical alterations.

4.3
Load Bearing Capacity

As detailed in preceding sections, the beam design adhered to the GFRP guideline ACI CODE-440.11-22 [71], with a shear strength set at 70% of the load required to induce bending failure. However, despite this consideration, arch action predominated, resulting in failure by bending. For beam 04, the consideration of the sisal yarn was analogous to the bamboo stirrups, but considering mechanical and physical properties mentioned in Table 7, section 3.2.3. The sisal yarn was transversely grouped into three bundles and spaced at each 20 mm. Table 11 provides a comparative analysis of the theoretical and experimental outcomes for each respective beam.

Table 11 - Ultimate load from three-point bending tests, expected loads calculated from design codes NBR6118 (beam 01), RILEM TC 162-TDF (beam 02), and ACI CODE-440.11-22 (beams 03, 04, 05, 06, 07, 08) and failure modes.

BEAM	$P_{ultimate}$ test [kN]	$P_{ultimate}$ expected [kN] - shear	$P_{ultimate}$ expected [kN] - bending	Failure Mode
01	129.4	136.64	-	SHEAR
02	52.96	59.6	96.0	SHEAR
03	62.10	35.55	92.55	BENDING-SHEAR
04	59.59	28.8	93.0	BENDING
05	56.36	65.55	90.0	BENDING
06	52.26	19.20	81.75	BENDING
07	49.11	23.40	108.6	SHEAR
08	59.82	31.80	118.5	SHEAR

Significant differences between the expected and the actual ultimate load were observed for specimens 03, 07 and 08 indicating a conservative bias present in the GFRP guidelines that leads to an underestimation of beam shear capacity. The correlation V_t/V_{exp} ranged from 0.48 to 0.57. However, for beams with failure mode by bending (SYB, 05, 06), V_t/V_{exp} was slightly improved: 0.62 – 0.64.

For the 01 specimen, comprised of conventional reinforced concrete where steel was employed for both longitudinal and transverse reinforcement, the load prediction followed the NBR6118[2] standards. As expected, the percentual difference between expected and test result were noticeable low ($V_t/V_{exp} = 0.95$).

In the case of concrete reinforced with sisal fiber, it was found that the utilization of the RILEM TC 162-TDF [105] method was applicable for load prediction ($V_t/V_{exp} = 1.13$), despite being tailored for steel fiber use . Additionally, the utilization of separate portions, V_c and V_f, considering ACI CODE-440.11-22 [71] was deemed inadequate for estimating beam strength.

4.4 Shear Mechanisms

The following sections describe the methods used for calculating the shear mechanisms acting on the beams. The analysis was performed for specimens 02, 07, and 08, since these beams presented the critical crack diagonally inclined, allowing for the investigation of the shear mechanisms. Aggregate interlock, dowel effect, residual strength, compression chord, arching action, and stirrup contribution were calculated according to the script attached at the end of the thesis. The prediction theories adopted assume characteristic values for the shear strength. Similarly to Cavagnis [83], in order to discretize the shear critical crack in the DIC analysis, the shape of the crack was represented by a polyline with points spaced at a maximal distance corresponding to 10 mm (aggregate size).

4.1.1 Aggregate Interlock

The model used for calculating the aggregate interlock is based on the contact density model from Li and Maekawa [90] and takes into account the parameters μ (friction

[2] Brazilian guideline that specifies the requirements for the design and construction of conventional reinforced concrete structures.

coefficient) and k' (constant related to the maximum compression stress borne by the concrete in the direction ɵ), which are derived from push-off tests. As a reference, the results obtained by Resende [84] μ = 0,6 and k' = 12 MPa are utilized due to the use of similar aggregate (gravel size 0) with comparable concrete compression strength (around 34 MPa). Moreover, the ratio *r* corresponding to the sliding divided by the crack opening is calculated for each discretized segment (r = $\Delta/_{\omega}$).

The shear (τ_r) and normal (σ_r) stresses at the cracking surfaces are represented by the expressions 2.1 and 2.2 below.

$$\sigma_r = 7{,}92\, k' \int_{arctg(1/r)}^{\pi/2} \{cos\theta^{24} \cos[\theta + arctg(\mu)]\} d\theta \tag{2.1}$$

$$\tau_r = 7{,}92\, k' \int_{arctg(1/r)}^{\pi/2} \{cos\theta^{24} \,\mathrm{sen}[\theta + arctg(\mu)]\} d\theta \tag{2.2}$$

Solving the integral and applying the integration limits, one derives:

$$\sigma_r = 95{,}04 * (r^2+1)^{12} * (631r^2 - 420) * \left(\frac{\sqrt{1/_{r^2}+1}}{1024r^{24}}\right) \tag{3.1}$$

$$\tau_r = (r^2+1)^{-13} * \{2(r^2+1)^{12} * [3r^2 * (r^2+1)^2 - 44r^2(r^2+1) + 231(r^2+4)] * \sqrt{\left(1 - 1/_{r^2}\right)} - 1048576(r^2+1)^{11} * \mathrm{atan}\left(1/_r\right) + 1048576(r^2+1)^{11} * \mathrm{atan}\left(\sqrt{r^2+1}/_r\right)\} \frac{95{,}04}{4194304} \tag{3.2}$$

The normal and shear stresses (σ_r, τ_r) are calculated according to the constant $r = \frac{\Delta}{\omega}$ of each discretized segment and by using Equation 4, the aggregate portion V_{ag} of the shear strength is calculated.

$$V_{ag} = b\left[\int_0^{l_{cr}} \tau_r \sin(\alpha)\, dl - \int_0^{l_{cr}} \sigma_r \cos(\alpha)\, dl\right] \tag{4}$$

With the width of rectangular cross section being $= 150\ mm$.

For each segment along the crack length ranging from 0 to l_{cr} , where w > w_{cr} , the shear and normal stresses are calculated as well as the angle α. Subsequently, these values are summed up to derive the total aggregate contribution V_{ag}.

$$V_{ag} = b_v \left[\left(\lim_{n \to lcr} \sum_{i=0}^{n} \tau_{r_i} \sin(\alpha)\, l_i \right) - \left(\lim_{n \to lcr} \sum_{i=0}^{n} \sigma_{r_i} \cos(\alpha)\, l_i \right) \right] \quad (5)$$

4.1.2
Concrete residual strength

The residual strength is a mechanism activated by the shear crack development in concrete structures. Despite being disregarded by some researchers [102], [115], [116], [117], in the present study, the residual capacity will be computed for crack segments with $w < w_{cr}$. The method adopted for beams 07 and 08 follows Resende [84] approach, where the assessment of residual strength of concrete V_{res} relies on the relationship between normal residual stress and crack opening, as proposed by Hordijk [118].

From FIB Model Code 2010 [119], one derives the fracture energy $G_{fracture}$, w_1 and w_{cr}, allowing the calculation of the residual tensile stress σ_{res} of concrete. By applying Equations 6.1 and 6.2 to each discretized segment of the critical crack, the residual strength V_{res} is determined according to Equation 7.

$$\sigma_{res} = \begin{cases} f_{ct} \cdot \left(1 - 0.8\left(\frac{w}{w_1}\right)\right), if\ w \leq w_1 & (6.1) \\ f_{ct} \cdot \left(0.25 - 0.05\left(\frac{w}{w_1}\right)\right), if\ w_1 \leq w \leq w_{cr} & (6.2) \end{cases}$$

$$V_{res} = b_v \int_0^{l_{cr}} \sigma_{res} \cdot \cos(\alpha)\, dl \quad (7)$$

For the concrete beam reinforced with discrete sisal fibers (SFB), residual strength was computed according to the crack opening width of the discretized segment. A graph of crack opening w versus residual stress σ_{res} (Figure 30) shows the position of w_a from which it should be taken into account the residual strength from fibers ($w \geq w_a$). Before the intersection of the curves ($f_{ct} < f_{Fts}$), only the residual strength for plain concrete is accounted.

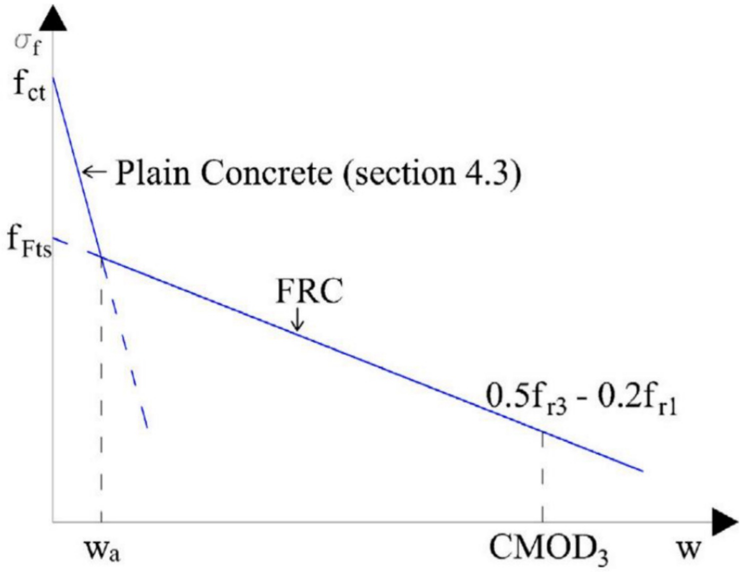

Figure 30 - Crack opening w versus residual stress σ_{res} for plain concrete and fiber reinforced concrete. [120]

Fib Model Code 2010 [119] was adopted in order to obtain the post-cracking residual strength (f_{FTu}). For linear model, f_{FTu} can be calculated using equation 8, where f_{R1} is the stress for crack opening of 0.5 mm (SLS) and f_{R3} is the stress for crack opening equal to 2.5 mm (ULS). Figure 31 illustrates crack opening *versus* stress for a softening material submitted to a bending test and the correspondent post-cracking model.

$$f_{FTu} = f_{FTs} - \frac{w_u}{CMOD_3}(f_{FTs} - 0{,}5f_{R3} + 0{,}2f_{R1}) \geq 0 \qquad (8)$$

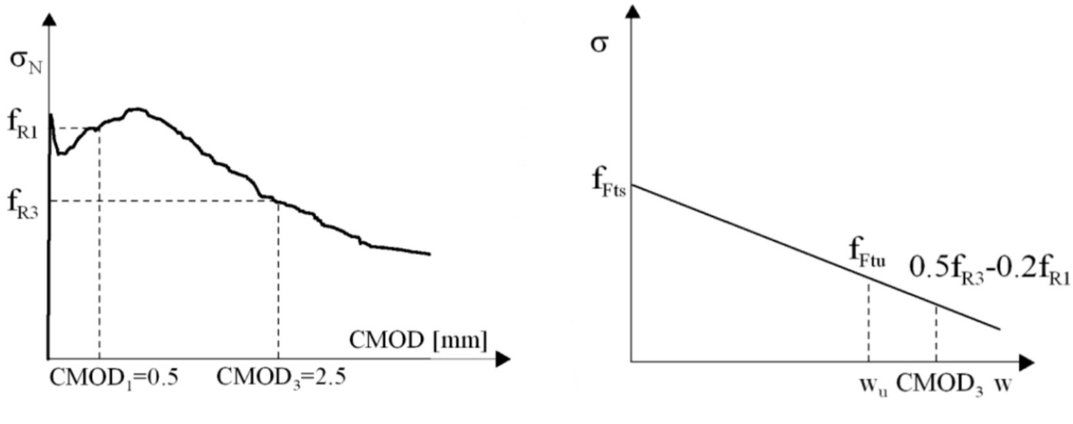

(a) (b)

Figure 31 - Stress-crack opening graphs for fiber reinforced concrete (FRC): (a) typical results from a bending test on a softening material (b) linear post-cracking constitutive law. [119]

In the aforementioned equation, the service residual strength is calculated as f_{FTs}= 0,45.f_{R1}; f_{R1} and f_{R3} are defined based on graphs obtained in the three-point bending test of a notched prism and the crack opening w varies according to the discretized cracking segment. Residual strength accounted with fiber contribution was calculated based on the results presented by Castoldi [106], since the author utilized the same content of sisal fiber used in the present research. CMOD of 0.5 mm resulted in f_{R1}= 0,80 MPa and CMOD of 2.5 mm led to f_{R3} = 0,54 MPa.

$$f_{FTu} = 0{,}45.0{,}80 - \frac{w_u}{2{,}5}(0{,}45.0{,}80 - 0{,}5.0{,}80 + 0{,}2.0{,}54) \geq 0 \tag{9.1}$$

$$f_{FTu} = 0{,}36 - 0{,}0272w_u \geq 0 \tag{9.2}$$

Given the post-cracking residual strength f_{FTu} and the angle α of each discretized crack segment, the contribution of fibers V_{fib}can be computed as follows:

$$V_{fib} = b_v \int_0^{l_{cr}} \sigma_f \cos(\alpha)\, dl \tag{9.3}$$

4.1.3
Dowel action

The dowel action was assessed using two distinct methods based on DIC analysis of crack patterns. When a dowel crack was identified in the images, the Cavagnis *et al.* [95] approach was applied. However, this method proved unsuitable for analyzing beams without dowel cracks, leading to unrealistic and significantly larger results. In such cases, the Cavagnis *et al.* [98] approach, which incorporates an equation proposed by Ruiz *et al.* [121], was utilized. Furthermore, when dowel cracks were present, both methods provided similar results. For beam 02 with discrete fibers, the model proposed by Resende [84] was employed since Cavagnis *et al.* [95], [98] developed their methodology for structures without shear reinforcement or fibers.

Cavagnis *et al.* [95] considers the mechanical behavior of the longitudinal bar as a beam on an elastic foundation (concrete), with free span $l_{da} = l_d + d_b$ where l_d is the cracking due dowel action and d_b is the bar diameter. This mechanism is activated by the transverse displacement of the bending reinforcement that is quantified through the crack developed along the longitudinal direction. An average of the culm diameters was used to obtain d_b values, resulting in d_b = 19.5 mm, and l_d was measured by DIC for each image. The beam deflection is approximated by a third order polynomial, using the vertical displacement and rotations in the l_{da} edges (Figure 32). The polynomial constants were determined by solving a linear system using the values of v(x) obtained through digital image correlation (DIC) for positions x located at a distance $x_d = d_b / 2$ outside the length l_{da}. Expression 10 is used to calculate the shear force carried by dowelling action.

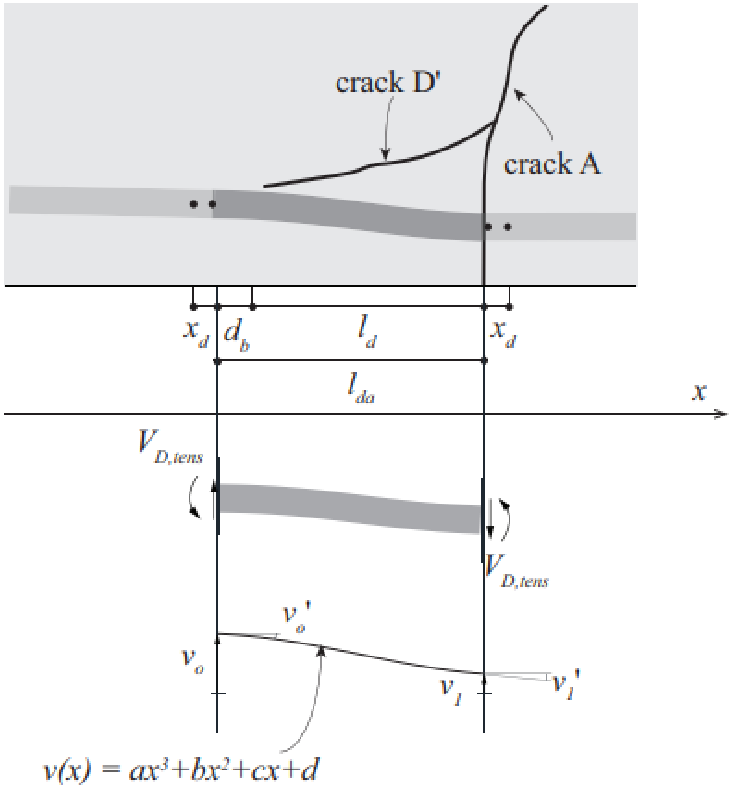

Figure 32 – Deflection of the longitudinal reinforcement in the proximity of the dowelling action. [83]

$$V_{dowel} = \frac{6.n.E_{bamboo}.I}{{l_{da}}^3} . \left[v_0 - v_1 + \frac{l_{da}}{2}(v'_0 + v'_1) \right] \tag{10}$$

Where n is the number of bars and I is moment of inertia of the longitudinal bars calculated as $I = \frac{\pi(D_{ex}^4 - D_{in}^4)}{64}$ for bamboo.

To calculate the embedded length of the bar in an elastic foundation, the Hetényi [122] solution for the proportionality equation between the reaction (p) and the vertical displacement (y) of the bar was employed, based on material characterization test results. By considering a semi-infinite bar length and p = kΦy, the following graph was generated. The vertical axis is represented by the reaction force p per unit length along the semi-infinite bar and the horizontal axis refers to the longitudinal position x along the bamboo length divided by its outer diameter Φ (Figure 33).

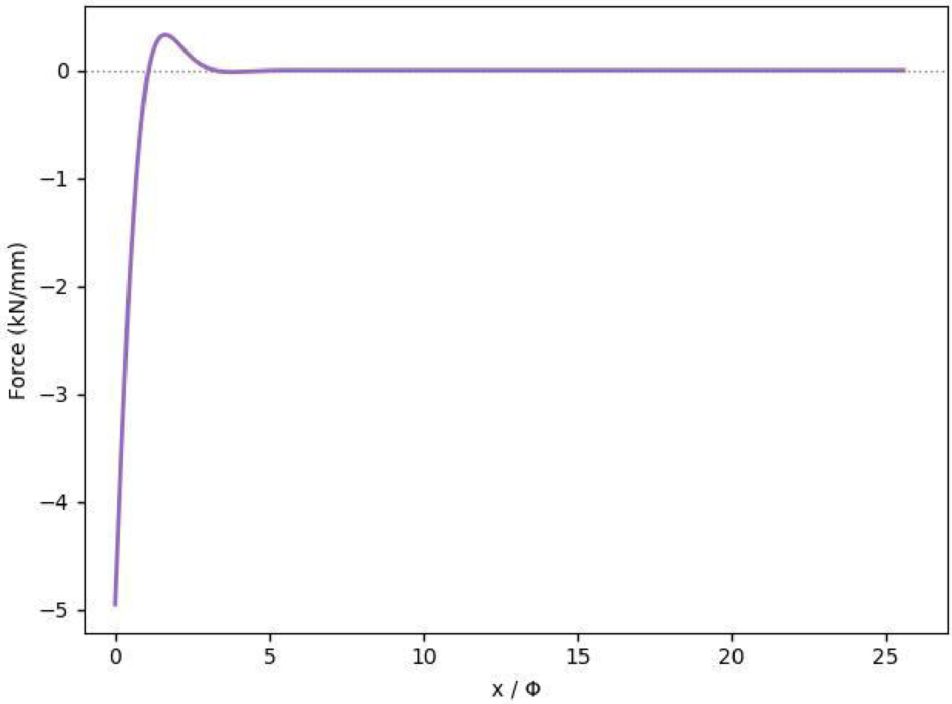

(a)

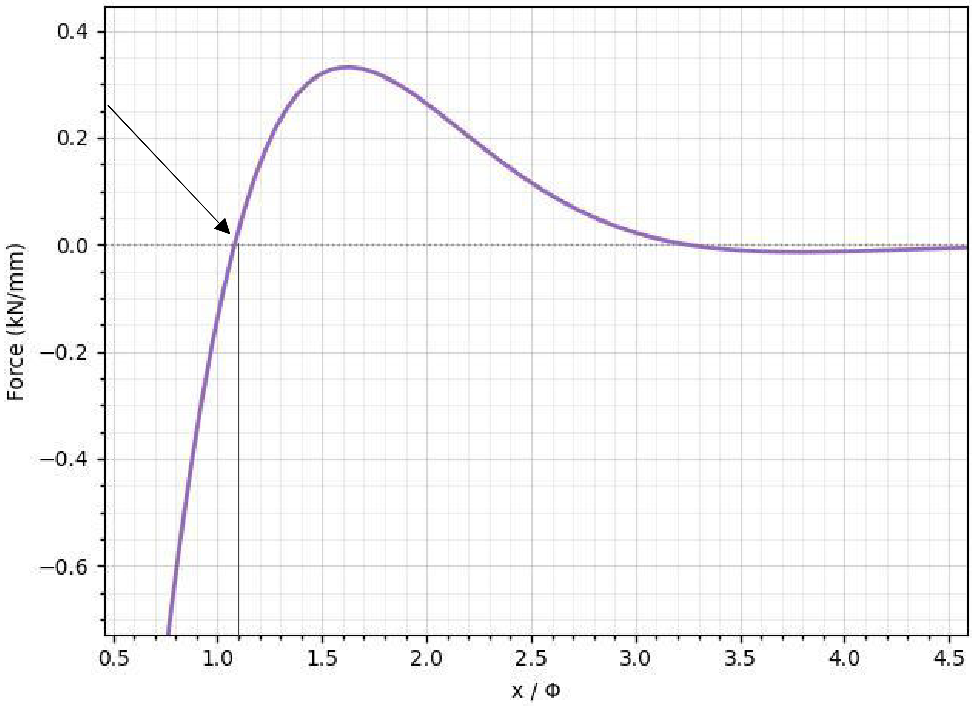

(b)

Figure 33 - Graph of reaction force versus x/Φ considering a semi-infinite bar length generated for beam 08: (a) Distribution of force per length unit along the bamboo reinforcement subjected to Vd = 26 kN at one edge (b) Length where tensile force acts: ld = 1.1Φ.

As indicated in Figure 33, the length (l_d) for which the tensile force acts corresponds to 1.1Φ. This length is used to calculate the dowel effect for the methods of

Vintzeleou and Tassios [93] and Cavagnis [98]. Equation 11 recommended by Cavagnis [98] allows the computation of the shear force V_{dR}, with $f_{ct,ef}$ equals to (k_b . f_{ct}). In this expression, f_{ct} is the tensile strength of the concrete and k_b is the smaller between the two values 0,063ε_b - 0,25 ≤ 1 and $0.063\left(\frac{d-c}{w_c}\right)^{0.25}$0,25 ≤ 1 , in which ε_b is the flexural reinforcement strain (bamboo strain) and w_c is the opening of the critical shear crack developed along the longitudinal reinforcement direction.

$$V_{dR} = n.b_{ef}.f_{ct,ef}.l_d \tag{11}$$

The method proposed by Vintzeleou and Tassios [93] assumes a finite length for the bar, with V_{dowel} obtained by equating the total concrete compressive force F_{cc} (expression 12.1) to the tensile force F_{ct}, resisted by the net width of the section b_n at the reinforcement level (expression 12.2). The appropriate dowel length for the bar was determined using a similar approach as previously described, but with the consideration of finite length. In this case, Equation 12.3 can be utilized, resulting in the same value as for semi-infinite length l_d = 1.1Φ (Figure 34).

$$F_{cc} = \int_0^{l_d} p\, dx = 1.208\, V_d \tag{12.1}$$

$$F_{ct} = f_{ct} b_n l_d \tag{12.2}$$

$$\mathrm{p} = \frac{2V_d\beta[\mathrm{sen}(\beta L)\cosh(\beta x)\cos(\beta x') - \mathrm{senh}(\beta L)\cos(\beta x)\cosh(\beta x')]}{\mathrm{senh}^2(\beta L) - \mathrm{sen}^2(\beta L)} \tag{12.3}$$

with x’ = (L-x).

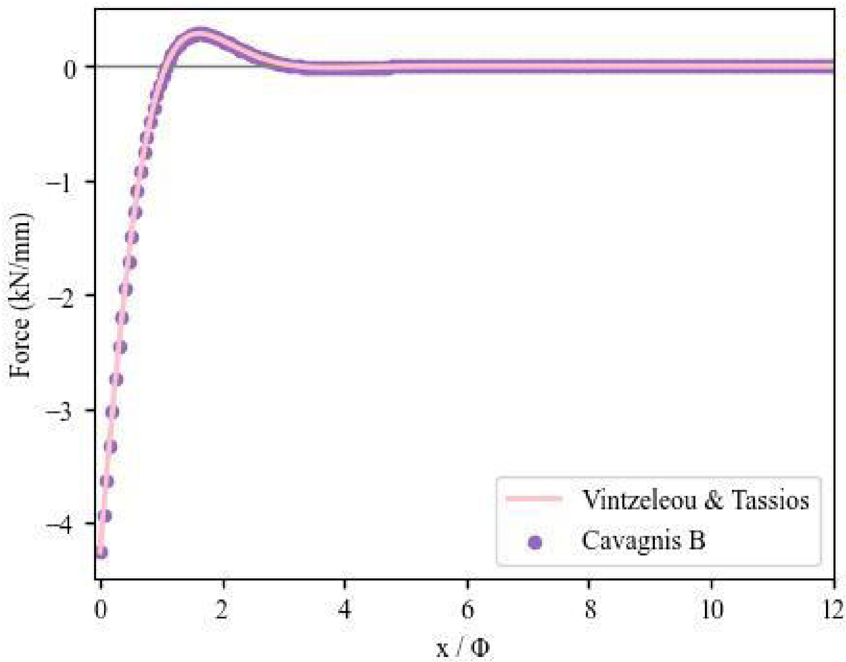

Figure 34 - Distribution of force per length unit along the bamboo longitudinal reinforcement using methods proposed by Vintzeleou and Tassios [93] and Cavagnis [98].

The proximity between the methods proposed by Vintzeleou and Tassios [93] and Cavagnis [98] is evident, yet the calculation proceeded using the approach outlined by Cavagnis [98]. In summary, Resende [84] was employed for specimen 02, given its application for fiber-reinforced concrete. As for the beams 07 and 08, methods developed by Cavagnis [95] and Cavagnis [98] were applied, depending on the observed crack pattern.

4.1.4
Compression chord and arching action

The compression chord or arching action was computed following expressions stated by Cavagnis [83]. Segments with lengths up to 6 mm were discretized in the section located above the tip of the critical shear crack. By using digital image correlation (DIC), principal strains e_1 (major) and e_2 (minor) were obtained along these segments from which one derived the principal stresses σ_1 and σ_2. The following expressions (15.1, 15.2, 16) were employed.

$$\sigma_1 = E_c.\varepsilon_1 \tag{15.1}$$

$$\sigma_1 = 0, \text{ se } E_c.\varepsilon_1 > f_{ct} \tag{15.2}$$

$$\sigma_2 = \frac{E_c.\varepsilon_2}{1+\left(\frac{\varepsilon_2}{\varepsilon_0}\right)^{\alpha}} \tag{16}$$

With: $\varepsilon_0 = \frac{\alpha.f_{c,eff}}{E_c.(\alpha-1)^{\left(1-\frac{1}{\alpha}\right)}}$ and $\alpha = 0.5 + \frac{f_{c,eff}}{20} + \frac{f_{c,eff}{}^2}{1500}$

Two different models were proposed by Cavagnis [83] to calculate the parameter $f_{c,eff}$. Considering post-cracked concrete, Cavagnis [83] recommends the use of expression 17 shown below, while for uncracked concrete it can be adopted Kupfer's failure criterion (Figure 35). Kupfer's failure criterion was adjusted to the strength obtained from compression tests and the arching action was calculated for both methods providing similar results. Finally, according to the cracking pattern it was chosen the method that best fitted in the shear prediction ($f_{c,eff} \leq f_{c,k}$), represented by the bolded values in Table 13.

$$f_{c,eff} = f_c.\frac{1}{0.8+170\varepsilon_1} \leq f_c \tag{17}$$

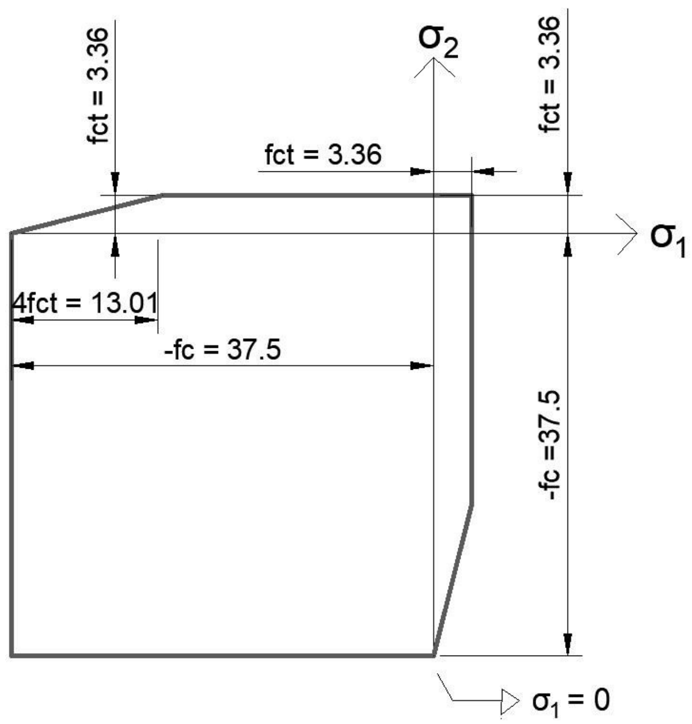

Figure 35 - Kupfer's failure criterion used to determine fc,eff for uncracked concrete.

After calculating the principal stresses with their respective orientations (θ_1 and θ_2), σ_1 and σ_2 were decomposed into the vertical direction (shear direction). The equation provided below (18) was utilized to calculate the arching effect. Table 12 summarizes the results of arching action based on the two different methods of $f_{c,eff}$ calculation for beams 02, 07 and 08.

$$V_{arching} = \sum \sigma_1 \text{sen}\theta * b_v * l_{segment} + \sum \sigma_2 \cos\theta * b_v * l_{segment} \qquad (18)$$

Table 12 - Arching effect calculated for beam 02, 07 and 08 using Kupfer's failure criterion and expression (17), developed for $f_{c,eff}$.

Arching Effect [kN]					
Time (s)	Kupfer's failure criterion (1)	$f_{c,eff}$ expression (2)	$\sum V_{calculated}$ (kN)		$V_{experimental}$ (kN)
			(1)	(2)	
BEAM 02					
540	**9.01**	7.55	22.94	21.48	28.27
620	**3.74**	3.28	25.29	24.83	29.54
680	-	-	-	-	23.73
740	-	-	-	-	20.97
BEAM 07					
404	**6.72**	6.73	16.28	16.29	26.34
434	**5.99**	7.02	17.25	18.28	27.40
464	**5.77**	5.54	35.34	35.11	25.63
494	5.7	**1.74**	24.11	20.15	26.11
BEAM 08					
384	**18.08**	17.66	37.58	37.16	28.35
404	12.14	**10.81**	28.54	27.21	28.58
444	8.00	**6.64**	20.11	19.37	30.24
484	7.82	**7.45**	19.93	19.56	31.72
544	7.19	**6.62**	37.37	36.80	33.24

Furthermore, from VIC-2D, the direction of the experimentally measured principal compressive strains at $V/V_{max} = 0.91$ (picture number 222) were obtained for beam 08 – Figure 36.a. Minor directions indicate the contribution of the direct strut to the shear force transferring. Also, the major direction (stress strain) is represented for the concerned beam at about 90% of the maximum load – Figure 36.b.

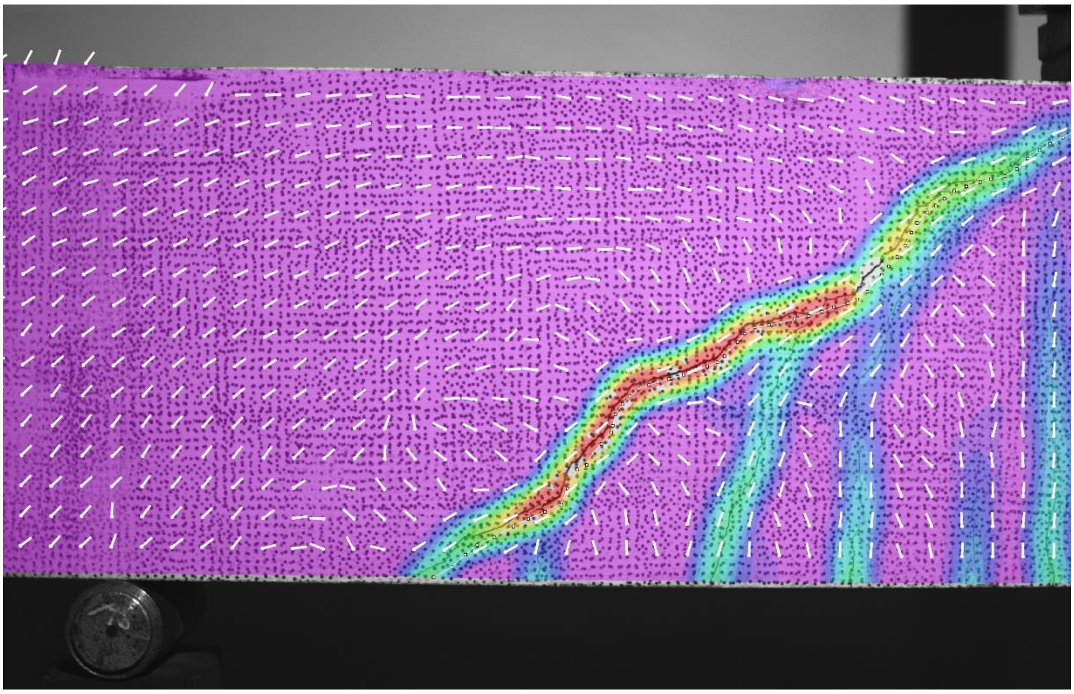

(a)

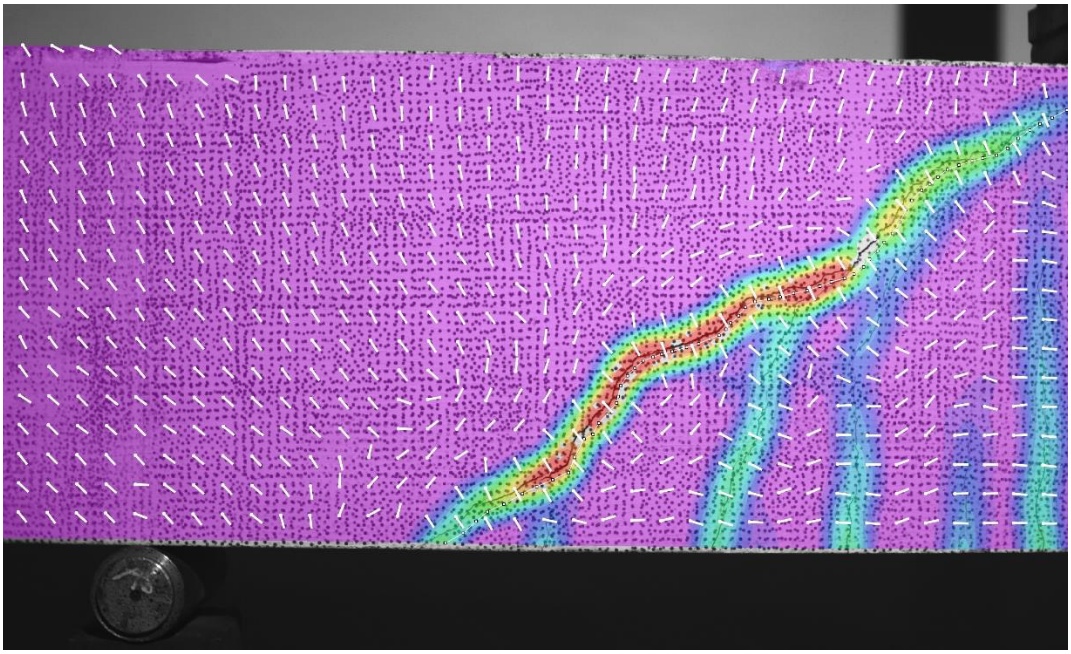

(b)

Figure 36 - Strain field acting in beam 08 (picture 222: V/Vmax = 0.91) indicating the development of tensile stress perpendicular to the crack formation and compression stress parallel to a direct strut: (a) Minor Direction (b) Major Direction.

4.1.5 Stirrups

For beam 08, stirrup contribution was computed by using sisal yarn physical and mechanical properties previously informed (section 3.5) and its bonding capacity was estimated from Silva *et al*. [123]. Pull-out tests conducted for twisted arch fiber type were used as reference, for curing age of 21 days considering that bond strength reaches its maximum capacity at 14 days with no further increment on strength for ages of 21 and 28 days. The diameter of the twisted sisal fibers used by Silva *et al.* [123] was approximately 600 μm and the results shown an interfacial shear strength of about 0.70 MPa with corresponding slip of 0.83 mm.

The results obtained for all the mechanisms previously explained are presented in figures 37, 38 and 39 with each mechanism indicated in Tables 13, 14 and 15 for beams 02, 07 and 08 respectively. As one can observe, the methods employed for beam 02 appear to accurately represent the experimental behavior of the beam – V_t/V_{exp} ranging from 0.81 to 1.05 - whereas specimens 07 and 08 did not demonstrate a strong approximation – V_t/V_{exp} ranging from 0.62 to 1.34.

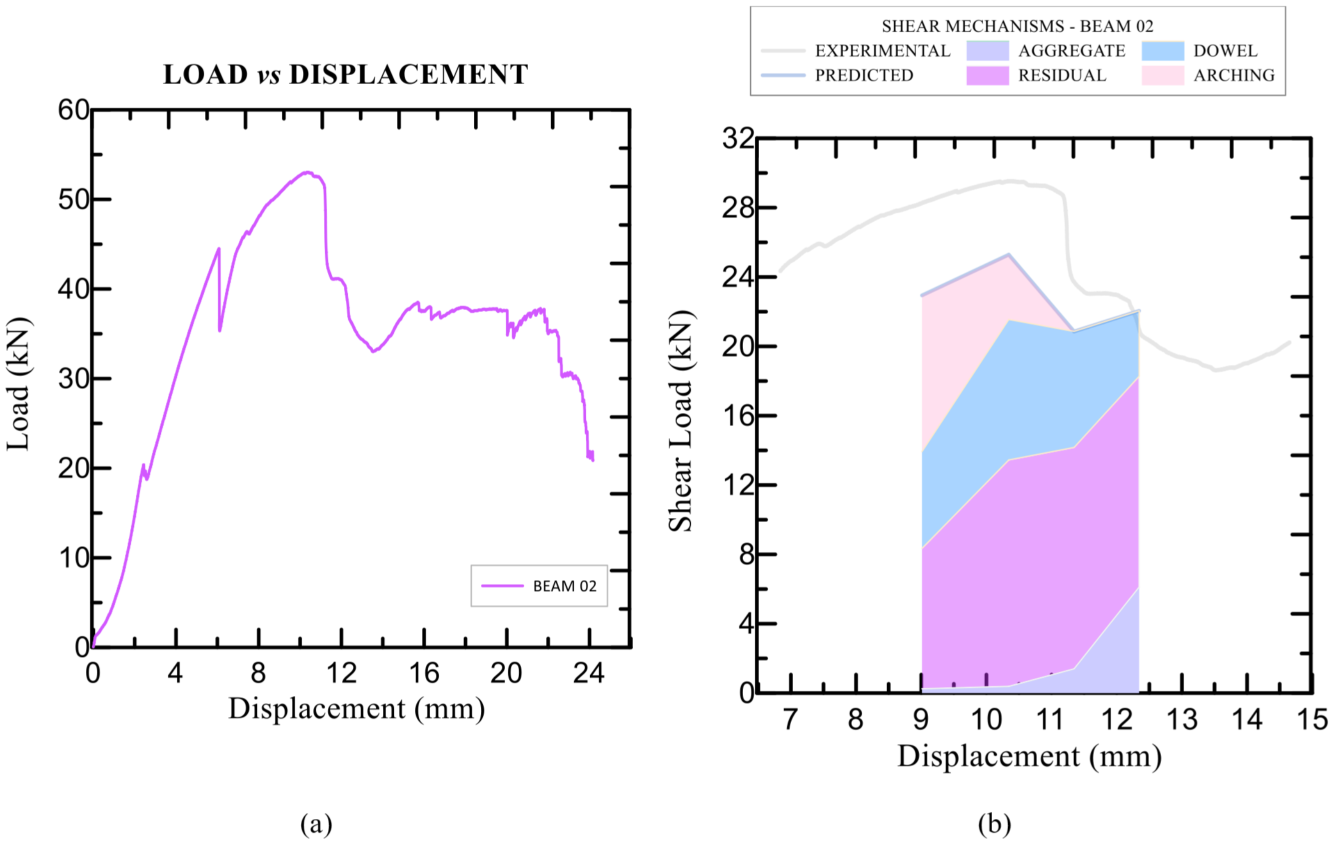

Figure 37 – Behavior of beam 02 specimen in a 3-point bending test: (a) load *versus* displacement for beam reinforced with sisal fiber (b) shear mechanisms acting on beam 02.

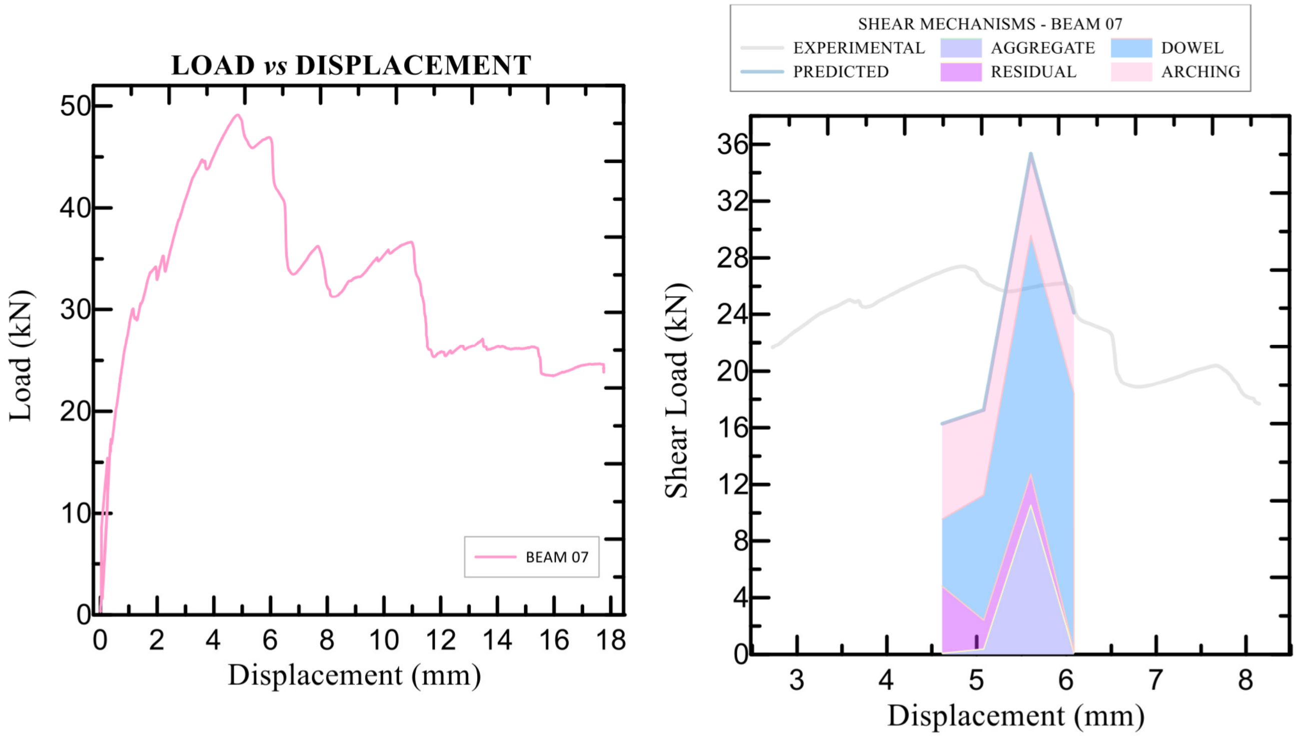

(a) (b)

Figure 38 – Behavior of beam 07 in a 3-point bending test: (a) load versus displacement for beam 07 (b) shear mechanisms acting on beam 07.

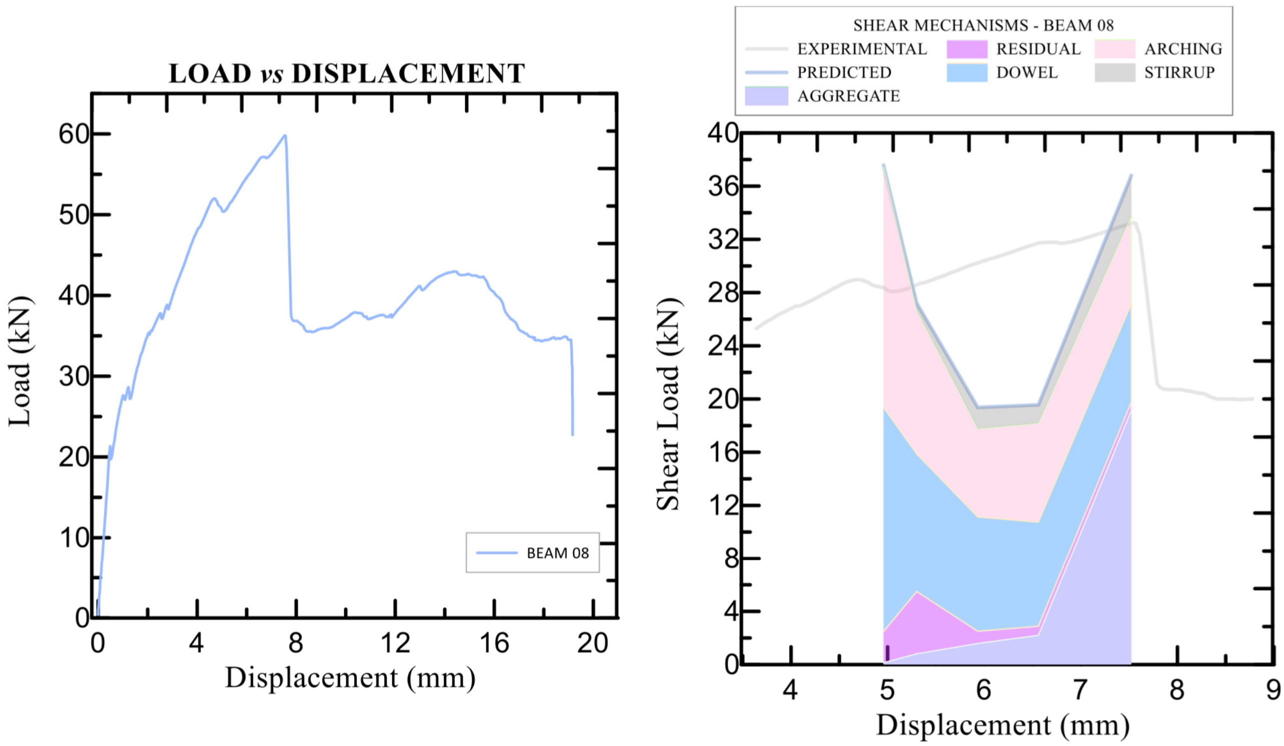

(a) (b)

Figure 39 – Behavior of beam 08 in a 3-point bending test: (a) Load versus displacement for beam 08 (b) shear mechanisms acting on beam 08.

Table 13 - Mechanism acting in specimen 02 with correspondent experimental shear load (kN).

BEAM 02							
Time (s)	V_{Agg}	V_{RS}	$V_{D,tens}$	V_C	$\sum V_{eng,res,pino,arco}$(kN)	$V_{experimental}$ (kN)	V_t/V_{exp}
540	0.25	8.10	5.58	9.01	22.94	28.27	0.81
620	0.39	13.06	8.10	3.74	25.29	29.54	0.86
680	1.40	12.77	6.69	-	20.86	23.73	0.88
740	6.12	12.16	3.77	-	22.05	20.97	1.05

Table 14 - Mechanism acting in specimen 07 with correspondent experimental shear load (kN).

BEAM 07							
Time (s)	V_{Agg}	V_{RS}	$V_{D,tens}$	V_C	$\sum V_{eng,res,pino,arco}$(kN)	$V_{experimental}$ (kN)	V_t/V_{exp}
404	0.086	4.72	4.76	6.72	16.28	26.34	0.62
434	0.382	2.04	8.84	5.99	17.25	27.40	0.63
464	10.56	2.19	16.82	5.77	35.34	25.63	1.34
494	0.114	0.098	18.20	5.70	24.11	26.11	0.92

Table 15 - Mechanism acting in specimen 08 with correspondent experimental shear load (kN).

BEAM 08							
Time (s)	V_{Agg}	V_{RS}	$V_{D,tens}$	V_C	$V_{stirrup}$	$\sum V_{calculated}$ (kN)	$V_{experimental}$ (kN)
384	0.14	2.35	16.88	18.08	0.13	37.58	28.35
404	0.81	4.69	10.37	10.81	0.53	27.21	28.58
444	1.59	0.92	8.62	6.64	0.98	19.37	30.24
484	2.2	0.69	7.85	7.45	1.37	19.56	31.72
544	19.15	0.63	7.38	6.62	3.02	36.80	33.24

As anticipated, the arching action gradually decreases as the load increases. Notably, while beam 02 exhibited an increase in residual strength attributed to fiber contributions with the load increment, specimens 07 and 08 experienced a reduction in residual strength and an increase in aggregate interlock. This phenomenon can be explained by the development of larger-sized cracks.

The dowell effect is significantly influenced by the location of the critical crack, as outlined by Cavagnis [83]. This research affirms that dowelling action is more constrained when the crack develops farther from the end support, like for beam 02 (24.3% - 32.0%). Conversely, it becomes more pronounced when the critical crack is in close proximity to it, as observed for beams 07 and 08 (29.2% – 75.5%).

Finally, due to the relatively low stiffness of sisal yarn, its contribution as a $V_{stirrup}$ was limited. Nevertheless, as the crack widened, $V_{stirrup}$ increased, as expected. For an accurate determination of the shear strength contribution from the transverse reinforcement, a deeper understanding of its bond with the concrete matrix is essential, thus requiring the execution of pull-out tests.

6.
FINAL REMARKS

The present work formulated strategies for using bamboo in reinforced concrete, particularly for low-rising buildings, focusing on the study of the shear behavior of the structures. Among all the options tested, the use of sisal yarn has shown greater feasibility as a building technique. The sisal yarn not only enhances strength but also offers the advantage of being a less time-consuming procedure compared to bamboo stirrups.

Furthermore, coating the bamboo has shown to be mandatory in order to improve its bonding with concrete, ensure an efficient load distribution and protect it from aging. Nevertheless, proper care should be taken into preparing the bamboo before applying the coating. It is suggested the use of castor oil since it is a more eco-friendly technique compared to the use of Sikadur.

In addition to the challenges in quality control, bamboo is a non-dimensional material. The irregular shape and varying sizes of unprocessed bamboo make it harder to establish standardized design codes. However, it is urgent to develop guidelines that address the utilization of non-conventional composite materials in the construction industry. Although the use of ACI CODE-440.11-22 [71] can effectively estimate the bending strength of beams, it has demonstrated a notably conservative tendency in shear design, which is consistent with the findings reported in the literature review [124].

Regarding the shear mechanisms, a distinct dominant mechanism was observed for each beam at the point of rupture. For beam 02 the residual strength was the major mechanism acting on the structure, while for beam 08, aggregate interlock prevailed and for 07 dowel action was the main contributor to resistant capacity of the beams. The sisal yarn contribution, calculated as stirrup mechanism, increased as the applied load neared the point of rupture. Nevertheless, due to its relatively lower rigidity, the sisal yarn's impact on the beam's strength did not emerge as the prevailing mechanism.

In all cases, the compression chord or arching effect decreased during the process of loading, playing an important role at load levels significantly lower than the maximum load. Furthermore, a decrease in the residual strength was observed for beams 07 and 08, correlating with the enlargement of cracks. Notably, specimen 02 exhibited a contrary trend, with an increase in the residual strength attributed to the activation of fiber contributions in the post-cracking stage. Aggregate interlock relies strongly on kinematic of the critical crack, being mobilized for higher crack opening and sliding.

The models derived from shear mechanisms, aimed at representing the structural behavior, proved to be well-suited for beam 02. However, for specimens 07 and 08, a deviation (V_t/V_{exp} ranging from 0.62 to 1.34) was observed between the expected and experimental results. In general, the predictive constitutive models must be refined to accurately capture bamboo's behavior and encompass the effects of shear-transfer actions, thus accounting for minor variations when compared to the experimental results.

Finally, it is demonstrated the potential of bamboo for utilization in the AEC (Architecture, Engineering, and Construction) industry. Bamboo culms can serve as a sustainable alternative to steel for structural applications in low-rise buildings, with the potential to support the local economy, reduce CO_2 emissions and address housing challenges through feasible solutions. However, it is noteworthy that many bamboo-related processes still rely heavily on manual craftsmanship. Therefore, there is a critical need to automate and standardize the procedures involved in working with bamboo. Suggestions for further work include:

- The use of a greener matrix such as utilizing recycled aggregates or replacing the Portland cement with a geopolymer cement with lower (or zero) clinker content should be considered.

- The interface and bonding between sisal yarn and concrete must be deeper investigated through execution of pull-out tests, for instance.

- Techniques to improve frictional adherence of bamboo in concrete could be explored, as well as ways to enhance strength at the nodes.

- Constitutive models adapted to bamboo's specific attributes, such as its tapered geometry and hollow structure, must be considered in calculations.

7. REFERÊNCIAS BIBLIOGRÁFICAS

[1] S. et al. Mehra, "Impact of construction material on environment.," *Ecological and*

Health Effects of Building Materials, pp. 427–442, 2022.

[2] R. An, B. Yu, R. Li, and Y. M. Wei, "Potential of energy savings and CO2 emission reduction in China's iron and steel industry," *Appl. Energy*, vol. 226, no. February, pp. 862–880, 2018, doi: 10.1016/j.apenergy.2018.06.044.

[3] K. Ghavami, "Ultimate load behaviour of bamboo-reinforced lightweight concrete beams," *Cem. Concr. Compos.*, vol. 17, no. 4, pp. 281–288, 1995, doi: 10.1016/0958-9465(95)00018-8.

[4] K. Ghavami, "Bamboo as reinforcement in structural concrete elements," *Cem. Concr. Compos.*, vol. 27, no. 6, pp. 637–649, 2005, doi: 10.1016/j.cemconcomp.2004.06.002.

[5] A. L. Beraldo, A. Azzini, K. Ghavami, and M. A. R. Pereira, "Bambu: Características e Aplicações," *Tecnologias e Materiais Alternativos de Construção*. pp. 253–276, 2010.

[6] O. H. Lopez, *Bamboo: the gift of the gods.* Bogotá: D'Vinni Ltda, 2003.

[7] A. L. Pereira, Marco Antonio dos Reis; BERALDO, *Bambu de corpo e alma*. Bauru – SP: Canal 6 Editora, 2007.

[8] E. N. Tokuda, J. de Toledo Viana, G. A. Nascimento Amorim, R. Dias, and S. Bigotto, "Design Procedure for Reinforced Concrete Beams and Reinforcement Replacement by Bamboo," *Comput. Water, Energy, Environ. Eng.*, vol. 09, no. 03, pp. 37–47, 2020, doi: 10.4236/cweee.2020.93004.

[9] A. Sabbir, S. M. A. Hoq, and S. F. Fancy, "Determination of Tensile Property of Bamboo for Using as Potential Reinforcement in the Concrete," no. October, pp. 47–51, 2011.

[10] S. Qaiser, A. Hameed, R. Alyousef, F. Aslam, and H. Alabduljabbar, "Flexural strength improvement in bamboo reinforced concrete beams subjected to pure bending," *J. Build. Eng.*, vol. 31, no. February, p. 101289, 2020, doi: 10.1016/j.jobe.2020.101289.

[11] G. C. dos S. Ferreira, "Vigas de concreto armadas com taliscas de bambu

Dendrocalamus Giganteus," 2007. doi: 10.47749/T/UNICAMP.2007.404877.

[12] H. Archila, S. Kaminski, D. Trujillo, E. Zea Escamilla, and K. A. Harries, "Bamboo reinforced concrete: a critical review," *Mater. Struct. Constr.*, vol. 51, no. 4, 2018, doi: 10.1617/s11527-018-1228-6.

[13] K. Harries and C. Rogers, "Experimental demonstration of the poor structural experimental demonstration of the poor structural performance of bamboo-reinforced concrete," *Int. Conf. Non-conventional Mater. Technol. NOCMAT 2022*, no. June, pp. 1–8, 2022, doi: 10.5281/zenodo.6569780.

[14] H. G. Geymayer and F. B. Cox, "Bamboo reinforced concrete," *J. Am. Concr. Inst.*, 1970.

[15] A. Agarwal, B. Nanda, and D. Maity, "Experimental investigation on chemically treated bamboo reinforced concrete beams and columns," *Constr. Build. Mater.*, vol. 71, pp. 610–617, 2014, doi: https://doi.org/10.1016/j.conbuildmat.2014.09.011.

[16] B. Mondal, D. Maity, and P. K. Patra, "Load and resistance factor design for bamboo reinforced concrete beam in ultimate flexural limit state," *Struct. Saf.*, vol. 102, p. 102323, 2023, doi: https://doi.org/10.1016/j.strusafe.2023.102323.

[17] P. R. Mali and D. Datta, "Experimental evaluation of bamboo reinforced concrete beams," *J. Build. Eng.*, vol. 28, no. March 2019, p. 101071, 2020, doi: 10.1016/j.jobe.2019.101071.

[18] L. Tian, "Flexural Behavior of Sprayed Lightweight Composite Mortar-original Bamboo Composite Beams : Experimental Study," no. March, 2019, doi: 10.15376/biores.14.1.500-517.

[19] G. C. et al. FERREIRA, "Flexural and shear behaviour of concrete beams reinforced with bamboo.," *Int. J. Sustain. Mater. Struct. Syst.*, vol. 2, no. 3–4, pp. 335–347, 2016.

[20] A. Mark and A. O. Russell, "A comparative study of Bamboo reinforced concrete beams using different stirrup materials for rural construction," *Int. J. Civ. Struct.*

Eng., vol. 2, no. 1, pp. 407–423, 2011, doi: 10.6088/ijcser.00202010120.

[21] O. F. da Silva, "ESTUDO SOBRE A SUBSTITUIÇÃO DO AÇO LISO PELO BAMBUSA VULGARIS , COMO REFORÇO EM VIGAS DE BAMBUSA VULGARIS , COMO REFORÇO EM VIGAS DE CONCRETO, PARA O USO EM CONSTRUÇÕES RURAIS," Universidade Federal de Alagoas, 2007.

[22] M. S. Sandanayake, "Environmental Impacts of Construction in Building Industry—A Review of Knowledge Advances, Gaps and Future Directions," *Knowledge*, vol. 2, no. 1, pp. 139–156, 2022, doi: 10.3390/knowledge2010008.

[23] L. Osorio, E. Trujillo, F. Lens, J. Ivens, I. Verpoest, and A. W. Van Vuure, "In-depth study of the microstructure of bamboo fibres and their relation to the mechanical properties," no. June, 2018, doi: 10.1177/0731684418783055.

[24] R. Manandhar, J. Kim, and J. Kim, "Environmental , social and economic sustainability of bamboo and bamboo-based construction materials in buildings," *J. Asian Archit. Build. Eng.*, vol. 18, no. 2, pp. 49–59, 2019, doi: 10.1080/13467581.2019.1595629.

[25] Pr. SUSTAINABILITY, "SimaPro database manual," *Pré Sustain. Amersfoort, Netherlands*, 2020.

[26] J. J. A. Janssen, *Designing and Building with Bamboo*, no. 20. Netherlands: International Network for Bamboo and Rattan, 2000.

[27] N. Serres, S. Braymand, and F. Feugeas, "Environmental evaluation of concrete made from recycled concrete aggregate implementing life cycle assessment," *J. Build. Eng.*, vol. 5, pp. 24–33, 2016, doi: 10.1016/j.jobe.2015.11.004.

[28] L. BLACK, "Low clinker cement as a sustainable construction material.," *Sustain. Constr. Mater.*, pp. 415–457, 2016.

[29] P. Azarsa and R. Gupta, "Durability and leach-ability evaluation of K-based geopolymer concrete in real environmental conditions," *Case Stud. Constr. Mater.*, vol. 13, p. e00366, 2020, doi: 10.1016/j.cscm.2020.e00366.

[30] R. A. Sá, M. G. Sá, K. Sankar, and W. M. Kriven, "Geopolymer-bamboo

composite – A novel sustainable construction material," *Constr. Build. Mater.*, vol. 123, pp. 501–507, 2016, doi: 10.1016/j.conbuildmat.2016.07.037.

[31] Ana Carolina Constâncio Trindade, "A study on the mixture design and mechanical performance of strain-hardening geopolymer composites (SHGC) under extreme conditions Ana Carolina Constâncio Trindade A study on the mixture design and mechanical performance of strain-hardening geopolymer c," 2021.

[32] N. Shehata, E. Taha, and M. Ali, "Recent progress in environmentally friendly geopolymers : A review," *Sci. Total Environ.*, vol. 762, p. 143166, 2021, doi: 10.1016/j.scitotenv.2020.143166.

[33] S. Canavan, D. M. Richardson, V. Visser, J. J. Le Roux, M. S. Vorontsova, and J. R. U. Wilson, "The global distribution of bamboos : assessing correlates of introduction and invasion," *AoB Plants*, 2016, doi: 10.1093/aobpla/plw078.

[34] O. H. López, "Manual de construción con bambú." Estudos Técnicos Colombianos Ed. Bogotá: Universidad Nacional de Colombia, Centro de Investigación de Bambu y Madera – CIBAM, 1974.

[35] T. S. . A. P. S. G. Filgueiras, "A Checklist of the Basal Grasses and Bamboos in Brazil (POACEAE)," *J. Am. Bamboo Soc.*, vol. 18, 2004.

[36] Guadua Bamboo, "Cucuta bridge," *http://www.guaduabamboo.com*, 2016.

[37] V. M. Andrade Molina, "Bambú en la construcción análisis de diferentes casos de estudio con sistemas constructivos en bambú.pdf," Universidade de Évora, 2019.

[38] A. et al. Gatóo, "Sustainable structures : bamboo standards and building codes," *Eng. Sustain.*, vol. 167, no. ES5, pp. 189–196, 2014.

[39] D. R. Akwada and E. Akinlabi, "ECONOMIC , SOCIAL AND ENVIRONMENTAL ASSESSMENT OF BAMBOO FOR ECONOMIC , SOCIAL AND ENVIRONMENTAL ASSESSMENT OF BAMBOO FOR," no. August, 2018.

[40] J. L. Guedes Pinto, P. F. da Rocha, and C. C. D. d´Oliveira Bastos, "Construções

com bambu.," *Tec-Usu*, vol. 1, no. 1, pp. 1–32, 2018.

[41] T. Gangwar, "Microimaging-informed continuum micromechanics accurately predicts macroscopic stiffness and strength properties of hierarchical plant culm materials," no. March, 2019, doi: 10.1016/j.mechmat.2019.01.009.

[42] H. Arifin, A. A. Afriansya, A. A. Amiruddin, N. M. Nurazzi, and M. N. F. Norrrahim, "Bamboo reinforced polymer composite - A comprehensive review Bamboo reinforced polymer composite - A comprehensive review," *IOP Conf. Ser. Mater. Sci. Eng.*, vol. 344, pp. 0–10, 2018, doi: 10.1088/1757-899X/344/1/012008.

[43] P. L. FILGUEIRAS, T. S.; VIANA, "Bambus brasileiros: morfologia, taxonomia, distribuição e conservação.," *Bambus no Brasil: da biologia à tecnologia.*, Rio de Janeiro, pp. 10–27, 2017.

[44] J. G. De Almeida, "Potencialidades do Bambu," *Sustentabilidade em Debate*, no. 2009, pp. 178–195, 2016, doi: 10.18472/SustDeb.v7n3.2016.21887.

[45] W. Liese, "Anatomy and properties of bamboo," in *Proceedings of the International Bamboo Workshop*, 1985, pp. 196–208.

[46] K. Ghavami, "Bamboo: Low cost and energy saving construction materials.," *Mod. bamboo Struct.*, vol. 1, no. 1, pp. 5–21, 2008.

[47] W. Liese, *The Anatomy of Bamboo Culms*. Leiden, The Netherlands: BRILL, 1998. doi: 10.1163/9789004502468.

[48] W. Liese and H. Tang, "Properties of the Bamboo Culm," 2015, pp. 227–256. doi: 10.1007/978-3-319-14133-6_8.

[49] G. O. García, "El bambú como agente de cambio: La actualización de su aprovechamiento em la región de Bengala," Madrid: Universidade Politécnica de Madrid.

[50] D. Kravtsova, "Estudo experimental de bambu da e spécie ' Phyllostachys Pubescens ' sob t orção e f lexão Daria Kravtsova Estudo experimental de bambu da e spécie ' Phyllostachys Pubescens ' sob t orção e f lexão," Pontifícia

Universidade Católica do Rio de Janeiro (PUC-Rio), 2011.

[51] T. Tan *et al.*, “Mechanical properties of functionally graded hierarchical bamboo structures,” *Acta Biomater.*, vol. 7, no. 10, pp. 3796–3803, 2011, doi: 10.1016/j.actbio.2011.06.008.

[52] I. de O. et al. Da Mota, “Estudo das Propriedades Físicas e Mecânicas do Bambu Brasileiro (Bambusa vulgaris vittata) para Aplicação na Construção de Sistemas Hidráulicos Alternativos de Distribuição de Água à Baixa Pressão,” *Rev. Estud. Ambient.*, vol. 19, no. 1, pp. 18–26, 2017, doi: 10.7867/1983-1501.2017v19n1p18-26.

[53] L. E. Ghavami, Khosrow; Barbosa, Normando Perazzo; MOREIRA, “Bambu como Material de Engenharia,” in *Avaliação de Desempenho de Tecnologias Construtivas Inovadoras: Conforto Ambiental, Durabilidade e Pós-Ocupação*, 2017, pp. 305–348.

[54] H. K. Chow, “Bamboo as a material for reinforcing concrete,” *PhD Thesis*, 1914.

[55] A. M. Argollo Ferrão, “TALISCAS DE BAMBU EM MATRIZES DE CONCRETO: CARACTERiSTICAS FISICO-MECANICAS,” *Master Thesis*, 1992.

[56] A. Hidayat, N., & Aldo, “Bamboo Reinforcement Concrete Beam as Innovation for Low-cost Earthquake Resistant House.,” *J. Phys. Conf. Ser.*, vol. 1625, no. 1, pp. 012–026, 2020.

[57] A. C. B. Filho, H. C. L. Júnior, N. P. Barbosa, and F. L. Willrich, “Comportamento estrutural de vigas de concreto reforçadas com ripas de bambu cravejadas de pinos Structural behavior of concrete beams reinforced with pinned bamboo-splints,” no. 81, pp. 1115–1122, 2010.

[58] C. A. C. of South Carolina. Engineering Experiment Station and H. E. Glenn, *Bamboo Reinforcement in Portland Cement Concrete*. 1950. [Online]. Available: https://books.google.com.br/books?id=7O85xAEACAAJ

[59] L. P. Mesquita, C. J. Czarnieski, A. C. B. Filho, and F. L. Willrich, “Determinação

da tensão de aderência do bambu-concreto Determination of the bamboo-concrete bond stress," no. 45, pp. 505–516, 2006.

[60] A. Khatib and G. Nounu, "Corrugated bamboo as reinforcement in concrete," vol. 170, no. Table 1, pp. 311–318, 2017.

[61] A. Javadian, I. F. C. Smith, N. Saeidi, and D. E. Hebel, "Mechanical Properties of Bamboo Through Measurement of Culm Physical Properties for Composite Fabrication of Structural Concrete Reinforcement," vol. 6, no. February, pp. 1–18, 2019, doi: 10.3389/fmats.2019.00015.

[62] A. Azadeh and H. H. Kazemi, "New Approaches to Bond between Bamboo and Concrete," in *Non-Conventional Materials and Technologies for Sustainable Engineering*, 2014, vol. 600, pp. 69–77. doi: 10.4028/www.scientific.net/KEM.600.69.

[63] M. Al-fasih, "Tensile properties of bamboo strips and flexural behaviour of the bamboo Tensile properties of bamboo strips and flexural behaviour of the bamboo reinforced concrete beams," *Eur. J. Environ. Civ. Eng.*, vol. 0, no. 0, pp. 1–17, 2021, doi: 10.1080/19648189.2021.1945954.

[64] M. Muhtar, "The Measurement of the Local Slip in Bamboo-Reinforced Concrete Beams Using," *J. Reniwable Mater.*, 2021, doi: 10.32604/jrm.2021.015452.

[65] A. P. Adewuyi, A. A. Otukoya, and O. A. Olaniyi, "Comparative Studies of Steel , Bamboo and Rattan as Reinforcing Bars in Concrete : Tensile and Flexural Characteristics," no. June, pp. 228–238, 2015.

[66] C. Paper, R. Sutharsan, and C. Ganesh, "Experimental study on Bamboo as a reinforcing material in concrete," no. January, 2020, doi: 10.1063/1.5141561.

[67] M. A. Salau, "Characteristic Strength of Concrete Column Reinforced with Bamboo Strips," *J. Sustain. Dev.*, vol. 5, no. 1, pp. 133–143, 2012, doi: 10.5539/jsd.v5n1p133.

[68] A. Kaware, "Analysis Of Bamboo Reinforced Concrete Column," *Int. J. Innov. Res. Sci.*, vol. 2, no. 6, pp. 1–10, 2013.

[69] M. Lei *et al.*, “Experimental Investigation on Short Concrete Columns Reinforced by Bamboo Scrimber under Axial Compression Loads,” vol. 2020, 2020.

[70] R. Ismail, Y. C. Bon, and N. Adiba, “Strength Behavior of Bamboo-Reinforced Concrete Slabs Strength Behavior of Bamboo-Reinforced Concrete Slabs,” *IOP Conf. Ser. Mater. Sci. Eng. Pap.*, pp. 0–8, 2018, doi: 10.1088/1757-899X/431/11/112003.

[71] ACI (American Concrete Institute), “Building Code Requirements for Structural Concrete Reinforced with Glass Fiber-Reinforced Polymer (GFRP) Bars—Code and Commentary. ACI 440.11-22.,” Farmington Hills, MI: ACI., 2022.

[72] H. C. L. Júnior, F. L. Willrich, and G. Fabro, “Vigas de concreto reforçadas com bambu Dendrocalamus giganteus II : Modelagem e critérios de dimensionamento,” *Rev. Bras. Eng. Agrícola e Ambient. v.9, n.4, p.652-659*, no. 1985, pp. 652–659, 2005.

[73] U. S. N. Civil, E. Labaoratory, P. Hueneme, F. E. Brink, and P. J. Rush, “BAMBOO REINFORCED CONCRETE,” no. February, 1966.

[74] A. Javadian, I. F. C. Smith, and D. E. Hebel, “Application of Sustainable Bamboo - Based Composite Reinforcement in Structural - Concrete Beams : Design and Evaluation,” pp. 1–26, 2020, doi: 10.3390/ma13030696.

[75] B. Masson, “The improvement of bamboo reinforced concrete beams structural behavior under bending, with variation of the bamboo-concrete interface.,” Pontifícia Universidade Católica do Rio de Janeiro (PUC-Rio), 2023.

[76] W. Ritter, *The hennebique design method (Die bauweise hennebique).* Schweizerische Bauzeitung (Zurich), 1899.

[77] E. Mörsch, *Concrete-steel Construction:(Der Eisenbetonbau).* Engineering news publishing Company, 1909.

[78] J. R. de Carvalho, Roberto Chust; Figueiredo Filho, *Cálculo e detalhamento de estruturas usuais de concreto armado: segundo a NBR 6118*. São Carlos: EdUFSCar, 2014.

[79] C. A. X. Villela, “Aplicação da Teoria do Campo de Compressão Modificada aos Perfis Retos de Concreto Armado e Protendido.” Master Thesis, 1993.

[80] F. P. Hirata, “Análise comparativa entre modelos de predição de norma e dados de ensaios na determinação da resistência ao cisalhamento,” *Master Thesis*, 2013.

[81] A. Bogdan and Podgorniak-Stanik, “The influence of concrete strength, distribution of longitudinal reinforcement, amount of transverse reinforcement and member size on shear strength of reinforced concrete members.,” Toronto, ON, Canada: University of Toronto, 1998.

[82] E. C. Bentz, F. J. Vecchio, and M. P. Collins, “Simplified Modified Compression Field Theory for Calculating Shear Strength of Reinforced Concrete Elements,” *ACI Struct. J.*, no. 103, 2007.

[83] F. Cavagnis, “Shear in reinforced concrete without transverse reinforcement : from refined experimental measurements to mechanical models PAR,” *PhD Thesis*, vol. 8216, 2017.

[84] T. L. de Resende, “Contribuição dos mecanismos resistentes à força cortante em vigas de concreto armado sem e com fibras de aço,” Pontifícia Universidade Católica do Rio de Janeiro (PUC-Rio), 2020.

[85] T. A. Gomes, “Mecanismos de Resistência ao Cortante em Vigas de Concreto Armado com Barras de PRFV e Fibras de Basalto,” Pontifícia Universidade Católica do Rio de Janeiro (PUC-Rio), 2022.

[86] J. C. Walraven and H. W. Reinhardt, “THEORY AND EXPERIMENTS ON THE MECHANICAL BEHAVIOUR OF CRACKS IN PLAIN AND REINFORCED CONCRETE SUBJECTED TO SHEAR LOADING,” *Heron*, 1981.

[87] J. . Walraven, *Aggregate interlock: A theoretical and experimental analysis*. Delft University Press, 1980.

[88] T. Ulaga, “Betonbauteile mit Stab- und Lamellenbewehrung,” 2003.

[89] R. Guidotti, “Poinçonnement des planchers-dalles avec colonnes superposées fortement sollicitées,” *PhD Thesis*, vol. 4812, 2010.

[90] B. Li and K. Maekawa, "Contact density model for cracks in concrete," *IABSE reports = Rapp. AIPC = IVBH Berichte*, vol. 54, pp. 51–62, 1987.

[91] L. Resende, D. C. T. Cardoso, and L. C. D. Shehata, "Experimental and theoretical investigation on the stress transfer across cracks due to combined action of steel fibers and aggregate interlock," *Cem. Concr. Compos.*, vol. 124, no. September, 2021, doi: 10.1016/j.cemconcomp.2021.104239.

[92] A. Hillerborg, M. Modéer, and P.-E. Petersson, "Analysis of crack formation and crack growth in concrete by means of fracture mechanics and finite elements," *Cem. Concr. Res.*, vol. 6, no. 6, pp. 773–781, 1976, doi: https://doi.org/10.1016/0008-8846(76)90007-7.

[93] E. N. Vintzēleou and T. P. Tassios, "Mathematical models for dowel action under monotonic and cyclic conditions," *Mag. Concr. Res.*, vol. 38, no. 134, pp. 13–22, 1986, doi: 10.1680/macr.1986.38.134.13.

[94] A. C. I. S. Journal and M. Fern, "Post-Punching Behavior of Flat Slabs," no. September 2013, 2016.

[95] F. Cavagnis, M. Fernández Ruiz, and A. Muttoni, "An analysis of the shear-transfer actions in reinforced concrete members without transverse reinforcement based on refined experimental measurements," *Struct. Concr.*, vol. 19, no. 1, pp. 49–64, 2018, doi: 10.1002/suco.201700145.

[96] A. M. López, M. F. Ruiz, and P. F. M. Sosa, "The influence of transverse reinforcement and yielding of flexural reinforcement on the shear-transfer actions of RC members," *Eng. Struct. J.*, vol. 234, no. July 2020, 2021, doi: 10.1016/j.engstruct.2021.111949.

[97] G. N. J. Kani, "The Riddle of Shear Failure and its Solution," *ACI J. Proc.*, vol. 61, no. 4, 1964, doi: 10.14359/7791.

[98] F. Cavagnis, M. Fernández Ruiz, and A. Muttoni, "A mechanical model for failures in shear of members without transverse reinforcement based on development of a critical shear crack," *Eng. Struct.*, vol. 157, pp. 300–315, 2018, doi: https://doi.org/10.1016/j.engstruct.2017.12.004.

[99] J. Huber, P.; Huber, T. ; Kollegger, “Investigation of the shear behavior of RC beams on the basis of measured crack kinematics.,” *Eng. Struct.*, pp. 41–58, 2016.

[100] S. Campana, A. Anastasi, and M. Ferna, “Analysis of shear-transfer actions on one-way RC members based on measured cracking pattern and failure kinematics,” *Mag. Concr. Res.*, vol. 65, no. 6, pp. 386–404, 2013.

[101] M. Shahnewaz, A. Rteil, and M. S. Alam, “Shear strength of reinforced concrete deep beams – A review with improved model by genetic algorithm and reliability analysis,” *Structures*, vol. 23, pp. 494–508, 2020, doi: https://doi.org/10.1016/j.istruc.2019.09.006.

[102] J. G. M. James K. Wight, *Reinforced Concrete - Mechanics & Design*, 6th ed., no. 1. 2004.

[103] T. L. Resende, “RESISTÊNCIA À FORÇA CORTANTE DE VIGAS DE CONCRETO AUTOADENSÁVEL,” *Master Thesis*, 2014.

[104] N. D. Tung, C. Betschoga, and N. V. Tue, “Analysis of the crack development and shear transfer mechanisms of reinforced concrete beams with low amounts of shear reinforcement,” *Eng. Struct.*, vol. 222, p. 111114, 2020, doi: https://doi.org/10.1016/j.engstruct.2020.111114.

[105] L. Vandewalle *et al.*, “RILEM TC 162-TDF Test and design methods for steel fibre reinforced concrete Recommendations,” *Mater. Struct.*, vol. 33, no. September, pp. 75–81, 2000.

[106] R. de S. Castoldi, “Propriedades mecânicas e durabilidade de concretos reforçados com fibras de polipropileno e sisal.,” *Master Thesis*, pp. 1–147, 2018.

[107] D. Ohrnberger, “The bamboos of the world: annotated nomenclature and literature of the species and the higher and lower taxa,” pp. 525–585, doi: 10.1016/B978-0-444-50020-5.50019-8.

[108] M. Ramakrishnan *et al.*, “Genetics and genomics of moso bamboo (Phyllostachys edulis): Current status, future challenges, and biotechnological opportunities toward a sustainable bamboo industry,” *Food Energy Secur.*, vol. 9, no. 4, pp. 1–

36, 2020, doi: 10.1002/fes3.229.

[109] ABNT NBR16828, *Bamboo Structures - Part 2: Determination of physical and mechanical properties of bamboo*. Rio de Janeiro, 2022.

[110] L. Henrique, S. Ribeiro, and L. M. De Aguiar, “Influence of section and moisture content on the tensile strength parallel to fibers of bamboo culms woody material 1,” 2019, doi: 10.1590/1983-40632019v4953562.2.

[111] N. V Santos and D. C. T. Cardoso, “3D printing of vegetable yarn-reinforced polymer components,” *J. Clean. Prod.*, vol. 415, p. 137870, 2023, doi: https://doi.org/10.1016/j.jclepro.2023.137870.

[112] A. Yeboah *et al.*, “Castor oil (Ricinus communis): A review on the chemical composition and physicochemical properties,” *Food Sci. Technol.*, vol. 41, no. December, pp. 399–413, 2021, doi: 10.1590/fst.19620.

[113] M. Vahanvati, “The Challenge of connecting bamboo Abstract : Challenges of building with bamboo in Australia,” *10th World Bamboo Congr. Damyang*, 2015.

[114] B. Masson, “The improvement of bamboo reinforced concrete beams structural behavior under bending, with variation of the bamboo-concrete interface.,” *Master Res. Rep.*, no. January, 2023.

[115] S. Sarkar, O. Adwan, and B. Bose, “Shear stress contributions and failure mechanisms of high strengh reinforced concrete beams,” *Mater. Struct.*, vol. 32, no. 2, pp. 112–116, 1999, doi: 10.1007/BF02479437.

[116] J. Kim and Y. Park, “Prediction of Shear Strength of Reinforced Concrete Beams without Web Reinforcement,” no. 93, pp. 213–222, 1997.

[117] Y. YANG, *Shear Behaviour of Reinforced Concrete Members without Shear Reinforcement*. TU Delft, 2014.

[118] D. A. Hordijk, “Tensile and tensile fatigue behaviour of concrete; experiments, modelling and analyses,” *Heron*, vol. 37, no. 1, pp. 1–79, 1992.

[119] International Federation for Structural Concrete (fib), *Model Code 2010-Final*

Draft: Volume 1, no. 1. 2012.

[120] T. A. Gomes, T. L. de Resende, and D. C. T. Cardoso, "Shear-transfer mechanisms in reinforced concrete beams with GFRP bars and basalt fibers," *Eng. Struct.*, vol. 289, p. 116299, 2023, doi: https://doi.org/10.1016/j.engstruct.2023.116299.

[121] Y. M. Miguel Fernandez Ruiz and Aurelio Muttoni, "Post-Punching Behavior of Flat Slabs," *ACI Struct. J.*, vol. 110, no. 5, doi: 10.14359/51685833.

[122] M. Hetényi, "Beams On Elastic Foundation Theory With Applications In The Fields Of Civil And Mechanical Engineering." Ann Arbor, MI: University of Michigan press, 1955.

[123] F. de A. Silva, "Durabilidade e propriedades mecânicas de compósitos cimentícios reforçados por fibras de sisal.," Universidade Federal do Rio de Janeiro (UFRJ), 2009.

[124] M. A. El Zareef, M. S. Elbisy, and M. Badawi, "Evaluation of code provisions predicting the concrete shear strength of FRP-reinforced members without shear reinforcement," *Compos. Struct.*, vol. 275, p. 114430, 2021, doi: https://doi.org/10.1016/j.compstruct.2021.114430.

Appendix A:

In Appendix A.1, the width, thickness, and nominal area ($A_{nominal}$) of each stirrup created are provided. Appendix A.2 presents the inner and outer diameters at the bottom of the bamboo (D_1 in, bottom and D_1 out, bottom), the outer diameters along two different cross sections of the culm (D_2 and D_3), the inner and outer diameters at the top of the bamboo (D_4 in, bottom and D_4 out, bottom), as well as the mean inner and outer diameters (Mean D_{in} and Mean D_{out}). Additionally, the average thickness (Average Thickness) and the approximated area (S approximated) of the bamboo cross-section are specified. The second row in the tables of Appendix A.2 indicates the measured culm, with "B" referring to the bottom, "M" to the middle, and "T" to the top sections.

A.1 Bamboo stirrups characteristics

STIRRUPS					
N° stirrup	Width (mm)		Thickness (mm)		$A_{nominal}$ mm²
1	6.75	5.71	1.33	1.4875	8.49
	5.5		1.31		
	5.3		1.91		
	6		1.4		
	5		-		
2	5.7	5.14	2.26	1.705	8.76
	4.2		1.5		
	5.3		1.49		
	5		1.57		
	5.5		-		
3	7.2	6.7925	1.24	1.635	11.106
	6.2		2.06		
	7.24		1.78		
	6.53		1.46		
	-		-		
4	5.2	5.09	1.26	1.454	7.401
	4.93		1.5		
	4.91		1.28		
	5.32		1.37		
	-		1.86		
5	6.5	5.7725	1.31	1.624	9.37
	5.6		2.07		
	7.05		1.6		
	3.94		1.4		
	-		1.74		
6	4.3	4.604	1.06	1.528	7.035
	4.08		2.11		
	5.13		1.36		
	4.02		1.08		

	5.49		2.03		
7	6.76	6.2375	1.27	1.53	9.54
	6.94		1.68		
	6.09		1.3		
	5.16		1.5		
	-		1.9		
8	6.3	5.7325	1.35	1.81	10.38
	7		1.87		
	5.29		1.96		
	4.34		1.75		
	-		2.12		
9	6.69	6.484	1.17	1.49	9.66
	7		2		
	5.95		1.1		
	6.25		1.05		
	6.53		2.13		
10	6.1	6.26	1.17	1.415	8.86
	5.15		1.6		
	5.85		1.49		
	7.2		1.4		
	7		-		
11	7.76	7.126	0.89	1.386	9.88
	5.9		2.12		
	7.61		1.75		
	7.36		1.18		
	7		0.99		
12	6.05	6.455	1.6	1.475	9.52
	6.91		1.3		
	5.76		0.9		
	7.1		2.1		
	-		-		
13	7.78	7.8575	1.27	1.552	12.19
	8.68		2.2		
	7.45		1.16		
	7.52		1.67		
	-		1.46		
14	6.8	6.038	1.2	1.5425	9.31
	6		1.6		
	5.04		2.06		
	6.9		1.31		
	5.45		-		
15	6	5.656	1.33	1.352	7.65
	4.66		1.7		
	4.8		1.14		
	7.06		1.24		
	5.76		1.35		
16	5.96	6.472	0.75	1.47	9.51
	6.75		2		
	5.94		1.3		
	6.5		1.19		
	7.21		2.11		
17	5.1	5.668	1.15	1.222	6.93
	5.9		2.02		

	5.77		0.87		
	6		0.82		
	5.57		1.25		
18	9.88	9.994	1.46	1.696	16.95
	9.14		1.6		
	9		2.24		
	10.57		1.8		
	11.38		1.38		
19	5.03	5.206	1.41	1.486	7.74
	5.51		1.22		
	4.96		1.57		
	4.8		1.15		
	5.73		2.08		
20	5.13	5.078	1.1	1.486	7.55
	5.3		1.82		
	4.47		1.41		
	4.72		0.96		
	5.77		2.14		
21	4.35	5.53	1.01	1.214	6.71
	6.1		1.31		
	5.73		1.2		
	5.27		1.4		
	6.2		1.15		
22	7	6.602	1.26	1.568	10.35
	7.24		2.29		
	6.54		1.2		
	5.33		1.71		
	6.9		1.38		
23	5.5	5.504	1.15	1.13	6.22
	5.3		1.23		
	4.4		1.18		
	6.6		1.08		
	5.72		1.01		
24	3.6	5.052	1.3	1.406	7.103
	4.68		1.65		
	6.24		1.38		
	4.97		1.5		
	5.77		1.2		
25	5.69	5.61	0.78	1.252	7.024
	5.9		1.08		
	5.35		1.41		
	6.6		1.16		
	4.51		1.83		

Total

	Width (mm)	Thickness (mm)	$A_{nominal}$ mm^2
Mean	6.067	1.48	8.96

Stirrups Used

	Width (mm)	Thickness(mm)	$A_{nominal}$ mm^2
Mean	6.15	1.47	9.026

A.2 Bamboo Longitudinal Reinforcement

	BEAM 02															
	IB		IIB		IIIB		IVB		IT		IIT		IIIT		IVT	
Number of nodes	7		7		6		8		6		7		7		7	
D1 in, bottom	14.61	14.255	14.53	14.725	13.17	12.83	8.97	9.175	11.68	11.635	12.59	12.66	13.92	13.46	11.53	11.095
	13.9		14.92		12.49		9.38		11.59		12.73		13		10.66	
D1 out, bottom	20.3	20.025	21.15	20.975	22.33	21.5	17.05	17.53	17.89	18.28	17.96	18.145	17.93	18.86	15.34	15.72
	19.75		20.8		20.67		18.01		18.67		18.33		19.79		16.1	
D2	18.71	19.03	19.75	20.075	21.14	20.515	16.48	16.78	15.6	16.125	16.84	17.295	15.57	16.185	13.77	14.04
	19.35		20.4		19.89		17.08		16.65		17.75		16.8		14.31	
D3 in, top	12.58	12.25	12.77	12.875	13.99	14.035	11.34	11.48	7.68	8.425	9.32	9.52	9	9.39	8.09	8.235
	11.92		12.98		14.08		11.62		9.17		9.72		9.78		8.38	
D3 out,top	17.48	18.175	18.82	18.935	19.7	18.9	15.08	15.67	12.24	12.795	14.3	15.14	13.9	14.6	11.23	11.6
	18.87		19.05		18.1		16.26		13.35		15.98		15.3		11.97	
Mean Din	13.253		13.8		13.433		10.328		10.03		11.09		11.425		9.665	
Mean Dout	19.077		19.995		20.305		16.66		15.73		16.86		16.55		13.79	
S approximated (m^2)	0.000148		0.000164		0.000182		0.000134		0.000115		0.000127		0.000113		7.59165E-05	
S approximated (mm^2)	147.883		164.431		182.103		134.223		115.404		126.662		112.561		75.917	
Average Thickness	5.824		6.195		6.873		6.333		5.703		5.77		5.123		4.122	

	BEAM 03															
	24B		25T		20B		26B		21B		27B		27T		26T	
Number of nodes	8		8		6		11		7		9		9		8	
D1 in, bottom	11.26		12.36		11.71		11.17		13.17		11.76		10.87		11.01	
	12.25	11.755	13.32	12.84	12.1	11.905	12.61	11.89	12.68	12.925	12.82	12.29	11.31	11.09	10.67	10.84
D1 out, bottom	16.23		18.97		19.07		18.01		19.16		19.37		16.03		15.05	
	18.02	17.125	17.93	18.45	17.93	18.5	19.92	18.965	18.96	19.06	17.76	18.565	14.98	15.505	16.1	15.575
D2	17.34		17.77		18.12		18.49		19.29		18.04		12.97		14.8	
	19	18.17	16.97	17.37	16.81	17.465	17.55	18.02	18.5	18.895	16.9	17.47	14.21	13.59	13.28	14.04
D3	19.65		15.61		17.56		16.61		17.87		16.36		12.44		13.08	
	18.83	19.24	14.76	15.185	16.12	16.84	17.42	17.015	18.8	18.335	16.91	16.635	11.51	11.975	11.5	12.29
D4 in, top	12.52		7.11		11.56		9.92		12.68		11.35		6.37		6.11	
	13.26	12.89	9.53	8.32	10.62	11.09	11.22	10.57	11.97	12.325	10.8	11.075	6.64	6.505	6.5	6.305
D4 out,top	20.11		13.63		15.05		15.65		17.41		15.17		9.36		9.48	9.94
	19.81	19.96	15.3	14.465	16.9	15.975	16.48	16.065	16.7	17.055	16.05	15.61	9.85	9.605	10.4	
Mean Din	12.3225		10.58		11.4975		11.23		12.625		11.6825		8.7975		8.5725	
Mean Dout	18.62375		16.3675		17.195		17.51625		18.33625		17.07		12.66875		12.96125	

S approximated (m²)	0.000153153	0.00012249	0.000128393	0.000141926	0.00013888	0.000121661	6.52675E-05	7.4225E-05
S approximated (mm²)	153.1526873	122.4896422	128.3933722	141.9262501	138.8799459	121.6613907	65.26754581	74.2250315
Average Thickness	6.30125	5.7875	5.6975	6.28625	5.71125	5.3875	3.87125	4.38875

	BEAM 04															
	29B		**22B**		**28B**		**23B**		**21T**		**25B**		**20T**		**24T**	
Number of nodes	8				8											
D1 in, bottom	12.33	12.52	12.96	13.12	13.23	12.47	12.06	12.81	11.97	12.245	14.27	13.785	10.69	11.21	11.16	11.645
	12.71		13.28		11.71		13.56		12.52		13.3		11.73		12.13	
D1 out, bottom	18.97	18.695	19.54	19.145	20.09	19.25	20.35	19.075	17.53	17.225	20.66	20.515	15.08	16.02	16.11	16.955
	18.42		18.75		18.41		17.8		16.92		20.37		16.96		17.8	
D2	19.2	18.76	19.45	18.795	18.88	18.2	16.27	17.44	16.53	15.97	20.22	19.975	15.89	14.89	16.2	15.535
	18.32		18.14		17.52		18.61		15.41		19.73		13.89		14.87	
D3	18.56	17.81	18.5	18.13	18.42	17.755	14.88	15.72	13.95	13.63	19.67	19.305	12.79	13.32	14.26	13.85
	17.06		17.76		17.09		16.56		13.31		18.94		13.85		13.44	
D4 in, top	11.24	11.655	12.46	12.095	10.91	11.41	9.96	10.6	8.42	7.95	13.39	12.74	7.49	7.965	8.14	8.65
	12.07		11.73		11.91		11.24		7.48		12.09		8.44		9.16	
D4 out,top	17.52	16.715	17.71	17.185	15.85	16.36	14.1	14.91	12.16	11.95	19	18.51	10.97	11.535	12	12.845
	15.91		16.66		16.87		15.72		11.74		18.02		12.1		13.69	
Mean Din	12.0875		12.6075		11.94		11.705		10.0975		13.2625		9.5875		10.1475	
Mean Dout	17.995		18.31375		17.89125		16.78625		14.69375		19.57625		13.94125		14.79625	
S approximated (m²)	0.000139575		0.000138579		0.000139434		0.000113703		8.94936E-05		0.000162841		8.04548E-05		9.10726E-05	
S approximated (mm²)	139.574968		138.5790942		139.4342701		113.7030064		89.49359395		162.8410449		80.454849		91.07261732	
Average Thickness	5.9075		5.70625		5.95125		5.08125		4.59625		6.31375		4.35375		4.64875	

	BEAM 05															
	30B		**32T**		**36B**		**37B**		**39B**		**31B**		**30T**		**31T**	
Number of nodes	7		6		7		5		7		6		8		6	
D1 in, bottom	14.59		12.04		11.76		10.85		14.16		10.67		12.81		10.8	
	13.79	14.19	11.3	11.67	10.65	11.205	9.95	10.4	14.93	14.545	11.51	11.09	12.24	12.525	9.82	10.31
D1 out, bottom	20.7		16.13		18.42		18.03		20.91		17.96		17.28		14.41	
	19.71	20.205	15.07	15.6	17.8	18.11	17.26	17.645	19.7	20.305	16.89	17.425	16.26	16.77	15.77	15.09
D2	19.79		15.52		19.66		17.95		20.82		17.69		14.55		14.8	
	18.83	19.31	14.07	14.795	20.71	20.185	17.01	17.48	19.3	20.06	16.41	17.05	15.71	15.13	13.39	14.095
D3	18.21	17.81	13.91	12.985	17.32	18.055	17.01	16.395	19.9	19.125	16.88	16.175	13.42	13.045	13.21	12.54

	17.41		12.06		18.79		15.78		18.35		15.47		12.67		11.87	
D4 in, top	12.58		8.72		10.29		9.87		13.36		9.98		7.18		7.42	
	11.86	12.22	7.28	8	11.36	10.825	9.03	9.45	12.31	12.835	10.81	10.395	6.25	6.715	6.6	7.01
D4 out,top	17.23		12.43		16.56		16.35		18.69		15.83		9.47		11.54	10.85
	16.23	16.73	10.85	11.64	17.91	17.235	15.31	15.83	17.21	17.95	14.47	15.15	10.39	9.93	10.16	
Mean Din	13.205		9.835		11.015		9.925		13.69		10.7425		9.62		8.66	
Mean Dout	18.51375		13.755		18.39625		16.8375		19.36		16.45		13.71875		13.14375	
S approximated (m^2)	0.000132251		7.2628E-05		0.000170503		0.000145295		0.000147179		0.000121895		7.5131E-05		7.67825E-05	
S approximated (mm^2)	132.250773		72.62796728		170.5034924		145.2953468		147.1785107		121.8947325		75.13095392		76.78253826	
Average Thickness	5.30875		3.92		7.38125		6.9125		5.67		5.7075		4.09875		4.48375	

	BEAM 06															
	35B		**38B**		**32B**		**34B**		**36T**		**33B**		**34T**		**35T**	
Number of nodes	7		7		7		9		7		7		8		5	
D1 in, bottom	9.5		12.73		14.04		11.96		10.54		11.63		9.92		10.32	
	9.39	9.445	14.48	13.605	13.23	13.635	10.7	11.33	11.11	10.825	12.56	12.095	10.81	10.365	9.35	9.835
D1 out, bottom	16.25		20.96		19.54		18.06		15.91		18.61		15.81		15.21	
	16.87	16.56	18.58	19.77	18.64	19.09	16.35	17.205	17.5	16.705	17.42	18.015	14.16	14.985	14.02	14.615
D2	15.94		20.06		16.94		17.75		15.1		18.2		14.46		13.92	
	16.56	16.25	18.03	19.045	18.14	17.54	15.98	16.865	16.6	15.85	16.78	17.49	12.87	13.665	11.97	12.945
D3	15.5		19.15		17.25		17.1		13.69		17.09		11.01		13.35	
	16.34	15.92	17.68	18.415	15.98	16.615	14.74	15.92	15.25	14.47	15.41	16.25	11.75	11.38	11.94	12.645
D4 in, top	8.45		12.3		12.05		10.82		8.54		11.17		7.1		7.29	
	9.29	8.87	11.02	11.66	11.33	11.69	9.99	10.405	9.06	8.8	9.86	10.515	5.64	6.37	7	7.145
D4 out,top	14.4		17.8		15.1		15.36		12.15		16.13		8.98		11.8	11.19
	15.25	14.825	16.45	17.125	16.13	15.615	14.59	14.975	13.25	12.7	14.2	15.165	10.44	9.71	10.58	
Mean Din	9.1575		12.6325		12.6625		10.8675		9.8125		11.305		8.3675		8.49	
Mean Dout	15.88875		18.58875		17.215		16.24125		14.93125		16.73		12.435		12.84875	
S approximated (m^2)	0.000132412		0.000146054		0.000106828		0.000114413		9.94762E-05		0.000119451		6.64558E-05		7.30501E-05	
S approximated (mm^2)	132.4122951		146.0538758		106.8277523		114.4133843		99.4762304		119.4511085		66.45581273		73.05010039	
Average Thickness	6.73125		5.95625		4.5525		5.37375		5.11875		5.425		4.0675		4.35875	

	BEAM 07															
	40B		41B		42B		43B		44B		51T		52T		53T	
Number of nodes	7+1		7+2		6		8		8+1		7		6+1		6	
D1 in, bottom	11.22		12.45		11.01		14.3		15.73		12.93		10.62		6.91	
	12.96	12.09	13.89	13.17	11.92	11.465	13.37	13.835	14.13	14.93	12.08	12.505	10.15	10.385	7.64	7.275
D1 out, bottom	18.08		20.11		19.78		21.87		22.67		18.76		16.38		16.32	
	19.81	18.945	18.74	19.425	18.01	18.895	20.58	21.225	24.33	23.5	17.53	18.145	15.37	15.875	15.14	15.73
D2	19.51		19.27		19.66		20.81		21.56		17.23		14.82		14.74	
	17.83	18.67	18.05	18.66	17.9	18.78	21.86	21.335	20.74	21.15	16.16	16.695	13.7	14.26	13.17	13.955
D3	19.63		16.94		19.52		21.78		19.81		15.14		3.35		12.91	
	17.56	18.595	17.96	17.45	18.28	18.9	20.58	21.18	21.03	20.42	16.16	15.65	12.2	7.775	11.43	12.17
D4 in, top	12.8		11.3		13.23		14.29		14.64		9.4		6.81		10.45	
	11.09	11.945	12.17	11.735	12.4	12.815	13.32	13.805	13.55	14.095	8.54	8.97	7.89	7.35	11.25	10.85
D4 out,top	19.43		15.88		19.22		18.79		20.34		13.46		11.89		16.36	15.765
	18.14	18.785	16.91	16.395	17.6	18.41	20.28	19.535	19.03	19.685	12.86	13.16	10.71	11.3	15.17	
Mean Din	12.0175		12.453		12.14		13.82		14.513		10.738		8.868		9.0625	
Mean Dout	18.749		17.983		18.746		20.819		21.189		15.913		12.3025		14.405	
S approximated (m^2)	0.000163		0.000132		0.000160		0.000190		0.000187		0.000108		5.71133E-05		9.84694E-05	
S approximated (mm^2)	162.6522842		132.187		160.254		190.402		187.200		108.317		57.113		98.469	
Average Thickness	6.73125		5.53		6.6063		6.999		6.676		5.175		3.435		5.343	

	BEAM 08															
	45T		46B		47B		48B		49B		50B		46T		47T	
Number of nodes	6		7		9		8		8		9		7		8	
D1 in, bottom	13.43		14.06		15.09		13.6		14.3		12.24		11.59		12.9	
	12.59	13.01	13.79	13.925	13.89	14.49	12.29	12.945	13.32	13.81	13.34	12.79	12.87	12.23	12.47	12.685
D1 out, bottom	19.22		21.02		22.64		21.85		21.46		21.64		17.92		17.93	
	17.6	18.41	20.5	20.76	21.65	22.145	20.25	21.05	20.23	20.845	20.31	20.975	16.29	17.105	17.16	17.545
D2	17.89		21.15		21.04		21.38		20.77		21.07		16.32		15.84	
	16.25	17.07	20.18	20.665	20.67	20.855	19.83	20.605	19.49	20.13	20.17	20.62	14.53	15.425	16.58	16.21
D3	16.4		20.36		19.67		21.04		20.05		19.82		13.49		13.86	
	14.84	15.62	19.05	19.705	19.34	19.505	19.22	20.13	18.7	19.375	18.98	19.4	12.61	13.05	12.94	13.4
D4 in, top	10.62		12.31		13.23		14.45		14.37		3.39		7.36		7.93	
	8.86	9.74	13.57	12.94	12.98	13.105	13.23	13.84	13.07	13.72	12.14	7.765	8.06	7.71	8.8	8.365
D4 out,top	14.34		17.78		19.31		18.11		19.97		20.03		12.37		11.16	11.715
	15.61	14.975	19.71	18.745	18.4	18.855	20.2	19.155	18.99	19.48	18.91	19.47	10.46	11.415	12.27	
Mean Din	11.375		13.4325		13.7975		13.3925		13.765		10.278		9.97		10.525	
Mean Dout	16.519		19.969		20.34		20.235		19.9575		20.116		14.249		14.718	

S approximated (m^2)	0.000113	0.0001715	0.0001754	0.0001807	0.00016401	0.000235	8.13877E-05	8.3118E-05
S approximated (mm^2)	112.688	171.467	175.414	180.717	164.012	234.863	81.388	83.118
Average Thickness	5.144	6.536	6.543	6.843	6.193	9.839	4.279	4.193

Appendix B:

In Appendix B, to calculate the effective depth (d), the nominal area (A), and the outer diameter (D_{out}) of each culm were utilized. Each area (A_i), along with its respective vertical coordinate y_i (with respect to the axis at the bottom of the beam), was multiplied and subsequently summed. This procedure enables the determination of the center of gravity (C.G.) and, consequently, the effective depth (d).

Furthermore, for bending design the longitudinal reinforcement area (A_f), longitudinal reinforcement ratio (ρ_f), distance from the extreme compression fiber to neutral axis at balanced strain condition (c_b) and nominal moment capacity (M_n) are calculated to obtain the ultimate load $P_{u,b}$. In the case of shear design, the ratio of depth of neutral axis to reinforcement depth (k) and ratio of modulus of elasticity of Bamboo bars to modulus of elasticity of concrete (n_f) are employed to derive the nominal shear strength provided by concrete (V_c) and shear resistance provided by the stirrups (V_f). The sum of these values represents the total shear strength (V_{total}).

Beam's Design

Effective Depth (d) - Beam 03

Total Area:		806.503	mm²		$\sum A_i \cdot y_i$
(1st layer)	A	153.15	122.49	128.39	16178.74
	D out	18.62	16.37	17.20	
(2nd layer)	A	141.93	138.88	121.66	35228.86
	D out	17.52	18.34	17.07	
C.G. = 63.74 mm			d = 186.26 mm		

BEAM 03					
Bending:					
A_f	ρ_f	$c_b = \left(\frac{\varepsilon_{cu}}{\varepsilon_{cu}+\varepsilon_{fu}}\right)d$	$M_n = A_f f_{fu}\left(d - \frac{\beta_1 c_b}{2}\right)$	Load for M_n=17.48	70% of $P_{u,b}$
806.503 mm²	2.89 %	40.49 mm	17.301 kN.m	86.38 kN	23.98 kN (design)
Shear:					
$k=\sqrt{2\rho_f n_f+(\rho_f n_f)^2}-\rho_f n_f$	n_f	$V_c = \frac{2}{5}\sqrt{f'_c} b_w (kd)$	$V_f = \frac{A_{fv} f_{fv} d}{s}$	V_{total}	Load for V = 13.56 kN
0.124	0.306	8152.98 N	5407.72 N	13.56 kN	33.18 kN (nominal)

BEAM 04					
Bending:					
A_f	ρ_f	$c_b = \left(\frac{\varepsilon_{cu}}{\varepsilon_{cu}+\varepsilon_{fu}}\right)d$	$M_n = A_f f_{fu}\left(d - \frac{\beta_1 c_b}{2}\right)$	Load for M_n=17.48	70% of $P_{u,b}$
783.626 mm²	2.70%	42.1035 mm	17.478 kN.m	86.8 kN	24.10 kN (design)
Shear:					
$k=\sqrt{2\rho_f n_f+(\rho_f n_f)^2}-\rho_f n_f$	n_f	$V_c = \frac{2}{5}\sqrt{f'_c} b_w (kd)$	$V_f = \frac{A_{fv} f_{fv} d}{s}$	V_{total}	Load for V = 11.06 kN
0.122	0.312	8122.477 N	2937.72 N	11.06 kN	26.88 kN (nominal)

BEAM 05					
Bending:					
A_f	ρ_f	$c_b = \left(\frac{\varepsilon_{cu}}{\varepsilon_{cu}+\varepsilon_{fu}}\right)d$	$M_n = A_f f_{fu}\left(d - \frac{\beta_1 c_b}{2}\right)$	Load for M_n=17.48	75% of $P_{u,b}$
789.751 mm²	2.85 %	40.22 mm	16.827 kN.m	84 kN	25.00 kN (design)

Shear:					
$k=\sqrt{2\rho_f n_f+(\rho_f n_f)^2}-\rho_f n_f$	n_f	$V_c=\frac{2}{5}\sqrt{f'_c}b_w(kd)$	$V_f=\frac{A_{fv}f_{fv}d}{s}$	V_{total}	Load for V = 24.50 kN
0.123	0.301	7450.742 N	17047.094 N	24.50 kN	61.18 kN (nominal)

BEAM 06					
Bending:					
A_f	ρ_f	$c_b=\left(\frac{\varepsilon_{cu}}{\varepsilon_{cu}+\varepsilon_{fu}}\right)d$	$M_n=A_f f_{fu}\left(d-\frac{\beta_1 c_b}{2}\right)$	Load for M_n=17.48	70% of $P_{u,b}$
718.635 mm²	2.58%	40.430 mm	15.391 kN.m	76.30 kN	21.34 kN (design)
Shear:					
$k=\sqrt{2\rho_f n_f+(\rho_f n_f)^2}-\rho_f n_f$	n_f	$V_c=\frac{2}{5}\sqrt{f'_c}b_w(kd)$	$V_f=\frac{A_{fv}f_{fv}d}{s}$	V_{total}	Load for V = 7.58 kN
0.120	0.316	7583.786 N	0	7.58 kN	17.64 kN (nominal)

BEAM 07					
Bending:					
A_f	ρ_f	$c_b=\left(\frac{\varepsilon_{cu}}{\varepsilon_{cu}+\varepsilon_{fu}}\right)d$	$M_n=A_f f_{fu}\left(d-\frac{\beta_1 c_b}{2}\right)$	Load for M_n=17.48	70% of $P_{u,b}$
941.0133 mm²	3.36 %	40.573 mm	20.225 kN.m	101.36 kN	28.07 kN (design)
Shear:					
$k=\sqrt{2\rho_f n_f+(\rho_f n_f)^2}-\rho_f n_f$	n_f	$V_c=\frac{2}{5}\sqrt{f'_c}b_w(kd)$	$V_f=\frac{A_{fv}f_{fv}d}{s}$	V_{total}	Load for V = 9.14 kN
0.129	0.283	9139.33 N	0	9.14 kN	21.84 kN (nominal)

BEAM 08					
Bending:					
A_f	ρ_f	$c_b = \left(\frac{\varepsilon_{cu}}{\varepsilon_{cu}+\varepsilon_{fu}}\right)d$	$M_n = A_f f_{fu}\left(d-\frac{\beta_1 c_b}{2}\right)$	Load for M_n=17.48	70% of $P_{u,b}$
1039.16 mm²	3.76%	40.017 mm	22.0287 kN.m	110.6 kN	30.59 kN (design)
Shear:					
$k=\sqrt{2\rho_f n_f+(\rho_f n_f)^2}-\rho_f n_f$	n_f	$V_c=\frac{2}{5}\sqrt{f'_c}b_w(kd)$	$V_f=\frac{A_{fv}f_{fv}d}{s}$	V_{total}	Load f/ V=12.17 kN $\frac{P(L-a)}{L}+\frac{G.L}{2}$
0.137	0.290	9382.50 N	2792.13 N	12.17 kN	29.68 kN (nominal)

BEAM 02					
Shear – Fiber Contribution (Rilem TC 162-TDF):					
k_f	$k_1=\frac{1600-d}{1000}$	τ_f	b_w	d	$V_f = 0.7.k_f.k_1.\tau_f.b_w.d$
1	1.414	0.0756	150	186.5	2093.34 N
Shear – Concrete Contribution (Rilem TC 162-TDF, ACI 440.1R-15):					
$k=1+\sqrt{\frac{200}{d}}$	σ_{cp}	V_c	n_f	$k=\sqrt{2\rho_f n_f+(\rho_f n_f)^2}-\rho_f n_f$	$V_c=\frac{2}{5}\sqrt{f'_c}b_w(kd)$
2.04	0	31047.64N	0.333	0.134	12110.11 N
V_{total} (RILEM):		33.14 kN	V_{total} (ACI 440.1R-15):		14.20 kN
LOAD (kN)		59.6 kN	LOAD (kN)		24.9 kN